2016

# COMPARING METEORIC 10Be, IN SITU 10Be, AND NATIVE 9Be ACROSS A DIVERSE SET OF WATERSHEDS

Emily Sophie Greene
*University of Vermont*

# COMPARING METEORIC $^{10}$Be, IN SITU $^{10}$Be, AND NATIVE $^{9}$Be ACROSS A DIVERSE SET OF WATERSHEDS

A Thesis Presented

by

Emily Sophie Greene

to

The Faculty of the Graduate College

of

The University of Vermont

In partial Fulfillment of the Requirements
for the Degree of Master of Science
Specializing in Geology

October, 2016

Defense Date: May 24, 2016
Thesis Examination Committee:

Paul R. Bierman, Ph.D., Advisor
Giuseppe A. Petrucci, Ph.D., Chairperson
Nicolas Perdrial, Ph.D.
Cynthia J. Forehand, Ph.D., Dean of the Graduate College

## ABSTRACT

The cosmogenic nuclide $^{10}$Be is a tool for quantifying earth surface processes that occur on millennial timescales. $^{10}$Be is produced in the atmosphere (meteoric $^{10}$Be) or in mineral grains (*in situ* $^{10}$Be). Well-understood nuclear physics, physical mixing processes, and the denudation of regolith control concentrations of *in situ* $^{10}$Be; in contrast, a combination of geomorphic, pedogenic, geochemical, and biological processes influence meteoric $^{10}$Be concentrations. Some have hypothesized that meteoric $^{10}$Be can be used as a tracer of sediment movement if meteoric $^{10}$Be is normalized against the concentration of native $^{9}$Be in grain coatings. This study aims to better understand Be dynamics in river sediment systems by further characterizing a large dataset of fluvial sediments (202 total samples from 7 study areas) that have previously been analyzed for *in situ* and meteoric $^{10}$Be.

I determined $^{9}$Be and major element compositions of grain coatings (as the acid-extractable fraction) and grains (by total digestion) of fluvial sediments. I compiled the emical data with characteristics of sample watersheds that I acquired using ArcGIS and with meteoric and *in situ* $^{10}$Be data from previous studies. With this dataset, I performed a statistical analysis testing relationships between the concentration of meteoric $^{10}$Be and $^{9}$Be in acid-extractable grain coatings, meteoric $^{10}$Be/$^{9}$Be ratios, $^{9}$Be concentrations in mineral grains, watershed characteristics, and major element compositions of fluvial sediment grains and grain coatings. I calculated meteoric $^{10}$Be/$^{9}$Be-derived denudation rates using a published mass balance model and compared them to *in situ* $^{10}$Be-derived denudation rates. Though this thesis focuses on fluvial sediment samples, I also measured $^{9}$Be concentrations of soil, suspended sediment, and glacial lake sediment samples with known meteoric $^{10}$Be or *in situ* $^{10}$Be concentrations, which can be used in future studies of $^{9}$Be and $^{10}$Be dynamics.

I find that meteoric $^{10}$Be and $^{9}$Be concentrations in grain coatings are significantly influenced by geochemical and geomorphic conditions in watersheds. HCl-extracted $^{9}$Be is significantly correlated to total meteoric $^{10}$Be concentrations in all but one study area, suggesting that meteoric $^{10}$Be and $^{9}$Be are well mixed in most, but not all, soil systems. Trends in meteoric $^{10}$Be do not mirror trends in *in situ* $^{10}$Be. Though normalizing meteoric $^{10}$Be against $^{9}$Be concentrations improves the correlation between meteoric $^{10}$Be and *in situ* $^{10}$Be in fluvial sediments, the spatial variation in parent $^{9}$Be concentrations and meteoric $^{10}$Be delivery rates, combined with the observation that meteoric $^{10}$Be and $^{9}$Be are not always well mixed, makes it difficult to interpret changes in meteoric $^{10}$Be/$^{9}$Be across study areas. A mass balance model for deriving meteoric $^{10}$Be/$^{9}$Be denudation rates helps control for some variation in $^{9}$Be concentrations and meteoric $^{10}$Be delivery rates across study areas, but uncertainties in quantifying these variables for each watershed introduce noise into the correlations between meteoric $^{10}$Be/$^{9}$Be -derived denudation rates and $^{10}Be_{is}$-derived denudation rates. When considering all samples, meteoric $^{10}$Be/$^{9}$Be-derived and $^{10}Be_{is}$-derived denudation rates are significantly correlated and have similar central tendencies. However, the $^{10}Be_{met}/^{9}Be_{reactive}$ -derived measure is less sensitive to changes in denudation than the $^{10}Be_{is}$ –derived measure.

## CITATIONS

Material from this thesis is submitted to Geochimica et Cosmochimica Acta on May 18, 2016 in the following form:

Greene, E.S., Bierman, P.R., & Perdrial, N.. (2016). Towards a better understanding of Beryllium-10 and Beryllium-9 dynamics in river sediments. *Geochim. Cosmochim. Acta.*

## TABLE OF CONTENTS

CITATION ..... ii

LIST OF FIGURES..... vi

LIST OF TABLES ..... vii

**CHAPTER 1: Introduction** ..... 1

**CHAPTER 2: Background** ..... 10

2.1. Production of cosmogenic $^{10}Be$ (*in situ* and meteoric) ..... 10

2.2. Inputs of $^{9}Be$, $^{10}Be_{met}$ and $^{10}Be_{is}$ to soils and watersheds ..... 11

2.2.1 $^{10}Be_{is}$ production rates ..... 12

2.2.2. $^{10}Be_{met}$ delivery rates ..... 12

2.2.3. Sources of $^{9}Be$ to soils and sediments ..... 15

2.3. $^{10}Be_{met}$ and $^{9}Be_{reactive}$ sorption and remobilization in soils and sediments ..... 17

2.4. $^{10}Be_{met}/^{9}Be_{reactive}$ and $^{10}Be_{is}$ as tracers of mass in soils and fluvial sediments ..... 23

2.5. $^{10}Be_{met}/^{9}Be_{reactive}$-derived denudation rate model ..... 27

**CHAPTER 3:** Manuscript for *Geochimica et Cosmochimica Acta* ..... 37

1. INTRODUCTION..... 39

2. BACKGROUND ..... 41

2.1 $^{9}Be$ geochemistry ..... 43

2.2 $^{10}Be_{met}$ and $^{9}Be_{reactive}$ concentrations in soil profiles ..... 44

2.3 $^{10}Be_{met}/^{9}Be_{reactive}$ denudation rate model ..... 46

3. EXPERIMENTAL APPROACH AND METHODS ..... 47

3.1 $^{9}Be_{reactive}$ extraction ..... 48

3.2 $^{9}Be_{min}$ total digestion ..... 49

3.3 $^{9}Be$ organic fraction extraction ..... 50

3.4 $^{10}Be_{met}/^{9}Be_{reactive}$-derived denudation rate calculations ..... 50

4. RESULTS ..... 52

4.1 Grain coatings leached with HCl ..... 52

4.2 Significant correlations between $^{10}Be_{is}$, $^{10}Be_{met}$, $^{10}Be_{met}/^{9}Be_{reactive}$ and $^{10}Be_{is}$-derived denudation rates ..... 53

4.3 Chemical compositions of grain coatings and mineral matrixes ..... 54

4.4 Variation in correlations between basin characteristics and Be isotopes by study area ..... 55

4.5 $^{10}Be_{met}/^{9}Be_{reactive}$ and $^{10}Be_{is}$-derived denudation rates significantly correlate across all samples ..... 57

5. DISCUSSION ..... 59

5.1 $^{9}Be_{reactive}$ and total $^{10}Be_{met}$ are primarily associated with HCl-extractable grain coatings ..... 58

5.2 Heterogeneous distributions of $^{9}Be_{min}$ and $^{9}Be_{reactive}$ within and across study areas ..... 61

5.3 Study site-specific influences on $^{9}Be_{reactive}$ and $^{10}Be_{met}$ concentrations in sediment grain coatings ..... 64

5.4 Assumptions required to calculate $^{10}Be_{met}/^{9}Be_{reactive}$-derived denudation rates introduce uncertainties ..... 68

5.5 Basin characteristics do not primarily influence Be isotopes or denudation rates ... ..... 72

6. CONCLUSIONS ..... 74

Chapter 3 References ..... 76

Chapter 3 Tables ..... 82

Chapter 3 Figures and captions ..... 86

Supplement Information ..... 95

**CHAPTER 4:** Conclusions and future work ..... 96

4.1 Conclusions ..... 96

4.1 Future work ..... 98

**CITED REFERENCES** ..... 100

**APPENDIX A:** complete data tables ..... Electronic

## LIST OF FIGURES

**Chapter 3:** Manuscript for submission to *Geochimica et Cosmochimica Acta*

**Figure 1.** Locations of study areas and associated coding ..... 1

**Figure 2.** Schematic diagram of $^{10}Be_{is}$, $^{10}Be_{met}$, and $^{9}Be$ behavior in a soil system ..... 2

**Figure 3.** HCl-extractable elemental concentrations over time ..... 3

**Figure 4.** Correlations between $^{10}Be_{met}$ and $^{10}Be_{is}$ and $^{10}Be_{met}/^{9}Be_{reactive}$ and $^{10}Be_{is}$ ..... 4

**Figure 5.** Comparison of $^{10}Be_{met}$ and $^{9}Be_{reactive}$ for each study area ..... 5

**Figure 6.** Correlations between $^{10}Be_{met}$ and HCl-extractable Al, Fe, and Mn ..... 6

**Figure 7.** Histograms of $^{9}Be_{min}+^{9}Be_{reactive}$ in each study area ..... 7

**Figure 8.** Boxplot of f.factors calculated for each study area ..... 8

**Figure 9.** Comparison of $^{10}Be_{met}/^{9}Be_{reactive}$- derived denudation rates and $^{10}Be_{is}$-derived denudation rates ..... 9

## LIST OF TABLES

**Chapter 1:** Introduction

**Table 1.** Compiled environmental and chemical data from study regions ..... 1

**Chapter 3:** Manuscript for submission to *Geochimica et Cosmochimica Acta* ..... 2

**Table 1.** Physical characteristics of the studied watersheds ..... 3

**Table 2.** Correlations between Be isotope data for each study area and for all samples ..... 4

**Table 3.** Correlations between Be isotopes and basin characteristics for each study area and for all samples ..... 5

**Table 4.** Mean denudation rates calculated from $^{10}Be_{is}$ and $^{10}Be_{met}/^{9}Be_{reactive}$ mass balance model ..... 6

# CHAPTER 1: INTRODUCTION

Recent realizations that earth surface processes may drive climate fluctuations and moderate tectonics have reinvigorated research in geochemical tracers relevant to pedogenesis and denudation (Raymo et al., 1988; Vance et al., 2009; Crowley et al., 2015; von Blanckenburg et al., 2015). The ability to quantify physical and chemical weathering rates could help understand the factors that control soil formation, hillslope processes, and sediment transport across a variety of spatial and temporal scales (Lal, 1991; Bierman, 1994; Gosse & Phillips, 2001; Portenga & Bierman, 2011). Cosmogenic nuclides have aided in quantifying earth surface processes (Granger & Schaller, 2014; Dixon & Riebe, 2014). The long half-life of $^{10}$Be (1.39 million years) (Nishiizumi et al., 2007; Chmeleff et al., 2010; Korschinek et al., 2010) renders it especially useful as an indicator of millennial-scale denudation rates (Nishiizumi et al., 1986; Bierman, 1994; Granger et al., 1996; Bierman & Caffee, 2002). Developing methods that can quantify the rate and spatial distribution of sediment generation and transport in fluvial systems is important for validating or refuting the proposed links between tectonics, climate, and geomorphology.

Early studies of terrestrial cosmogenic isotopes measured the concentration of meteoric $^{10}$Be ($^{10}Be_{met}$) – the $^{10}$Be that is formed in the atmosphere and delivered to landscapes via precipitation or dry deposition (Lal & Peters, 1967; Monaghan et al., 1983; Pavich et al., 1984;1986). As advances in accelerator mass spectrometry allowed for lower detection limits, researchers developed techniques to quantify basin scale denudation rates and soil production rates using measurements of *in situ* $^{10}$Be ($^{10}Be_{is}$), which is produced within mineral grains on earth's surface at concentrations 3-4 orders of

magnitude lower than the rate of $^{10}Be_{met}$ delivery (Nishiizumi et al., 1986; Elmore & Phillips 1987; Bierman & Turner, 1995; Bierman & Steig, 1996; Heimsath et al., 1997;1999).

While $^{10}Be_{is}$ concentrations in fluvial sediments have been used to quantify millennial scale denudation rates around the globe (Portenga & Bierman, 2011), grain size dependencies and the potential for remobilization make $^{10}Be_{met}$ concentrations difficult to interpret in terms of denudation rates (Brown et al., 1992; Willenbring & von Blanckenburg, 2010; Graly et al., 2010; Ouimet et al., 2015). This is problematic because in many respects, using $^{10}Be_{met}$ as a proxy for denudation rates is advantageous; $^{10}Be_{met}$ is orders of magnitude more abundant than $^{10}Be_{is}$ and measureable in all types of substrates, not just the sand-size quartz required for $^{10}Be_{is}$ analysis (Stone, 1998).

Some (Barg et al., 1997; von Blanckenburg et al., 2012; Bacon et al., 2012) have hypothesized $^{9}Be$ that has weathered out of bedrock ($^{9}Be_{reactive}$) can be used to help interpret $^{10}Be_{met}$ data in denudation rate studies. Given that native $^{9}Be_{reactive}$ has the same chemical behavior as $^{10}Be_{met}$ in weathering and pedogenic reactions, the $^{10}Be_{met}/^{9}Be_{reactive}$ ratio could be used to normalize the $^{10}Be_{met}$ nuclide inventory against post-deposition chemical processes and grain size dependencies (Barg et al., 1997; von Blanckenburg et al., 2012; 2014; 2015, Bacon et al., 2012, Wittmann et al., 2012). It has recently been proposed that measuring the $^{9}Be$ distribution between the phase that is dissolved in river water ($^{9}Be_{diss}$), the phase that is sorbed to grains ($^{9}Be_{reactive}$), and the phase that is crystalized into a mineral lattice ($^{9}Be_{min}$) can be used in a mass balance formulation to derive $^{10}Be_{met}/^{9}Be_{reactive}$-based denudation rates (von Blanckenburg et al., 2012; Bouchez et al., 2014; von Blanckenburg & Bouchez, 2014; von Blanckenburg & Scheussler,

2014). If the assumptions of this mass balance model are supported in more study areas, $^{10}Be_{met}/^{9}Be_{reactive}$ ratios could become a powerful tool for determining rates of denudation from fluvial sediments, ancient soils, and lacustrine or marine sediment cores around the globe (Merrill et al., 1959; Brown et al., 1988; Bacon et al., 2012; Wittmann et al., 2012; von Blanckenburg et al., 2012;2014).

My thesis examines previous assumptions about Be isotope dynamics in sediments by comparing concentrations of $^{9}Be$ and $^{10}Be$ in a diverse set of fluvial sediment samples that have extant measurements of $^{10}Be_{is}$, $^{10}Be_{met}$, and $^{10}Be_{is}$-derived denudation rates. Chemical characterization of the HCl-extractable phase of sediments allows for the measurement $^{9}Be_{reactive}$, and chemical characterization of the digested residual material after HCl extraction allows for the measurement of $^{9}Be_{min}$. These data, combined with $^{10}Be_{met}$ and $^{10}Be_{is}$ measurements from previous studies, can be used to draw conclusions about Be isotope dynamics in soils and fluvial sediments from varied climatic, lithological, and tectonic settings.

With this dataset of diverse and well-characterized samples, I address several geologically relevant questions. First, I test assumptions about isotope mixing and Be remobilization by statistically analyzing $^{10}Be_{is}$, $^{10}Be_{met}$, $^{9}Be_{reactive}$, $^{9}Be_{min}$, and $^{10}Be_{met}/^{9}Be_{reactive}$ concentrations, watershed characteristics such as elevation, mean annual precipitation (MAP), and total basin relief, and major elemental abundances of HCl-extractable grain coatings. I then calculate $^{10}Be_{met}/^{9}Be_{reactive}$-derived denudation rates using several methods and compare them to $^{10}Be_{is}$-derived denudation rates determined from previous studies. Finally, using the $^{10}Be_{is}$-derived denudation rates as a framework, I assess which set of assumptions used to calculate $^{10}Be_{met}/^{9}Be_{reactive}$-derived denudation

rates results in the most accurate denudation rate estimate.

This project is possible because I have access to fluvial sediment samples that were previously analyzed for $^{10}Be_{met}$ and $^{10}Be_{is}$ concentrations. These samples were collected by others from watersheds around the globe in diverse climactic, tectonic, and chemical environments (Trodick, 2011; Portenga and Bierman, 2011; Nichols et al., 2014; Neilson, 2016). Table 1 summarizes the climatic and environmental setting for my study areas.

Chapter 2 of this thesis focuses on background information relating to the cosmogenic nuclide $^{10}Be$, the biogeochemistry and natural distribution of $^{9}Be$, and models of using meteoric and *in situ* $^{10}Be$ to quantify millennial-scale denudation rates in fluvial systems. Chapter 3 consists of a manuscript for submission to Geochimica et Cosmochimica Acta. Chapter 4 consists conclusions and future work. Electronic appendixes include supplementary data tables of measured samples (soils, suspended sediments, and glacial lake sediments).

| Location | Climate | Tectonic setting | Bedrock description | ID | n | Mean MAP (mm/yr) | Mean basin size ($km^2$) | Mean elevation (m) | Mean total basin relief (m) | Mean latitude (°) | $^{10}Be_{is}$-derived denudation rate (t $km^{-2}$ $yr^{-1}$) |
|---|---|---|---|---|---|---|---|---|---|---|---|
| Potomac River | temperate, never glaciated | passive margin | gneiss, sandstone, shale and carbonates | POT | 62 | 730-1030 | 1050 | 354 | 330 | 39.1 | 29.8 |
| Barron River (NE Australia) | humid temperate, never glaciated | passive margin | granite and biogenetic carbonate | QLD | 8 | 1930-2250 | 330 | 475 | 730 | 16.9 | 73.7 |
| Georges River (SE Australia) | humid temperate, never glaciated | passive margin | sandstone, granodiorite | G | 14 | 970-1260 | 90 | 390 | 730 | 41.3 | 43.6 |
| China, Mekong River (SW China) | tropical, never glaciated | tectonically active | lightly metamorphosed granite and sedimentary red beds, mafic intrusions, carbonates | CH1 xx | 64 | 510-1660 | 28200 | 2290 | 2880 | 25.4 | 403 |
| | | | | CHa | 15 | 960-1040 | 40 | 3040 | 960 | 27.1 | 160 |
| | | | | CHb | 24 | 1080-1250 | 580 | 1700 | 1450 | 24.0 | 311 |
| | | | | CHc | 15 | 1520-1610 | 140 | 1596 | 790 | 21.8 | 128 |

Table 1. Compiled environmental and chemical data from study regions.

## CITATIONS


Bacon, A.R., Richter D., Bierman, P.R., & Rood, D.H. (2012). Coupling meteoric $^{10}Be$ with pedogenic losses of $^{9}Be$ to improve soil residence time estimates on an ancient North American interfluve. *Geology, 40,* 847-850.

Barg, E., Lal, D., Pavich, M.J., Caffee, M.W., & Southon, J. R. (1997). Beryllium geochemistry in soils; evaluation of $^{10}Be/^{9}Be$ ratios in authigenic minerals as a basis for age models. *Chemical Geology, 140,* 237-258.

Bierman, P.R. (1994). Using *in situ* produced cosmogenic isotopes to estimate rates of landscape evolution; a review from the geomorphic perspective. *Journal of Geophysics Research B: Solid Earth, 99,* 13885-13896.

Bierman, P., & Caffee, M. (2002). Cosmogenic exposure and erosion history of Australian bedrock landforms. *Geological Society of America Bulletin, 114,* 787-803.

Bierman, P., & Turner, J. (1995). $^{10}Be$ and $^{26}Al$ evidence for exceptionally low rates of Australian bedrock erosion and the likely existence of pre-Pleistocene landscapes. *Quaternary Research*, *44*, 378-382.

Bierman, P., & Steig, E.J. (1996). Estimating rates of denudation using cosmogenic isotope abundances in sediment. *Earth Surface Processes and Landforms, 21* 125-139.

Bouchez, J., Gaillardet, J., & von Blanckenburg, F. (2014). Weathering intensity in lowland river basins: from the Andes to the Amazon mouth. *Procedia Earth and Planetary Science, 10*, 280-186.

Brown, L., Pavic, M.J., Hickman, R.E., Klein, J., & Middleton, R. (1988). Erosion of the eastern United States observed with $^{10}Be$. *Earth Surface Processes and Landforms, 13*, 441-457.

Brown, E.T., Edmond, J.M., Raisbeck, F.M., Bourlès, D. L., Yiou, F., & Measures, C.I. (1992). Beryllium isotope geochemistry in tropical river basins. *Geochimica et Cosmochimica Acta, 56,* 1607-1624.

Dixon, J., & Riebe, C. (2014). Tracing and pacing soil across slopes. *Elements, 10,* 363-368

Elmore, D., & Phillips, F., (1987). Accelerator mass spectrometry for measurement of long-lived radioisotopes. *Science*, *236,* 543-550.

Gosse, J.C., & Phillips, F.M. (2001). Terrestrial *in situ* cosmogenic nuclides: theory and application. *Quaternary Science Reviews, 20,* 1475-1560.

Graly, J.A., Bierman, P.R., Reusser, L.J., & Pavich, M.J. (2010). Meteoric $^{10}$Be in soil profiles - a global meta-analysis. *Geochimica et Cosmochimica Acta, 74,* 6814-6829

Granger, D.E., Kirchner, J.W., & Finkel, R. (1996). Spatially averaged long-term denudation rates measured from in situ-produced cosmogenic nuclides in alluvial sediments. *Journal of Geology, 104,* 249-257.

Granger. D.E., & Schaller, M. (2014). Cosmogenic nuclides and denudation at the watershed scale. *Elements, 10,* 369-393.

Heimsath, A.M., Dietrich, W.E., Nishiizumi, K., & Finkel, R.C. (1997). The soil production function and landscape equilibrium. *Nature, 388,* 358-361.

Heimsath, A.M., Dietrich, W.E., Nishiizumi, K., & Finkel, R.C. (1999). Cosmogenic nuclides, topography and the spatial variation of soil depth. *Geomorphology, 27*, 151-172.

Jungers, M.C., Bierman, P.R., Matmon, A., Nichols, K., Larsen, J., & Finkel, R. (2009). Tracing hillslope sediment production and transport with *in situ* and meteoric $^{10}$Be. *Journal of Geophysical Research, 114,* F04020.

Korschinek G., Bergmaier, A. Faestermann, T., Gerstmann, U.C., Knie, K., Rugel, G. Wallner, A., Dillmann, I., Dollinger, G., von Gostomski, C.L., Kossert, K., Poutivtsev M., & Remmert, A. (2010). A new value for the half-life of $^{10}$Be by heavy-ion elastic recoil detection and liquid scintillation counting. *Nuclear Instruments and Meth*ods *in Physical Research, 268,* 187–191.

Lal, D. (1991). Cosmic ray labeling of denudation surfaces: *in situ* nuclide production rates and denudation models. *Earth and Planetary Science Letters, 104,* 424-439.

Lal, D., & Peters, B. (1967). Cosmic ray produced radioactivity on the earth. *Handbuch der Physik*. Berlin: Springer.

Merrill, J. R., Lyden, E., Honda, M., & Arnold, J. R. (1959). The sedimentary geochemistry of the beryllium isotopes. *Geochimica et Cosmochimica Acta, 18,* 108-129.

Monaghan, M.C., Krishnaswami, S., & Thomas, J.H. (1983). $^{10}$Be concentrations and the long-term fate of particle-reactive nuclides in five soil profiles from California, *Earth and Planetary Science Letters, 65,* 51-60.

Neilson, T.B. (2015). *Using long- and short-lived sediment-associated isotopes to track denudation and sediment movement through rivers in Yunnan, SW China.* (MS thesis). University of Vermont, Burlington.

Nichols, K.K., Bierman, P.R., & Rood, D.H. (2014). $^{10}$Be constrains the sediment sources and sediment yields to the Great Barrier Reef from the tropical Barron River catchment, Queensland, Australia. *Geomorphology*, *224,* 102-110.

Nishiizumi, K, Lal, D., Klein, J., Middleton, R., & Arnold, J. R. (1986). Production of $^{10}$Be and $^{26}$Al by cosmic rays in terrestrial quartz *in situ* and implications for denudation rates. *Nature, 319,* 1468-1470.

Nishiizumi, K., Imamura, M., Caffee, M.W., Southon, J.R., Finkel, R.C., & McAninch, F. (2007). Absolute calibration of $^{10}$Be AMS standards, *Nuclear Instruments and Methods in Physical Research B, 258,* 403-413.

Ouimet, W., Dethier, D., Bierman, P., Wyshnystzky, C., Shea, N., & Rood, D. (2015) Spatial and temporal variations in meteoric $^{10}$Be inventories and long-term deposition rates, Colorado Front Range. *Quaternary Science Reviews, 109*, 1-12.

Pavich, M.P., Brown, L., Klein, J., & Middleton, R. (1984). $^{10}$Be accumulation in a soil chronosequence. *Earth and Planetary Science Letters, 68,* 198-204.

Pavich, M.P, Brown, L., Harden, J., Klein, J., & Middleton, R. (1986). $^{10}$Be distribution in soils from Merced River terraces, California. *Geochimica et Cosmochimica Acta, 50,* 1727-1735.

Portenga, E.W., & Bierman P.R. (2011). Understanding Earth's eroding surface with $^{10}$Be. *GSA Today, 21,* 4-10.

Raymo, M.E., Ruddiman, W.F., & Froelich, P.N. (1998). Influence of late Cenozoic mountain building on ocean geochemical cycles. *Geology, 16,* 649-653.

Stone, J. (1998). A rapid fusion method for separation of beryllium-10 from soils and silicates. *Geochemica et Cosmochimica Acta. 62,* 555-561.

Trodick, C.D. (2011). *In situ and meteoric $^{10}$Be concentrations of fluvial sediment collected from the Potomac River Basin.* (MS thesis). University of Vermont, Burlington.

Vance, D., Teagle, D., & Foster, G. (2009). Variable Quaternary chemical weathering fluxes and imbalances of marine geochemical budgets. *Nature, 458,* 493-496.

von Blanckenburg, F., Bouchez, J., & Wittmann, H. (2012). Earth surface denudation and weathering from the $^{10}$Be (meteoric)/$^{9}$Be ratio. *Earth and Planetary Science Letters, 351*, 295-305.

von Blanckenburg, F., & Bouchez, J. (2014). River fluxes to the sea from the ocean's $^{10}$Be/$^{9}$Be ratio. *Earth and Planetary Science Letters, 387,* 34-43.

von Blanckenburg, F., & Schuessler, J.A. (2014). Element cycling in the critical zone as viewed by new isotope tools. *Procedia Earth and Planetary Science, 10,* 173-178.

von Blanckenburg, F., Bouchez, J., Ibarra, D., & Maher, K. (2015). Stable runoff and weathering fluxes into the oceans over Quaternary climate cycles. *Nature Geoscience*, *8,* 538-542.

Willenbring, J., & von Blanckenburg, F. (2010). Meteoric cosmogenic beryllium-10 adsorbed to river sediment and soil: applications for earth-surface dynamics. *Earth Science Rev*iews, *98,* 105-122.

Wittmann, H., von Blanckenburg, F., Bouchez, J, Dannhaus, N., Naumann, R., Christl, M., & Gaillardet, J. (2012). The dependence of meteoric $^{10}$Be concentrations on particle size in Amazon River bed sediment and the extraction of reactive $^{10}$Be/$^{9}$Be ratios. *Chemical Geology, 318,* 126-138.

# CHAPTER 2: BACKGROUND AND LITERATURE SURVEY

## 2.1. Production of cosmogenic $^{10}$Be (*in situ* and meteoric)

High-energy and charged atomic nuclei, electrons, positrons, and subatomic particles, called cosmic rays, are principally generated from galactic supernovas (Dunai, 2010). The energy of these particles is well above the binding energy of atomic nuclei, and cosmic rays can thus interact with atoms in Earth's atmosphere via spallation reactions that produce a nuclear cascade of secondary comic rays – high-energy neutrons, with lesser numbers of pions and muons (Dunai, 2010). $^{10}$Be is a cosmogenic radionuclide formed from the interaction of secondary cosmic rays with O, Mg, Si or Fe (Lal, 1988). The vast majority of $^{10}$Be is produced in the atmosphere, where $^{10}$BeO or $^{10}$Be(OH)$_2$ attaches to aerosols and is deposited to Earth's surface via precipitation or dry deposition processes (McHarque & Damon, 1991; Graly et al., 2011). $^{10}$Be formed in the atmosphere is called meteoric $^{10}$Be ($^{10}$Be$_{met}$). The concentration of $^{10}$Be$_{met}$ in soils and sediments is influenced by the sorption potential and specific surface area of particles, and therefore depends on environmental conditions that dictate the grain size and chemistry of the substrate (Takahashi et al., 1999; Willenbring & von Blanckenburg, 2010; Wittmann et al., 2012). The dependency of $^{10}$Be$_{met}$ concentrations on environmental conditions is an important difference between studies using $^{10}$Be$_{met}$ and studies using *in situ* $^{10}$Be.

Uncertainties surrounding the rate of $^{10}$Be$_{met}$ delivery and the strength of $^{10}$Be$_{met}$ sorption to soils and sediments have drawn many researchers to focus on *in situ*–produced cosmogenic nuclides. *In situ* $^{10}$Be ($^{10}$Be$_{is}$) is produced on earth's surface, where secondary cosmogenic neutrons and muons generate $^{10}$Be$_{is}$ that is trapped within a

mineral lattice (Lal, 1991). The physics of *in situ* cosmogenic nuclide production is well understood; nuclide production rates depend on latitude, elevation and solar modulation, and nuclide attenuation lengths are based on the penetrated mass of substrate (Lal & Peters, 1967; Lal 1991). Models of nuclide concentrations as a function of depth have been supported by several field studies (Brown et al., 1992; Gosse & Phillips, 2001; Balco et al., 2008). However, methodological constraints limit $^{10}Be_{is}$ measurements to areas where quartz-bearing rocks crop out and where sand-size quartz grains can be separated (Stone, 1998). Between the requirement for quartz mineralogy and the requirement for sand-size or greater sediment grains, some substrates are disqualified from $^{10}Be_{is}$ analysis, such as some soil samples, marine sediment cores, and lacustrine sediment cores (Bierman et al., 2002; Nishiizumi et al., 1986). As interest in quantifying earth surface processes expands, there has been renewed research into understanding the variables that influence $^{10}Be_{met}$ concentration in natural systems including rivers, soils, lakes, and oceans, so that $^{10}Be_{met}$ can be employed as a dating tool or denudation rate proxy, especially in environments where $^{10}Be_{is}$ analysis is not possible (Barg et al., 1997; Lebatard et al., 2008; Graly et al., 2011; Willenbring & von Blanckenburg, 2010; von Blanckenburg et al., 2012;2015; Sujan et al., 2015).

### 2.2. Inputs of $^{9}Be$, $^{10}Be_{met}$ and $^{10}Be_{is}$ to soils and watersheds

In order to quantify denudation rates using Be isotopes, the inputs of $^{10}Be_{met}$, $^{10}Be_{is}$, and $^{9}Be$ concentrations must be understood across variables such as elevation, latitude, precipitation regime, and, in the case of $^{9}Be$, bedrock lithology. This requires a

quantitative understanding of the cosmogenic radiation flux, the $^{10}Be_{met}$ delivery rate, the $^{9}Be$ concentration of parent bedrock, and the degree of bedrock and regolith weathering.

### 2.2.1 $^{10}Be_{is}$ production rates.

Production rates for $^{10}Be_{is}$ depend on irradiation conditions including altitude, latitude, and the degree of shielding, the sample's depth, the substrate's density, and the slope of the exposed surface (Lal, 1991; Nishizumi, 1986; Heimsath et al., 1997; Dunne et al., 1999; Dunne & Elmore, 2003). Quantifying the influence of these variables enables the calculation of soil production rates and soil denudation rates (Nishizumi et al., 1986; Bierman & Steig, 1996; Heimsath et al., 1997; Balco et al., 2008; Jungers et al., 2009). By combining studies of nuclide production rates and calculation schemes for surface exposure ages and denudation rates (Dunne, 1999; Dunai, 2000; Dunai, 2001; Desilets & Zreda, 2003; Lifton et al., 2005; Desilets et al., 2005; Lifton et al., 2008), Balco et al. (2008) developed an online calculator that converts nuclide abundances to exposure ages or basin-scale denudation rates. Calibration information regarding elevation, latitude, substrate thickness and density, and exposure geometry are included in the online CRONUS calculator (Balco et al., 2008).

### 2.2.2. $^{10}Be_{met}$ delivery rates.

$^{10}Be_{met}$ delivery rates are more difficult to quantify than $^{10}Be_{is}$ production rates because $^{10}Be_{met}$ deposition depends on irradiation conditions as well as precipitation regimes and atmospheric mixing rates (Lal, 1967; Heikkila, 2007; Graly et al., 2011). Though $^{10}Be_{met}$ concentrations in continuous ice and sediment layers indicate that $^{10}Be_{met}$ delivery rates are influenced by the solar modulation function and geomagnetic field strength, the integrated effect is minimal over kyr timescales (Field et al., 2006; Heikkila

et al., 2008; Willenbring & von Blanckenburg, 2010). In order to constrain $^{10}Be_{met}$ delivery rates in soils, Graly et al. (2011) integrated $^{10}Be_{met}$ concentrations in dated terrestrial soil profiles and compared these results to short-term measurements of $^{10}Be_{met}$ in precipitation. By measuring $^{10}Be_{met}$ inventories in dated soils and $^{10}Be_{met}$ concentrations in precipitation, they concluded that short-term $^{10}Be_{met}$ deposition rates predicted long-term deposition rates with uncertainties of 20 percent. Using dust-corrected $^{10}Be_{met}$ fallout data from around the globe, Graly et al. (2011) parameterized an empirical formula for $^{10}Be_{met}$ flux that is a function of mean annual precipitation (MAP) and latitude.

Several studies have considered the potential influence for $^{10}Be_{met}$ or $^{10}Be_{is}$ deposition via aeolian fluxes (Brown et al., 1992; Lal, 2007; Heikkia et al., 2008; Willenbring & von Blanckenburg, 2010). Because the half-life of $^{7}Be$ is short (53 days), it is possible to disentangle the contribution of directly deposited "primary" $^{10}Be_{met}$ from "recycled" $^{10}Be_{met}$ delivered via terrestrial dust inputs. Heikkia et al. (2008) found that dust corrected $^{10}Be_{met}$ data in two locations (the high altitude Jungfraujoch site in Switzerland and Dunidin, New Zealand) had from 6.2% to 16.1% recycled $^{10}Be_{met}$ concentrations, respectively. Though Brown et al. (1992) found that the largest component $^{10}Be_{met}$ flux to the oceans is associated with aeolian material, trends in ice cores indicated a less significant aeolian $^{10}Be_{met}$ flux (Lal, 2007). Using a technique that infers dust flux from measuring calcium concentrations (Lal, 2007), Willenbring & von Blanckenburg (2010) concluded that dust contributed less than 5% of total $^{10}Be_{met}$ flux to the Greenland ice during the Holocene and less than 20% of the total $^{10}Be_{met}$ flux during the highest dust flux times. These studies indicated that in climate regimes where $^{10}Be_{met}$ delivery is

primarily via rainfall, delivery rates for $^{10}Be_{met}$ are relatively consistent over time (Willenbring & von Blanckenburg, 2010; Graly et al., 2010).

Variation in the average $^{10}Be_{met}$ deposition rate could result from different historic rainfall regimes, and this uncertainty can sometimes be difficult to constrain (Pavich et al., 1986; Reusser et al., 2010; Ouimet et al., 2015). Ouimet et al. (2015) found that $^{10}Be_{met}$ inventories measured at six dated sites near the Boulder Creek Critical Zone Observatory, Front Range, Colorado resulted in calculations of $^{10}Be_{met}$ deposition rates that matched neither primary $^{10}Be_{met}$ deposition rates predicted by global latitude-based models nor regional precipitation-specific models. Previous analysis of soils in the Front Range suggested that long-term dust accumulation rates could not explain the high-end deviation from model predictions (Ouimet et al., 2015). Lower than expected $^{10}Be_{met}$ inventories in the older sites suggested either loss of $^{10}Be_{met}$ through physical denudation or selective removal of near-surface soil enriched in $^{10}Be_{met}$ (Ouimet et al., 2015). The authors suggested that the higher inventories may reflect the addition of $^{10}Be_{met}$ due to snowdrifts or interflow and proposed that the effective local $^{10}Be_{met}$ deposition rate is ~30 to 50% higher than predicted by global or annual precipitation- specific models. Reusser et al. (2010) similarly found that the integrated $^{10}Be_{met}$ inventory of a well-dated 4.1 m soil profile in New Zealand had lower $^{10}Be_{met}$ concentrations than expected given measurements of modern $^{10}Be_{met}$ concentrations in local rainfall. Reusser et al. (2010) suggested that either long-term precipitation and/or dust flux were less than contemporary values by ~ 30%. In all, studies of $^{10}Be_{met}$ fluxes indicate that local calibration of deposition rates may be important in $^{10}Be_{met}$ studies around the globe.

### 2.2.3. Sources of $^{9}$Be to soils and sediments.

Nearly all the Be in soils, sediments, and bedrock is $^{9}$Be, the only stable isotope of Be. In soil systems, weathering processes partially dissolve $^{9}$Be from primary minerals ($^{9}Be_{min}$) (Graly et al., 2010; Bacon et al., 2012; von Blanckenburg et al., 2012). The released $^{9}$Be either sorbs onto the mineral surface, is incorporated into precipitates that frequently compose grain coatings ($^{9}Be_{reactive}$), or is dissolved into water ($^{9}Be_{diss}$) (von Blanckenburg et al., 2012; Wittmann et al., 2012).

Total $^{9}$Be concentrations generally range from 1-15 ppm in upper crust materials (Veselý et al., 2002) and the global average concentration of Be in bedrock estimated to be 2.5 ppm (Grew et al., 2002; von Blanckenburg et al., 2012). The US Department of Health and Human Services' summary of trace element concentrations in surficial materials found that $^{9}$Be concentrations of soils (average US concentration of 0.6 ppm), surface water (average US concentration of 0.2 ppm), and air (average US concentration of 0.03 ng/m$^3$) are much lower than $^{9}$Be concentrations of bedrock (Smith et al., 2002).

$^{9}$Be concentrations in the reactive or dissolved phase are related to the $^{9}$Be abundance of the local bedrock. Brown et al. (1992) collected suspended sediments and water samples from a group of acidic and intensely weathered tributaries to the Amazon River, finding that $^{9}Be_{diss}$ concentrations in river water spanned over two orders of magnitude (45 to 5800 pM) and reflected regional geology. Brown et al. (1992) measured higher concentrations of $^{9}Be_{diss}$ in tributaries draining basins dominated by granites and lower concentrations in tributaries that drained catchments with mafic intrusions or carbonate lithologies. The study concluded that the major controls on $^{9}Be_{reactive}$ and $^{9}Be_{diss}$ were the concentration of $^{9}$Be in the bedrock of the watershed and the degree of sorption of $^{9}$Be to

particle surfaces, with the relative influence of these controls determined by the extent to which river water interacted with flood plain sediments and the pH of river water. This study suggested that $^{9}Be$ concentrations of parent material could influence $^{9}Be_{reactive}$ concentrations in sediment grain coatings and river water in conjunction with geomorphic and geochemical conditions. Despite the variation of $^{9}Be$ concentration in parent materials (bedrock and regolith), many use the simplifying assumption that the average $^{9}Be$ concentration of unaltered bedrock for the source area for a study is the same as the global mean crustal abundance of $^{9}Be$ (Grew, 2002; Lebatard et al., 2008; Kabata-Pendias & Szteke, 2015; von Blanckenburg et al., 2012). This assumption is likely most valid in study areas with heterogeneous bedrock or bedrock that has the mean global crustal abundance of $^{9}Be$ (von Blanckenburg et al., 2012).

There are several trends in $^{9}Be$ concentration by rock and mineral types. $^{9}Be$ is incompatible during crustal petrogeneis, and is thus enriched in highly differentiated igneous rocks; granitoids have an average Be concentration of 3.1 ± 1.5 ppm while mafic rocks have an average Be concentration of 0.6 ± 0.4 ppm (von Blanckenburg et al., 2012). In natural systems, several studies have indicated that Be preferentially sorbs to clay minerals (Meehan & Smythe, 1967; You et al., 1989; Kabata-Pendias & Szteke, 2015) and percentage clay composition correlates to maximum $^{10}Be_{met}$ concentrations in many published soil profiles (Pavich et al., 1984; Bacon et al., 2012; Jungers et al., 2009; Graly et al., 2010). This trend is likely due to the physical and chemical characteristics of clay minerals. Clay minerals have greater surface area per unit mass due to their platy structure and high specific surface area. Clay minerals also have a wide range of cation exchange capacities, which vary by mineral from 3 to 150 meq/100g dry weight

(vermiculite has the highest cation exchange capacity), compared to 1 to 2 meq/100g for feldspars and quartz and 4 meq/100g for hydrous oxides of aluminum and iron (Birkeland, 1999). Be concentrations in metamorphic rocks are not influenced by increasing metamorphic grade and metamorphic rocks with clay-rich protoliths generally have high Be concentrations; metabauxites tend to have between 5 and 10 ppm Be (Grew, 2002). Such variation in the Be concentration of bedrock and mineral grains is significant because different compositions of parent material that form soils will result in regional differences in $^{9}Be_{diss}$, $^{9}Be_{reactive}$, and $^{9}Be_{min}$ concentrations.

### 2.3. $^{10}Be_{met}$ and $^{9}Be_{reactive}$ sorption and remobilization in soils and sediments

Landscapes are frequently mantled by regolith and soil, which are comprised of primary minerals, secondary weathering products, organic matter from vegetation, aerosols introduced with rainfall, and particles carried by the wind (Birkeland, 1999). Soil and regolith shields the underlying bedrock from cosmic radiation, subjecting individual sediment grains to different cosmic ray exposure histories and a differing proximity to $^{10}Be_{met}$ sources such as rainwater and dust. $^{10}Be_{met}$, $^{9}Be_{reactive}$, and $^{10}Be_{is}$ must be mixed via chemical or mechanical processes for the Be inventory to be homogenized in the soil profile (Monaghan et al., 1983; Jungers et al., 2009; Bacon et al., 2010; von Blanckenburg et al., 2012).

The ability for $^{9}Be_{reactive}$ to migrate upward from the weathering front and for $^{10}Be_{met}$ to migrate downward from the surface depends on the chemistry of the soil and the degree of physical mixing (Birkeland, 1999; Gabet et al., 2003; Jungers et al., 2009). Dissolved compounds and colloids can move with pore water until changing chemical

conditions or dehydration causes them to precipitate out of solution or sorb to available sites on mineral grains. Slight changes in salinity of pore water can cause organic material and iron compounds to flocculate (Mattock, 1954). Changes in pH can cause chelating agents to dissociate from metals, also inducing precipitation (Birkeland, 1999). Ions and particles can also be transferred upward via capillary forces, evapotranspiration, and biological activity (e.g. plants uptake ions and release them back to the surface in litterfall). Physical mixing processes such as burrowing and tree throw mix mineral grains throughout the soil column (Jungers et al., 2009; Birkeland, 1999).

The degree to which $^{10}Be_{met}$ and $^{9}Be$ dissolve into the surrounding water depends on the strength of the interaction between Be compounds and the solids in the soil or river system. The distribution coefficient ($K_d$) of Be (defined as the ratio of Be sorbed to the sediment or soil grains to Be dissolved in the aqueous phase) depends on pH, specific surface area, and grain mineralogy of the soils or sediment grains, which in turn depend on climate and bedrock lithology (Measures & Edmond, 1983; Hawley et al., 1986; You et al., 1989; You et al., 1994; Aldahan et al., 1998). Studies in the field and controlled laboratory experiments have used $^{9}Be$, $^{10}Be_{met}$, and $^{7}Be$ isotopes to determine the optimal conditions for high Be sorption to soils and sediments (Bourlès et al., 1988; Hawley et al., 1986; You et al., 1989).

Field and laboratory studies indicate that pH is an important control on the degree of Be solubility in a soil system (You et al., 1989; Measures & Edmund, 1983; Takahashi et al., 1999; Bacon et al., 2012). Experimentally observed trends and theoretical models show that $K_d$ of Be decreases 4 orders of magnitude as pH is lowered from 6 to 0 (You et al., 1989). In a field study, Measures & Edmond (1983) showed that the mobility of $^{9}Be$

in continental waters depended of pH, with acidic streams (pH < 6) being strongly enriched in Be compared to alkaline rivers sourced in predominantly carbonate bedrock catchments, though it is difficult to disentangle the effect of low parent $^{9}Be$ concentration in carbonates (average $^{9}Be$ concentration of 0.57 ppm) from the effect of decreased mobility in more basic conditions (Grew, 2002). In a another field study, Brown et al., (1992) found that dissolved $^{9}Be$ concentrations in highly acidic (~pH 4 river water) Rio Negro represented ~65 percent of total $^{9}Be$ in the watershed, indicating the acidic conditions in the watershed contributed to Be dissolution from soil and sediment grains.

Organic matter readily complexes with Be ions, influencing Be mobility in soils. Above pH 5, organic ligands can remain deprotonated and available to form organometallic complexes with cations (Birkeland, 1999). Organic-rich soils in strongly acidic to neutral conditions have lower Be mobility because Be can be sequestered in organometallic $Be^{2+}$ complexes that have a strong affinity for positively charged Fe-oxy-hydroxides, Al hydroxides, and clay minerals (Barg et al., 1997; Bacon et al., 2010; Willenbring & von Blanckenburg, 2010; Wittmann et al., 2012). Takahashi et al. (1999) found that in soils with pH between 3 and 11, nearly all Be takes the form of the hydroxylated species ($Be(OH)_x^{-n}$). $Be(OH)_x^{-n}$ humate complexes readily sorb to positively charged crystalline oxide or amorphous oxy-hydride surfaces (Takahashi et al., 1999). Consequently, Takahashi et al. (1999) observed that when dissolved $Be^{2+}$ (pH 7.5) was mixed with humic acids in the presence of kaolinite, over 70% of Be was adsorbed to the kaolinite in the form of hydroxylated Be humate complexes. These studies indicate that if significant concentrations of organic acids are present, Be will remain adsorbed to the crystalline oxide or amorphous oxy-hydride surfaces, even at relatively low pH.

At a given pH, $K_d$ also varies greatly depending on the mineralogy of the grain. Aldahan et al. (1998) show that at pH 7, the amount of Be sorbed to biotite is up to 40 times higher than the amount of Be sorbed to albite. This result can partly be explained by the higher specific surface area of biotite, which often results in enhanced ion exchange capabilities (Aldahan et al., 1998; Birkeland, 1999). Aldahan et al., 1998). Biotite has a specific surface area that is approximately 21 times greater than albite for the grain size fraction from 20-63 mm, and 110 greater than albite for the grain size fraction from 63-124 mm (Aldahan et al., 1998). Differences in the mineral structures of albite and biotite also contribute to their different $K_d$. The easily leachable cations from interlayer and octahedral layers of biotite (compared to tetrahedral rings of albite) and the relative ease with which biotite is weathered in acidic solutions provide more available sites for Be absorption (Acker & Bricker, 1992). In a study of the sorption potential of Be to various substrates, You et al. (1989) determined that man-made $Mn0_2$ and *in situ* weathering products of andesite have the highest $K_d$ (more than $1 \times 10^6$), while most mud, silt, and clay sediments have a $K_d$ on the order of $10^5$.

Several studies have found that the amount of Fe and Al associated with grains correlates to the $^9Be_{reactive}$ concentration (Olsen et al., 1986; Jungers et al., 2009; Taylor et al., 2012; Wittmann et al., 2012). Jungers et al. (2009) found that $^{10}Be_{met}$ is correlated to citrate-bicarbonate-dithonite extractable aluminum concentrations ($R^2 = 0.65$), supporting the hypothesis that Be is co-precipitated with Al oxides. Using a sequential extraction leaching procedure on soils experimentally exposed to $^7$Be tracer in artificial rainwater, Taylor et al. (2012) found that soil-sorbed $^7$Be is strongly associated with the reducible fraction of the soil (42–62%) and that no detectable $^7$Be was extracted by the artificial

rainwater solution (pH 5.6) from experimental soils. These findings indicate that $^{7}Be$ is a largely immobile a tracer under common, oxic field conditions and reducible phases are thermodynamically favorable for $^{7}Be$. Where reducing conditions occur, there is a potential for Be concentrations in soils and sediments to decrease due to metal oxide dissolution from grain coatings (Taylor et al., 2012).

The degree to which Be cycles through the biosphere is not well constrained (Kabata-Pendias & Szteke, 2015; Veselý et al., 2002). The similar reactivity of Be and other common biologically relevant elements such as Mg, Ca, and Al has been used to explain why Be is incorporated into some organic materials. Like Mg and Ca, Be occurs naturally in the +2 oxidation state, and similar to $Al^{3+}$, $Be^{2+}$ has a high charge to ionic radius ratio. These similar physical characteristics could allow for $Be^{2+}$ to compete with $Mg^{2+}$, $Ca^{2+}$, and $Al^{3+}$ in plant nutrient cycling mechanisms (Willenbring et al., 2010; Conyers, 2014).

Most studies show that unlike heavy metals such as Pb, Be does not bioaccumulate significantly (Kabata-Pendias & Szteke, 2015). Meehan & Smythe (1967) found that the overall uptake of Be by living organisms is low, even in acidic soils where Be may be more mobile. Other research, however, shows that some plants absorb significant quantities of Be from the soil (Lundberg et al., 1983; Fishein et al., 1884; Veselý et al., 2002). Conyers (2014) reported $^{10}Be_{met}$ concentrations of the trees and surrounding soils in Martell Experimental Forest, Indiana. The study found that Hickory wood samples contained ~0.38 ppm $^{10}Be_{met}$ by dry weight in wood, and ~2.0 ppm $^{10}Be_{met}$ in fallen leaves, while the concentration of $^{10}Be_{met}$ in the surrounding soil was less than 0.2 ppm. These findings indicate that Hickory trees bioaccumulate Be, with tree litter acting as a mechanism for cycling Be through the soil column.

The high Be concentrations in coal also indicate that Be may bioaccumulate, or at least have a strong affinity for organic matter (Vesleý et al., 2002). Be concentrations in coal are commonly measured between 0 and 100 ppm, although concentrations as high as 1,000 ppm have also been observed (Veselý et al., 2002; Fishbein, 1984). Lundberg et al. (1983) found that handpicked organic material (partially decayed leafs, twigs, and bark) out of lacustrine sediment cores was greatly enriched in Be, with the organic containing ~5 ppm $^{9}$Be and 10 dpm/kg $^{10}Be_{met}$ and the bulk sediment containing from less than 0.1 ppm to 2 ppm $^{9}$Be and 2.7 dpg/kg $^{10}Be_{met}$. On balance, these studies indicate that biological processes may be significant in mobilizing Be throughout the soil column and that organic material may sequester Be in biogeochemical systems.

Another important consideration in determining the capacity for Be sorption in natural systems is the rate of sorption reactions. You et al. (1989) found that adsorption of Be onto soil is a two-stage process, with the second stage ~1,000 times slower than the first. The reaction curve of Be adsorption over time suggests that a steady state is quickly established for the first stage, which likely represents Be adsorbing to easily accessible exchange sites. The second part of the curve has a shallower slope and likely represents the stage at which exchanged Be slowly diffuses towards less accessible sites (You et al., 1989). Nyffeler et al. (1984) found similar trends to You et al. (1989) for Be adsorption kinetics in ocean sediment and seawater, and calculated the reaction rate constants for this kinetic model with a fast equilibrium stage followed by a slower adsorption stage. Understanding of these rate constants is important for interpreting Be data; in climates that experience monsoons or other or other high water discharge events, $^{10}Be_{met}$ may not

have time to sorb to soils and suspended sediments may not have time to equilibrate with dissolved Be in rivers (Nyffler et al., 1984; You et al., 1989).

In summary, the retention of Be in soils and sediments varies significantly by location. Even in locations where mineralogy, pH and redox conditions indicate that $K_d$ for Be will be large, the equilibrium rate for sorption reactions may be slow, adding to the spatial and temporal variability of Be dynamics. Due to the possibility of $^{10}Be_{met}$ remobilization via a variety of processes, for most applications it is necessary to normalize $^{10}Be_{met}$ concentrations to another element with similar reactivity such that remobilization occurs for both species. Because $^{9}Be$ has the same chemical reactivity as $^{10}Be$, most researchers have chosen to normalize with an operationally defined fraction of $^{9}Be_{reactive}$ that is thought to have the same speciation as $^{10}Be_{met}$ in soils and sediments (Bourlès et al., 1989; Barg et al., 1997; von Blanckenburg et al., 2012; Bacon et al., 2012).

### 2.4. $^{10}Be_{met}/^{9}Be_{reactive}$ and $^{10}Be_{is}$ as a tracers of mass in soils and fluvial sediments

There are several models that have been proposed to estimate site-specific soil denudation rates and integrated basin-scale denudation rates from $^{10}Be_{is}$ or $^{10}Be_{met}/^{9}Be_{reactive}$ concentrations in fluvial sediments and soils (Pavich et al., 1984; Pavich et al., 1986; Lal, 1991; Bierman & Steig, 1996; Brown et al., 1998, Heisinger & Nolte, 2000; Wittmann et al., 2012). Calculating quantitative denudation rates from these models requires assumptions about the ways that Be isotopes are influenced by bedrock weathering, soil development, and transport of grains from slopes and through fluvial systems.

An important implicit assumption in the models determining basin-scale denudation rates from $^{10}Be_{is}$ or $^{10}Be_{met}/^{9}Be_{reactive}$ is that the sampled grains are representative of the total sediment or soil in the system; in other words, it is assumed that the soil profile is well-mixed (Bierman & Steig, 1996; Lal, 1991) and that sediment is derived from the entire drainage basin. Observing how $^{10}Be_{is}$, $^{10}Be_{met}$ and $^{9}Be_{reactive}$ concentrations change with depth can provide information about relative rates of physical mixing compared to remobilization in biogeochemical processes.

The total inventory of $^{10}Be_{is}$ in stable or eroding regolith profiles provides an estimate of the duration of time over which $^{10}Be_{is}$ has accumulated. If it is assumed that regolith denudation occurs at the same pace as regolith production (the soil is in a steady state), the inventory of $^{10}Be_{is}$ in a regolith profile can be related to the denudation rate (Pavich et al., 1984;1986; Brown et al., 1988). Because $^{10}Be_{is}$ is incorporated into the mineral matrix of grains, models for $^{10}Be_{is}$ mixing need only be concerned with physical processes of redistributing mineral grains throughout the soil column. Most studies measuring $^{10}Be_{is}$ in soil profiles have shown that the concentration of $^{10}Be_{is}$ is roughly uniform above the soil-saprolite boundary or above the regolith, indicating that the upper section of the soil column is well-mixed via biological processes like tree throw or animal burrowing on millennial timescales (Brown et al., 1995; Nichols et al., 2002; Jungers et al., 2009; Fulop et al., 2015). The uniform concentration with depth suggests that a soil or sediment sample is representative of the nuclide inventory, as long as it is sourced from within the mixed region of the profile. The assumption of uniform $^{10}Be_{is}$ distribution in the mixed zone of a soil profile allows $^{10}Be_{is}$ concentrations to be used in conjunction with the

CRONUS calculator to determine $^{10}Be_{is}$-derived basin scale denudation rates from fluvial sediments (Balco et al., 2008; Portenga & Bierman, 2011).

Many recent studies of $^{10}Be_{met}/^{9}Be_{reactive}$ ratios (Barg et al., 1997; Lebatard et al., 2008; Willenbring & von Blanckenburg, 2010; Graly et al., 2011; von Blanckenburg et al., 2015; Sujan et al., 2015) assume that $^{10}Be_{met}$, $^{10}Be_{is}$, and $^{9}Be_{reactive}$ are mixed in the soil system on timescales faster than would be sensitive to millennial scale denudation rates. This assumption is supported for $^{10}Be_{is}$ and $^{10}Be_{met}$ in a study by Jungers et al. (2009), where researchers observed that $^{10}Be_{is}$ profiles were well-homogenized with depth and $^{10}Be_{met}$ profiles increased in concentration with depth. This trend suggests that $^{10}Be_{met}$ equilibrates to chemical conditions of soil horizons at timescales faster than required for physical mixing processes that homogenize $^{10}Be_{is}$ concentrations. This study did not measure $^{9}Be_{reactive}$, which is primarily sourced from buried bedrock and regolith.

In order for $^{9}Be_{reactive}$ to effectively normalize $^{10}Be_{met}$ concentrations, it is important that both isotopes have equilibrated throughout the soil profile during mixing so that neither $^{9}Be_{reactive}$ nor $^{10}Be_{met}$ is preferentially leached or sorbed at various depths. If $^{10}Be_{is}$ or $^{10}Be_{met}/^{9}Be_{reactive}$ is not constant with depth, the weathering regime in the sub catchment (e.g. sheetwash instead of landsliding) may influence the $^{10}Be_{met}$, $^{9}Be_{reactive}$, or $^{10}Be_{is}$ concentrations of soils and fluvial sediments (Reusser & Bierman, 2010; Graly et al., 2010; Nichols et al., 2014). For example, if sediments were sourced from above the highest concentration $^{10}Be_{met}$ horizon or below the mixed layer for $^{10}Be_{is}$, analysis of the corresponding fluvial sediments would overestimate denudation rates (Bierman & Steig, 1996; Reusser & Bierman, 2010).

Measurements of $^{10}Be_{met}$ soil profiles frequently have mid-depth bulges in $^{10}Be_{met}$ concentration that correspond to horizons with high clay content and/or small grain size (Pavich et al., 1984; Bacon et al., 2012; McKean et al., 1993; Ouimet et al., 2015). Though varied biogeochemical conditions in a soil profile also influence $^{9}Be_{reactive}$ concentrations, not many studies have sampled $^{9}Be_{reactive}$ soil profiles and methods of extracting $^{9}Be_{reactive}$ vary. However, two studies of $^{9}Be_{reactive}$ profiles do not observe the similar trends between $^{9}Be_{reactive}$ and $^{10}Be_{met}$ with depth (Bacon et al., 2012; Barg et al., 1997). A18 m deep soil profile of $^{10}Be_{met}$ and hydroxylamine hydrochloride-extractable $^{9}Be$ from an Utisol showed that $^{9}Be_{reactive}$ concentrations increased steadily as sample depth approached the depth of the weathering front. In contrast, $^{10}Be_{met}$ concentrations had distinct bulges near the surface that correspond to soil horizons, and concentrations generally decreased with depth (Bacon et al., 2012). Due to differing pH, redox conditions, ion concentrations, organic content, biota, and mineralogy at depths in soil columns (Birkeland, 1999), there is potentially a different likelihood for $^{10}Be_{met}$ or $^{9}Be_{reactive}$ remobilization along the soil profile in this example (Pavich et al., 1984; Reusser et al., 2010; Bacon et al., 2012).

In the example of a highly weathered soil profile, the discrepancy between $^{10}Be_{met}$ and $^{9}Be_{reactive}$ distributions may reflect the fact that $^{9}Be_{reactive}$ is weathering from bedrock faster than it is mixed throughout the column, resulting in higher concentrations closer to the weathering front (Bacon et al., 2012). Barg et al. (1997) also found that $^{10}Be_{met}$ and $^{9}Be_{reactive}$ observed different trends in concentration at depth. Barg et al. (1997) separated the $^{9}Be_{reactive}$ and $^{10}Be_{met}$ into different phases using sequential extraction followed by a total digest of soil samples. In the “adsorbed phase,” which was extracted with 1M HCl,

$^{10}Be_{met}$ concentrations did not correlate to $^{9}Be$ concentrations and $^{10}Be_{met}/^{9}Be_{reactive}$ was variable with depth. The same trend was observed when considering $^{9}Be_{reactive}$ extracted from the authigenic clay fraction using oxalic acid. From these experiments, it is not clear if $^{9}Be_{reactive}$ mixes as quickly or thoroughly as $^{10}Be_{met}$ in soil columns. Despite differing trends along deep soil profiles, when considering the influence of isotope mixing on Be isotopes in fluvial sediments, it is most important that $^{10}Be_{met}$ and $^{9}Be_{reactive}$ are well mixed in the upper portion of the soil profile that (unless the predominate erosion regime is landsliding) is most likely to become fluvial sediment (Reusser & Bierman, 2010). More comparisons of $^{10}Be_{met}/^{9}Be_{reactive}$ and $^{10}Be_{is}$ concentrations in soil profiles and sediments may shed light on the respective timescales of $^{9}Be_{reactive}$ and $^{10}Be_{met}$ mixing and the effectiveness of $^{9}Be_{reactive}$ as a mechanism to normalize $^{10}Be_{met}$ against grain size dependencies and remobilization.

### 2.5. $^{10}Be_{met}/^{9}Be_{reactive}$-derived denudation rate model.

An objective of this study is to use a recently proposed mass balance model to estimate $^{10}Be_{met}/^{9}Be_{reactive}$-derived denudation rates and compare these rates to $^{10}Be_{is}$-derived denudation rates for the same samples (von Blanckenburg et al., 2012). In the mass balance model (eq. 1), $[^{9}Be]_{parent}$ is the $^{9}Be$ concentration in parent bedrock, $F_{met}^{^{10}Be}$ is the delivery rate of $^{10}Be_{met}$, $D$ is denudation rate, and $f_{reac}^{^{9}Be} + f_{diss}^{^{9}Be}$ is the fraction of $^{9}Be$ in the reactive phase and the fraction of $^{9}Be$ in the dissolved phase, which is simplified in this study as the *f.factor*.

$$D = \frac{F_{met}^{^{10}Be}}{[^{9}Be]_{parent} * (f_{reac}^{^{9}Be} + f_{diss}^{^{9}Be}) * \left( \frac{^{10}Be_{met}}{^{9}Be_{reactive}} \right)} \quad \text{eq. 1}$$

Studies using this equation have assumed that the concentration of parent bedrock is 2.5 ppm, the same as the global average Be concentration in crustal rocks (Grew, 2002; Veselý et al., 2002; von Blanckenburg et al., 2012; Bouchez et al., 2014). Von Blanckenburg et al. (2012) argue that for large catchments with heterogeneous lithologies such as the Amazon River, this assumption is unlikely to introduce significant error.

The *f.factor* can be thought of as the fraction of $^{9}Be$ that has been weathered from parent materials and is cycling through the biogeochemical system either as $^{9}Be_{diss}$ or $^{9}Be_{reactive}$. Von Blanckenburg et al. (2012) estimate the *f.factor* using modern sediment yield and river discharge as well as measured $^{9}Be_{reactive}$, $^{9}Be_{diss}$, and $^{9}Be_{min}$ concentrations. Using this method of calculating the *f.factor* for each sample and using 2.5 ppm as the $^{9}Be_{parent}$ concentration, von Blanckenburg et al. (2012) found that $^{10}Be_{met}/^{9}Be_{reactive}$-derived denudation rates are agreement within a factor of two with independent measures of denudation such as $^{10}Be_{is}$-derived denudation rates or modern river loads.

## CITATIONS


Acker, J.G., & Bricker, O.P. (1991). The influence of pH on biotite dissolution and alteration kinetics at low temperature. *Geochimica et Cosmocheimica acta, 56*, 3070-3092.

Aldahan, A., Ye, H.P., & Possnert, G. (1999). Distribution of beryllium between solution and minerals (biotite and albite) under atmospheric conditions and variable pH. *Chemical Geology, 156,* 209-229.

Bacon, A.R., Richter D., Bierman, P.R., & Rood, D.H. (2012). Coupling meteoric $^{10}$Be with pedogenic losses of $^{9}$Be to improve soil residence time estimates on an ancient North American interfluve. *Geology, 40,* 847-850.

Balco, G., Stone, J.O., Lifton, N.A. & Dunai. T.J. (2008). A quick and easily accessible means of calculating surface exposure ages or denudation rates from $^{10}$Be and $^{26}$Al measurements. *Quaternary Geochronology, 3,* 174-195.

Barg, E., Lal, D., Pavich, M.J., Caffee, M.W., & Southon, J.R. (1997). Beryllium geochemistry in soils; evaluation of $^{10}$Be/ $^{9}$Be ratios in authigenic minerals as a basis for age models. *Chemical Geology, 140,* 237-258.

Bierman, P., & Steig, E.J. (1996). Estimating rates of denudation using cosmogenic isotope abundances in sediment. *Earth Surface Processes and Landforms, 21* 125-139.

Bierman, P., Caffee M., Davis, P., Marsella, K., Pavich, M., Colgan, P., Mickelson, D., & Larsen, J. (2002). Rates and timing of earth surface processes from *in situ*-produced cosmogenic Be-10. *Reviews in Mineralogy and Geochemistry, 50,* 147-205.

Birkeland, P.W. (1999). *Soils and Geomorphology, 3rd edition*. Oxford: Oxford University Press.

Bourlès, D., Raisbeck, G.M., & Yiou, F. (1998). $^{10}$Be and $^{9}$Be in marine sediments and their potential for dating. *Geochimica et Cosmochimica Acta, 53,* 443-452.

Brown, L., Pavic, M.J., Hickman, R.E., Klein, J., & Middleton, R. (1988). Erosion of the eastern United States observed with $^{10}$Be. *Earth Surface Processes and Landforms, 13*, 441-457.

Brown, E.T., Edmond, J.M., Raisbeck, F.M., Bourlès, D.L., Yiou, F., & Measures, C.I. (1992). Beryllium isotope geochemistry in tropical river basins. *Geochimica et Cosmochimica Acta, 56,* 1607-1624.

Bouchez, J., Gaillardet, J., & von Blanckenburg, F. (2014). Weathering intensity in lowland river basins: from the Andes to the Amazon mouth. *Procedia Earth and Planetary Science, 10*, 280-186.

Chmeleff, J., von Blanckenburg, F., Kossert, K., & Jakob, D. (2010). Determination of the $^{10}$Be half-life by multicollector ICP-MS and liquid scintillation counting. *Nuclear Instruments and Methods in Physics Research, 268,* 192-199.

Conyers, G. (2014). *Cosmogenic beryllium cycling in a natural forest setting* (MS thesis). Perdue University, Indiana.

Crowley, J.W., Katz, R., Huybers, P., Langmuir, C.H., & Park, S. (2015). Glacial cycles drive variation in the production of oceanic crust. *Science, 347,* 1237-1240.

Delunel, R., van der Beek, P.A., Carcaillet, J., Bourlès, D.L., & Valla, P.G. (2010). Frost-cracking control on catchment denudation rates: Insights from in situ produced $^{10}$Be concentrations in stream sediments (Ecrins-Pelvoux massif, French Western Alps). *Earth and Planetary Science Letters, 293*, 72–83.

Desilets, D., & Zreda, M. (2003). Spatial and temporal distribution of secondary cosmic-ray nucleon intensities and applications to in situ cosmogenic dating. *Earth Planet. Sci. Lett.* 206, 21-42.

Desilets, D., Zreda, M., & Pradu, T. (2006). Extended scaling factors for *in situ* cosmogenic nuclides: New measurements at low latitude. *Earth and Planetary Science Letters, 246,* 265-276.

Dunai, T. (2000). Scaling factors for production rates of in situ produced cosmogenic nuclides: a critical reevaluation. *Earth and Planetary Science Letters, 176,* 157-169.

Dunai, T. (2001). Influence of secular variation of the geomagnetic field on production rates of *in situ* produced cosmogenic nuclides. *Earth and Planetary Science Letters, 193,* 197-212.

Dunai, T. (2010). *Cosmogenic Nuclides, Principles, Concepts and Applications in the Earth Surface Sciences*. Cambridge: Cambridge University Press.

Dunne, J., Elmore, D., & Muzikar, P. (1999). Scaling factors for the rates of production of cosmogenic nuclides for geometric shielding and attenuation at depth on sloped surfaces. *Geomorphology, 27,* 3-11.

Dunne, J., & Elmore, D. (2003). Monte Carlo simulations of low-energy cosmogenic neutron fluxes near the bottom of cliff faces. *Earth and Planetary Science Letters, 206,* 43-49

Elmore, D., & Phillips, F., (1987). Accelerator mass spectrometry for measurement of long-lived radioisotopes. *Science*, *236,* 543-550.

Fishbein, L. (1984). Overview of analysis of carcinogenic and/or mutagenic metals in biological and environmental samples. *International Journal of Environmental Analytical Chemistry, 12*, 113-170.

Fulop, R.H., Bishop, P., Fabel, D., Cook, G.T., Everest, J., Schnabel, C., Codilean, Q. T., & Xu, S. (2015). Quantifying soil loss with *in-situ* cosmogenic $^{10}$Be and $^{14}$C depth-profiles. *Quaternary Geology, 27,* 78-93.

Gabet, E.J., Reichman, O.J., & Seablooom, E. (2003). The effects of bioturbation on soil processes and hillslope evolution. *Annual Reviews in Earth and Planetary Science, 31,* 249 – 273.

Gosse, J.C., & Phillips, F.M. (2001). Terrestrial *in situ* cosmogenic nuclides: theory and application. *Quaternary Science Reviews, 20,* 1475-1560.

Graly, J.A., Bierman, P.R., Reusser, L.J., & Pavich, M.J. (2010). Meteoric $^{10}$Be in soil profiles - a global meta-analysis. *Geochimica et Cosmochimica Acta, 74,* 6814-6829.

Graly, J.A., Reusser, L.J., & Bierman, P.R. (2011). Short and long-term delivery rates of meteoric $^{10}$Be to terrestrial soils. *Earth and Planetary Science Letters, 302,* 329-336.

Grew, E.S. (2002). Beryllium in metamorphic environments (emphasis on aluminous compositions). *Reviews in Mineralogy and Geochemistry, 50,* 487-549.

Hawley, N., Robbins, J.A., & Eadie, B.J. (1986). The partitioning of $^{7}$beryllium in fresh water. *Geochimica et Cosmochimica Acta, 50,* 1127-1131.

Heikkila, U., Beer, J., & Alfimov, V. (2008). Beryllium-10 and beryllium-7 in precipitation in Dubendorf (440 m) and at Jungfraujoch (3580 m), Switzerland 1998-2005. *Journal of Geophysical Research, 113,* D11104.

Heisinger, B., & Nolte, E. (2000). *In situ* production of radionuclides: Exposure ages and erosion rates. *Nuclear Instruments and Methods in Physical Research B, 172,* 790-795.

Heimsath, A.M., Dietrich, W.E., Nishiizumi, K., & Finkel, R.C. (1997). The soil production function and landscape equilibrium. *Nature, 388,* 358-361.

Jungers, M.C., Bierman, P.R., Matmon, A., Nichols, K., Larsen, J., & Finkel, R. (2009). Tracing hillslope sediment production and transport with *in situ* and meteoric $^{10}$Be. *Journal of Geophysical Research, 114,* F04020.

Kabata-Pendias, A. & Szteke, V. (2015). *Trace Elements in Abiotic and Biotic Environments. 1st ed.*. Florida: Taylor & Francis Group, LLC.

Lal, D., & Peters, B. (1967). Cosmic ray produced radioactivity on the earth. *Handbuch der Physik*. Berlin: Springer.

Lal, D. (1988). *In situ*-produced cosmogenic isotopes in terrestrial rocks. *Annual Review of Earth and Planetary Science, 16,* 355-388.

Lal, D. (1991). Cosmic ray labeling of denudation surfaces: *in situ* nuclide production rates and denudation models. *Earth and Planetary Science Letters, 104,* 424-439.

Lal, D. (2007). Recycling of cosmogenic nuclides after their removal from the atmosphere; special case of appreciable transport of $^{10}$Be to polar regions by Aeolian dust. *Earth and Planetary Science Letters, 2007,* 177-187.

Lebatard, A.E., Bourlès, D.L. Duringer, P., Jolivet, M., Braucher, R., Carcaillet, J., Schuster, M., Arnaud, N., Monié, P., Lihoreau, F., Likius, A., Mackaye, H.T., Vignaud, P., & Brunet, M. (2008). Cosmogenic nuclide dating of Sahelanthropus tchadensis and Australopithecus bahrelghazali: Mio-Pliocene hominids from Chad. *Procedings of the National Academy of Sciences, 105,* 3226–3231.

Lifton, N., Bieber, J., Clem, J., Duldig, M., Everson, P., Humble, J., & Pyle R. (2005). Addressing solar modulation and long-term uncertainties in scaling secondary cosmic rays for *in situ* cosmogenic nuclide applications. *Earth and Planetary Science Letters, 239,* 140-161.

Lifton, N., Smart, D., & Shea, M. (2008). Scaling time-integrated *in situ* cosmogenic nuclide production rates using a continuous geomagnetic model. *Earth and Planetary Science Letters, 268,* 190-201.

Lundberg, L., Ticich, T., Herzog, G.F., Hughes, T., Ashley, G., Moniot, R.K., Tuniz, C., Kruse, T., & Savin, W. (1983). $^{10}$Be and Be in the Maurice River-Union Lake system of southern New Jersey. *Journal of Geophysical Res*earch*, 88,* 4498-4504.

Matmon, A., Bierman, P.R., Larsen, J., Southworth, S., Pavich, M., Finkel, R., & Caffee, M. (2003). Erosion of an ancient mountain range, the Great Smoky Mountains, North Carolina and Tennessee. *American Journal of Science*, *303,* 817-855.

Mattock, G. (1954). The hydrolysis and aggregation of the beryllium ion. *Journal of the American Chemical Society, 76,* 4835-4838.

McHarque, L.R., & Damon, P.E. (1991). The global beryllium-10 cycle. *Reviews in Geophysics, 29,* 141-158.

McKean, J., Dietrich, W.E., Finkel, R.C., Southon, J.R., & Caffee, M.W. (1993). Quantification of soil production and downslope creep rates from cosmogenic $^{10}$Be accumulations on a hillslope profile. *Geology, 22,* 343-346.

Measures, C.I., & Edmond, J.M. (1983). The geochemical cycle of $^{9}$Be: a reconnaissance. *Earth and Planetary Science Letters*, *66,* 101-110.

Meehan, W.R., & Smythe, L.E. (1967). Occurrence of beryllium as a trace element in environmental materials. *Environmental Science Technology, 10,* 839-844.

Merrill, J.R., Lyden, E., Honda, M., & Arnold, J.R. (1959). The sedimentary geochemistry of the beryllium isotopes. *Geochimica et Cosmochimica Acta, 18,* 108-129.

Monaghan, M.C., Krishnaswami, S., & Thomas, J.H. (1983). $^{10}$Be concentrations and the long-term fate of particle-reactive nuclides in five soil profiles from California, *Earth and Planetary Science Letters, 65,* 51-60.

Neilson, T.B. (2015). *Using long- and short-lived sediment-associated isotopes to track denudation and sediment movement through rivers in Yunnan, SW China.* (MS thesis). University of Vermont, Burlington.

Nichols, K.K., Bierman, P.R., & Rood, D.H. (2014). $^{10}$Be constrains the sediment sources and sediment yields to the Great Barrier Reef from the tropical Barron River catchment, Queensland, Australia. *Geomorphology*, *224,* 102-110.

Nishiizumi, K., Lal, D., Klein, J., Middleton, R., & Arnold, J.R. (1986). Production of $^{10}$Be and $^{26}$Al by cosmic rays in terrestrial quartz *in situ* and implications for denudation rates. *Nature, 319,* 1468-1470.

Nishiizumi, K., Imamura, M., Caffee, M.W., Southon, J.R., Finkel, R.C., & McAninch, F. (2007). Absolute calibration of $^{10}$Be AMS standards, *Nuclear Instruments and Methods in Physical Research B, 258,* 403-413.

Nyffeler, U.R., Li, Y.-U., & Santschi, P.H. (1984). A kinetic approach to describe trace-element distribution between particles and solution in natural aquatic systems. *Geochimica et Cosmochimica Acta, 48*, 1513-1522.

Olsen, C.R., Larsen, I.L., Lowry, P.D., Cutshall, N.H., & Nichols, M.M. (1986). Geochemistry and deposition of Be-7 in river-estuarine and costal waters. *Journal of Geophysical Research-Oceans, 91,* 896-908.

Ouimet, W., Dethier, D., Bierman, P., Wyshnystzky, C., Shea, N., & Rood, D. (2015) Spatial and temporal variations in meteoric $^{10}$Be inventories and long-term deposition rates, Colorado Front Range. *Quaternary Science Reviews, 109*, 1-12.

Pavich, M.P., Brown, L., Klein, J., & Middleton, R. (1984). $^{10}$Be accumulation in a soil chronosequence. *Earth and Planetary Science Letters, 68,* 198-204.

Pavich, M.P, Brown, L., Harden, J., Klein, J., & Middleton, R. (1986). $^{10}$Be distribution in soils from Merced River terraces, California. *Geochimica et Cosmochimica Acta, 50,* 1727-1735.

Portenga, E.W., & Bierman P.R. (2011). Understanding Earth's eroding surface with $^{10}$Be. *GSA Today, 21,* 4-10.

Raymo, M.E., Ruddiman, W.F., & Froelich, P.N. (1998). Influence of late Cenozoic mountain building on ocean geochemical cycles. *Geology, 16,* 649-653.

Reusser, L., Graly, J., Bierman, P., & Rood, D. (2010). A long-term meteoric $^{10}$Be accumulation rate in soil. *Geophysical Research Letters, 37,* L19403.

Reusser, L., & Bierman, P.R. (2010). Using meteoric $^{10}$Be to track fluvial sand through the Waipaoa River basin, New Zealand. *Geology, 38,* 47-50.

Smith, C., Ingerman, L., & Amata, R. (2002). U.S. Department of Health and Human Services. *Toxicological profile for beryllium.* Atlanta Georgia: Government Printing Office.

Stone, J. (1998). A rapid fusion method for separation of beryllium-10 from soils and silicates. *Geochemica et Cosmochimica Acta. 62,* 555-561.

Šujan, M., Braucher, R., Kováč, M., Bourlès, D.L., Rybár, S., Guillou, V., & Hudáčková, N. (2015). Application of the authigenic $^{10}$Be/$^{9}$Be dating method to Late Miocene-Pliocene sequences in the northern Danube Basin (Pannonian Basin System): confirmation of heterochronous evolution of sedimentary environments. *Global and Planetary Change, 137,* 35-53.

Takahashi, M., Ambe, S., Makide, Y., & Ambe, F. (1999). Comparison of adsorption behavior of multiple inorganic ions on kaolinite and silica in the presence of humic acid using the multi-tracer technique. *Geochimica et Cosmochimica Acta, 63l,* 815-836.

Taylor, A., Blake, W.H., Couldrick, L., & Keith-Roach, M.J. (2012). Sorption behavior of beryllium-7 and implications for its use as a sediment tracer. *Geoderma*, *187-188,* 16-23.

Trodick, C.D. (2011). *In situ and meteoric $^{10}$Be concentrations of fluvial sediment collected from the Potomac River Basin.* (MS thesis). University of Vermont, Burlington.

Vance, D., Teagle, D., & Foster, G. (2009). Variable Quaternary chemical weathering fluxes and imbalances of marine geochemical budgets. *Nature, 458,* 493-496.

Veselý J.S., Norton, A., Skřivan, P., Majer, V., Krám, P., Navrátil, T., & Kaste, J.M. (2002). Environmental chemistry of beryllium. *Reviews in Mineralogy and Geochemisty, 50,* 291-317.

von Blanckenburg, F., Bouchez, J., & Wittmann, H. (2012). Earth surface denudation and weathering from the $^{10}$Be (meteoric)/$^{9}$Be ratio. *Earth and Planetary Science Letters, 351*, 295-305.

von Blanckenburg, F., & Bouchez, J. (2014). River fluxes to the sea from the ocean's $^{10}$Be/$^{9}$Be ratio. *Earth and Planetary Science Letters, 387,* 34-43.

von Blanckenburg, F., & Schuessler, J.A. (2014). Element cycling in the critical zone as viewed by new isotope tools. *Procedia Earth and Planetary Science, 10,* 173-178.

von Blanckenburg, F., Bouchez, J., Ibarra, D., & Maher, K. (2015). Stable runoff and weathering fluxes into the oceans over Quaternary climate cycles. *Nature Geoscience*, *8,* 538-542.

Willenbring, J., & von Blanckenburg, F. (2010). Meteoric cosmogenic beryllium-10 adsorbed to river sediment and soil: applications for earth-surface dynamics. *Earth Science Rev*iews, *98,* 105-122.

Wittmann, H., von Blanckenburg, F., Bouchez, J, Dannhaus, N, Naumann, R., Christl, M., & Gaillardet, J. (2012). The dependence of meteoric $^{10}$Be concentrations on particle size in Amazon River bed sediment and the extraction of reactive $^{10}$Be/$^{9}$Be ratios. *Chemical Geology, 318,* 126-138.

You, C.-F., Lee, T., & Li, Y.H. (1989). The partition of Be between soil and water. *Chemical Geology, 77,* 105-118.

You, C.-F., Morris, J., Gieskes, J., Rosenbauer, R., Zheng, S., Xu, X., Ku, T., & Bischoff, J. (1994). Mobilization of beryllium in the sedimentary column at convergent margins *Geochimica et Cosmochimica Acta, 58,* 4887-4897.

*For submission to Geochimica et Cosmochimica Acta*
Wednesday, May 18, 2016

# Towards a better understanding of Beryillium-10 and Beryllium-9 dynamics in river sediments

Emily Sophie Greene*, Paul Bierman, Nicolas Perdrial

University of Vermont, Department of Geology, Burlington, Vermont, 05405-1758
*Corresponding author: esgreene@uvm.edu

Keywords: Beryllium-10, metal sorption, cosmogenic, denudation rates, erosion rates

## Abstract

The cosmogenic nuclide $^{10}Be$ ($t_{1/2}$ = 1.39 my) is a tool for understanding rates of sediment generation and transport across a variety of spatial and temporal scales. Concentrations of *in situ* $^{10}Be$ are controlled by well-understood nuclear physics, physical mixing processes, and the denudation of regolith; in contrast, meteoric $^{10}Be$ concentrations are influenced by a combination of geomorphic, pedogenic, geochemical, and biological processes. As a result, the concentration of meteoric $^{10}Be$ in detrital material reflects biogeochemical processes in watersheds.

This study aims to understand the processes controlling meteoric $^{10}Be$ and $^{9}Be$ concentrations in fluvial sediments. We chemically characterize grain coatings (as the acid-extractable fraction) and substrate composition (by total digestion) of 202 fluvial sediment samples in which others have measured the concentration of *in situ* and meteoric $^{10}Be$. Samples were collected from seven study areas in China, North America, and Australia with diverse geological settings. To help understand the impact of geochemical and environmental processes on meteoric $^{10}Be$ concentrations, we performed a statistical analysis testing relationships between meteoric $^{10}Be$ and $^{9}Be$ in acid-extractable grain coatings, meteoric $^{10}Be/^{9}Be$ ratios, watershed characteristics, and major element compositions of grains and grain coatings. We also compared meteoric $^{10}Be/^{9}Be$-derived denudation rates calculated with a published mass balance model to *in situ* $^{10}Be$-derived denudation rates.

We find that HCl-extracted $^{9}Be$ is significantly correlated to total meteoric $^{10}Be$ in all but one study area, suggesting that the HCl method of $^{9}Be$ extraction from grain coatings does not attack $^{9}Be$ in mineral matrices and that meteoric $^{10}Be$ and $^{9}Be$ are mixed in soil

systems. Meteoric $^{10}$Be is also significantly correlated to the concentration of total acid-extractable Al, Fe and Mn in most, but not all study areas, indicating that meteoric $^{10}$Be is frequently associated with metal oxides and oxy-hydroxides in grain coatings. Study areas display a range of $^{9}$Be concentrations in grain coatings (0.06-4.18 μg/g) and mineral matrixes (0.03-3.76 μg/g); the average sum of $^{9}$Be concentrations in mineral grains and coatings between study areas varies from 0.72 ± 0.28 to 2.09 ± 1.12 μg/g. Meteoric $^{10}$Be/$^{9}$Be is significantly correlated ($p < 0.05$) to mean annual precipitation in four of seven study areas, but is only significantly correlated to total basin relief in two of seven study areas. We find that meteoric $^{10}$Be/$^{9}$Be-derived denudation rates have a central tendency that is similar to *in situ* $^{10}$Be-derived denudation rates (205 ± 226 t km$^{-2}$ yr$^{-1}$ and 202 ± 226 t km$^{-2}$ yr$^{-1}$, respectively) and are significantly correlated to *in situ* $^{10}$Be-derived denudation rates when considering all samples ($R^2 = 0.38$, $p < 0.01$), but only have $R^2 > 0.30$ and $p < 0.05$ in one of seven individual study areas. These findings suggest that while meteoric $^{10}$Be/$^{9}$Be in fluvial sediments is related to denudation rates, meteoric $^{10}$Be/$^{9}$Be also reflects the heterogeneity of $^{9}$Be concentrations in parent material, pedogenic processes that generate grain coatings, and modification of grain coatings during sediment transport.

## 1. Introduction

Recent realizations that earth surface processes can drive climate fluctuations and influence plate tectonics have reinvigorated research in geochemical tracers relevant to pedogenesis and denudation (Raymo et al., 1988; Vance et al., 2009; Crowley et al., 2015; von Blanckenburg et al., 2015). The cosmogenic isotope $^{10}$Be ($T_{1/2}$ = 1.39 Myr) has

been used to quantify the rates of earth surface processes such as sediment generation and transport over timescales of $10^3$-$10^6$ years (Lal, 1991; McKean et al., 1993; Gosse and Phillips, 2001; Bierman and Nichols, 2004; Portenga and Bierman, 2011). Over 99% of $^{10}$Be is formed in the atmosphere and delivered to landscapes via precipitation and dry deposition ($^{10}Be_{met}$), but a small portion of $^{10}$Be is produced and trapped *in situ* within mineral grains ($^{10}Be_{is}$) (Lal and Peters, 1967; Gosse and Phillips, 2001; Willenbring and von Blanckenburg, 2010). Unlike $^{10}Be_{is}$, which requires sand-size quartz grains for analysis, $^{10}Be_{met}$ can be measured in all types and grain sizes of substrates (Kohl and Nishiizumi, 1992; Stone, 1998).

$^{10}Be_{is}$ concentrations in fluvial sediments have been used to quantify millennial scale denudation rates around the world (Portenga and Bierman, 2011; Granger and Schaller, 2014), but grain size dependencies and reversible sorption limit the certainty of quantitative estimates of denudation rates and soil production rates using $^{10}Be_{met}$ (Brown et al., 1992; von Blanckenburg, 2005; Willenbring and von Blanckenburg, 2010; Graly et al., 2010). Improved understanding of $^{10}Be_{met}$ delivery rates (Field et al., 2006; Heikkila et al., 2008; Graly et al., 2011) along with the possibility of normalizing $^{10}Be_{met}$ against grain size dependencies, mineralogical dependencies, and remobilization processes with the stable isotope $^9$Be (Brown et al., 1992; Bacon et al., 2012; Wittmann et al., 2012; von Blanckenburg et al., 2012) has reinvigorated research into $^{10}Be_{met}$ as a tracer for sediment movement in both hillslope and fluvial systems (Jungers et al., 2009; West et al., 2013; von Blanckenburg et al., 2012; Campforts et al., 2015).

This study aims to understand better $^9$Be and $^{10}Be_{met}$ dynamics by chemically characterizing grain coatings and mineral matrices of fluvial sediment samples that have

known $^{10}Be_{met}$ concentrations, $^{10}Be_{is}$ concentrations, and $^{10}Be_{is}$-derived basin-scale denudation rates from previous studies (Table 1; Fig. 1) (Trodick, 2011; Portenga and Bierman, 2011; Nichols et al., 2014; Neilson, 2016). These data, combined with $^{10}Be_{met}$ and $^{10}Be_{is}$ measurements and watershed characteristics determined from elevation and precipitation geospatial data, can be used to draw conclusions about Be isotope dynamics in fluvial sediments from varied climatic, lithological, and tectonic settings.

## 2. Background

$^{10}$Be is a cosmogenic radionuclide formed by the interaction of secondary cosmic rays with O, Mg, Si, or Fe (Lal and Peters, 1967; Gosse and Phillips, 2001). The vast majority of $^{10}$Be is produced in the atmosphere, where $^{10}BeO$ or $^{10}Be(OH)_2$ attaches to aerosols and is deposited on Earth's surface via precipitation or dry deposition processes (Lal, 1988; McHarque and Damon, 1991; Graly et al., 2011).

The concentration of $^{10}Be_{met}$ in soils and sediments is influenced by the sorption potential and specific surface area of particles and their coatings, and therefore depends on environmental conditions that dictate the grain size and chemistry of the substrate and groundwater (Takahashi et al., 1999; von Blanckenburg, 2005; Willenbring and von Blanckenburg, 2010; Graly et al., 2010; Wittmann et al., 2012). Jungers et al. (2009) found that $^{10}Be_{met}$ is correlated to citrate-bicarbonate-dithonite extractable aluminum in soils ($R^2 = 0.65$), which supports the hypothesis that $^{10}Be_{met}$ is co-precipitated with Al in grain coatings. Sequential chemical extractions of fluvial sediments, marine sediments, and soils have found that $^{10}Be_{met}$ is also held in exchangeable, carbonate, and organic fractions of grain coatings (Barg et al., 1997; Bourlès et al., 1989; Wittmann et al., 2012).

In contrast, $^{10}Be_{is}$ is formed and trapped within mineral grain matrixes (Lal, 1991; Gosse and Phillips, 2001). This difference in the location of $^{10}Be$ formation, either in mineral grains ($^{10}Be_{is}$) or in the atmosphere ($^{10}Be_{met}$), has important implications regarding whether $^{10}Be$ data are interpreted as a tracer of sediment transport, as a proxy for hillslope erosion rates, or more broadly as a tracer of biogeochemical processes in fluvial systems (Fig. 2).

$^{9}Be$ is a stable, naturally occurring isotope of Be that is weathered from bedrock and regolith and mixed through the soil column by processes such as bioturbation, clay translocation, and dissolution (Barg et al., 1997; Bacon et al., 2012; von Blanckenburg et al., 2012). $^{9}Be$ in fluvial systems is found in mineral grains ($^{9}Be_{min}$), in water ($^{9}Be_{diss}$) and in reactive grain coatings ($^{9}Be_{reactive}$) (von Blanckenburg et al., 2012). Several studies have proposed that $^{9}Be_{reactive}$ in grain coatings may help in the interpretation of $^{10}Be_{met}$; the ratio of $^{10}Be_{met}$ to $^{9}Be_{reactive}$ diminishes the influence of grain size and remobilization processes if these factors are equally likely to affect either isotope (Brown et al., 1992; Barg et al., 1997; Bourlès et al., 1989; Bacon et al., 2012; Wittmann et al., 2012; von Blanckenburg et al., 2012). Understanding the variables that influence sorption of $^{10}Be_{met}$ and $^{9}Be_{reactive}$ to fluvial sediment grains in a variety of environments is important for interpreting $^{10}Be_{met}/^{9}Be_{reactive}$ data in fluvial systems. If $^{9}Be_{reactive}$ normalizes $^{10}Be_{met}$ against grain size dependencies and remobilization processes, $^{10}Be_{met}/^{9}Be_{reactive}$ could be a viable alternative to $^{10}Be_{is}$ for quantifying basin-scale denudation rates in areas where lithology or grain size makes $^{10}Be_{is}$ analysis impossible. A better understanding of $^{10}Be_{met}/^{9}Be_{reactive}$ could also lead to new applications for $^{10}Be_{met}$ as a tracer of biogeochemical processes in fluvial systems.

*2.1 $^{9}$Be geochemistry*

Total $^{9}$Be concentrations generally range from <1-15 μg/g in upper crustal materials (Meehan and Smythe, 1967; Veselý et al., 2002; Grew et al., 2002). $^{9}$Be is incompatible during crustal petrogenesis, and thus is enriched in more highly differentiated igneous rocks; granitoids have an average $^{9}$Be concentration of 3.1 ± of 1.5 μg/g while mafic rocks have an average $^{9}$Be concentration of 0.6 ± 0.4 μg/g (von Blanckenburg et al., 2012). Carbonate sediments have a mean $^{9}$Be concentration of 0.6 ± 0.2 μg/g (Stauidgel et al., 1998), which is less than the average of 4.0 ± 3.5 μg/g $^{9}$Be in unmetamorphosed pelitic rocks (Grew, 2002). $^{9}$Be concentrations in coal typically range from 0 to 100 μg/g, although concentrations as high as 1,000 μg/g have also been measured (Veselý et al., 2002; Fishbein, 1984). Several studies have indicated that Be preferentially sorbs to clay minerals, and pelagic clays contain 2-3 μg/g $^{9}$Be (Grew, 2002; Pavich et al., 1984; Graly et al., 2010). Such variation in the $^{9}$Be concentrations of parent materials is significant because different compositions of bedrock and regolith that form soils, and subsequently sediment grain coatings, will result in local and regional differences in $^{9}Be_{diss}$, $^{9}Be_{reactive}$, and $^{9}Be_{min}$ concentrations.

The influence of parent $^{9}$Be concentration on $^{9}Be_{diss}$ and $^{9}Be_{reactive}$ is shown in a study of $^{9}$Be and $^{10}Be_{met}$ in suspended sediments and river water from tributaries with variable bedrock lithology (Brown et al. 1992). Brown et al. (1992) collected suspended sediments and water samples from a group of acidic and intensely weathered tributaries to the Amazon River, finding that $^{9}Be_{diss}$ concentrations in river water spanned over two orders of magnitude (45 to 5800 pM) and reflected regional geology. Brown et al. (1992)

measured higher concentrations of $^{9}Be_{diss}$ in tributaries draining basins dominated by granites and lower concentrations in tributaries draining catchments with carbonate lithologies or mafic intrusions. Brown et al. (1992) concluded that the major controls on $^{9}Be_{reactive}$ and $^{9}Be_{diss}$ concentrations were the abundance of $^{9}Be$ in the rocks of the watershed and the extent to which $^{9}Be$ adsorbed onto particle surfaces, with the relative influence of these controls determined by the extent to which river water interacted with flood plain sediments and the pH of river water. This shows that $^{9}Be$ concentrations in parent material can influence $^{9}Be_{reactive}$ concentrations in conjunction with geomorphic and geochemical conditions of the river system.

### *2.2 $^{10}Be_{met}$ and $^{9}Be_{reactive}$ concentrations in soil profiles*

$^{9}Be_{reactive}$ is primarily sourced from buried bedrock and regolith, while $^{10}Be_{met}$ is deposited on exposed surfaces. Dust can also contribute $^{10}Be_{met}$ and $^{9}Be$ to soil profiles, and the significance of aeolian flux to total $^{9}Be$ or $^{10}Be_{met}$ concentrations varies by region and climate (Lal, 2007; Heikkila, 2008; Willenbring and von Blanckenburg, 2010; Graly et al., 2011). In order for $^{9}Be_{reactive}$ to effectively normalize $^{10}Be_{met}$ concentrations, $^{10}Be_{met}$ and $^{9}Be_{reactive}$ must be mixed throughout the soil column. The rapidity of $^{10}Be_{met}$ remobilization is well demonstrated by the soils data of Jungers et al. (2009), which showed uniform $^{10}Be_{is}$ concentrations in soil samples from 28 soil pits (~60 cm deep) in the Great Smoky Mountains, North Carolina. Though $^{10}Be_{is}$ profiles in this study were homogenized with depth, $^{10}Be_{met}$ concentrations in the same profiles increased in concentration with depth. This trend suggests that $^{10}Be_{met}$ equilibrates to chemical

conditions of soil horizons at timescales faster than required for physical mixing processes.

In profiles extending below the uppermost soil horizons, $^{10}Be_{met}$ and $^{9}Be_{reactive}$ concentrations do not always have the same trends, which suggests that they are not completely and rapidly mixed in all study areas and at all depths (Barg et al., 1997; Bacon et al., 2012). $^{9}Be$ is primarily sourced from weathering bedrock (with some $^{9}Be$ deposited in dust at the surface) while $^{10}Be_{met}$ is deposited at the surface (Willenbring and von Blanckenburg 2010). Bacon et al. (2012), working with core samples collected to a depth of nearly 20 m, found that $^{9}Be_{reactive}$ concentrations increased steadily as sample depth approached the depth of the weathering front; in contrast, $^{10}Be_{met}$ concentrations increased and then decreased down the profile. A similar trend is found for $^{10}Be_{met}$ and $^{9}Be_{reactive}$ concentrations of leached soils compiled by Barg et al. (1997), which included soil profiles up to 11 m in depth from various temperate and tropical locations. The discrepancy between $^{10}Be_{met}$ and $^{9}Be_{reactive}$ distributions with depth may reflect the fact that $^{9}Be_{reactive}$ is weathering from bedrock faster than it is mixed throughout the regolith, resulting in higher concentrations of $^{9}Be_{reacitve}$ closer to the weathering front (Bacon et al., 2012). Although differing geochemical conditions along the profile may result in a different likelihood for $^{10}Be_{met}$ or $^{9}Be_{reactive}$ to remobilize if $^{10}Be_{met}$ and $^{9}Be_{reactive}$ do not have the same distributions, mixing the upper section of the soil profile that is most likely to be eroded is most important for influencing $^{10}Be_{met}/^{9}Be$ ratio in fluvial sediment grain coatings (Pavich et al., 1984; Bacon et al., 2012; von Blanckenburg et al., 2012). Despite the observed differences in distribution between $^{10}Be_{met}$ and $^{9}Be_{reactive}$ in profiles measured by Bacon et al. (2012) and Barg et al. (1997), Wittmann et al. (2012) found that

$^{9}Be_{reactive}$ normalizes $^{10}Be_{met}$ across grain sizes in Amazon River sediments, suggesting that $^{9}Be_{reactive}$ and $^{10}Be_{met}$ behave similarly in grain coatings of sediments that have eroded from hill slopes.

### *2.3 $^{10}Be_{met}$ / $^{9}Be_{reactive}$ denudation rate model*

Von Blanckenburg et al. (2012) derived a mass balance formula whereby measurements of $^{9}Be_{diss}$, $^{9}Be_{reactive}$, and $^{9}Be_{min}$ can be used to calculate $^{10}Be_{met}$/$^{9}Be_{reactive}$-derived denudation rates (eq. 1). The mass balance model includes assumptions about the parent $^{9}$Be concentration (the $^{9}$Be concentration of unaltered bedrock), $^{10}Be_{met}$ delivery rates, rapid soil mixing, and steady state weathering rates (von Blanckenburg et al., 2012).

$$D = \frac{F_{met}^{^{10}Be}}{[^{9}Be]_{parent} * (f_{reac}^{^{9}Be} + f_{diss}^{^{9}Be}) * \left( \frac{^{10}Be_{met}}{^{9}Be_{reactive}} \right)} \quad \text{eq. 1}$$

$$f.factor = \frac{F_{met}^{^{10}Be}}{[^{9}Be]_{parent} * D * \left( \frac{^{10}Be_{met}}{^{9}Be_{reactive}} \right)} \quad \text{eq. 1'}$$

In this equation, $[^{9}Be]_{parent}$ is the $^{9}$Be concentration in parent bedrock, $F_{met}^{^{10}Be}$ is the delivery rate of $^{10}Be_{met}$, $D$ is denudation rate, and $f_{reac}^{^{9}Be} + f_{diss}^{^{9}Be}$ is the sum of fractions of $^{9}$Be in the reactive phase and dissolved phase. $^{10}Be_{met}$ and $^{9}Be_{reactive}$ are the operationally defined "reactive" fractions of sediment grain coatings. In this study, $f_{reac}^{^{9}Be} + f_{diss}^{^{9}Be}$ is simplified to "f.factor." The f.factor can be estimated by using measured concentrations of $^{9}Be_{min}$, $^{9}Be_{reactive}$, $^{9}Be_{diss}$, sediment load, and discharge or, if there are independent

measures of denudation rates for the sampled basins (i.e. $^{10}Be_{is}$-derieved denudation rates, sediment load and discharge data), the f.factor can be calculated from algebraic rearrangement of eq. 1 (von Blanckenburg et al., 2012). If f.factors are calculated this way, they are calibrated values and will be, by their nature, well correlated with such measures of denudation rate. In studies thus far, it has been assumed that the concentration of parent bedrock is 2.5 μg/g, the global average Be concentration in crustal rocks (von Blanckenburg et al., 2012; von Blanckenburg and Bouchez, 2014). For large catchments with heterogeneous lithologies such as the Amazon River, assuming $^{9}Be_{parent}$ to be 2.5 μg/g is unlikely to introduce significant error (von Blanckenburg et al., 2012). However, in studies of basins with less heterogeneous parent lithologies, we consider the hypothesis that $^{9}Be_{min}$+$^{9}Be_{reactive}$ may be a more accurate estimation of the $^{9}Be_{parent}$ concentrations.

## 3. Experimental Approach and Methods

This study leverages a large dataset (n = 202) of fluvial sediment samples that others have already collected and measured for *in situ* and total meteoric $^{10}$Be (Trodick 2011; Portenga and Bierman, 2011; Nichols et al., 2014; Neilson, 2016). Samples were sieved in the field; sand-size grains (250-850 μm) were collected and pulverized in a shatterbox. In this study, we further analyzed the powdered fluvial sediment for $^{9}Be_{reactive}$ and $^{9}Be_{min}$ concentrations.

There is consensus that $^{10}Be_{met}$ is primarily contained in stable grain coatings that form during pedogenesis (Barg et al., 1997; Stoops et al., 2010; Wittmann et al., 2012). In order to further our understanding of $^{10}Be_{met}$ dynamics, we selectively removed grain

coatings using acid leaching (HCl) and refer to the concentration of Be in these coatings as $^{9}Be_{reactive}$. $^{9}Be$ incorporated in silicate minerals or lithic grains is not accessible in remobilization reactions on timescales relevant to denudation nor is it leached by HCl. $^{9}Be$ concentrations in mineral grains provide information about sources of $^{9}Be$ to the reactive fraction and are quantified in this study for a large subset (n = 140) of the fluvial sediment samples.

### *3.1 $^{9}Be_{reactive}$ extraction*

To test and refine HCl extraction of Be, we conducted several experiments using three very different sample types, all of which had been powdered: fluvial sediment, soil, and glacial lake sediment. We did these experiments to ensure that our procedure removed the entire grain coating without removing Be from underlying mineral grains. For each sample, we reacted 0.250 g in 2 mL of warm, sonicated 6 M or 3 M HCl for 1, 4, 8, and 24 hours (24 extractions total). The leachate was analyzed for Be, Al, Fe, Mn, Na, Ca, K, Mg, Si, and Ti concentrations using Inductively Coupled Plasma Optical Emission Spectrometry (ICP-OES, JY Horiba Optima) at the University of Vermont.

To analyze the fluvial sediment samples in this study, we reacted 0.250 g of powdered fluvial sediment samples in 2 mL warm 6 M HCl for 24 hours in an ultrasonic bath. After centrifugation, we quantified Be concentrations using the 313.107 nm emission line on the ICP-OES because it has high sensitivity and does not have overlapping peaks with other extractable elements, which we verified by scanning emission spectra of multi-element standards and leached samples and by referring to published tables of elemental emission lines (Kramida et al., 2015). Although ICP-OES detects total Be, $^{9}Be_{reactive}$

concentrations are 10-12 orders of magnitude higher than $^{10}Be_{met}$ so that we effectively measure only $^{9}Be$. ICP-OES acquisition parameters are described in SI.

*3.2 $^{9}Be_{min}$ total digestion*

We analyzed a subset of samples from each study area (n = 140) for $^{9}Be_{min}$ concentrations by totally digesting of material remaining after $^{9}Be_{reactive}$ analysis. After the HCl acid-leach, the residual material was rinsed 3 times with MilliQ water and dried overnight. The residual material was digested using an open-beaker hotplate method. First, 2.5 mL of 1:1 $HNO_3$ was added to each sample. Samples were covered with a watch glass, heated to 95°C and refluxed for 15 minutes. This step was repeated twice with 1 mL of conc. $HNO_3$ added after each reflux. Samples were then heated for ~2 hours at 95°C, at which point there was ~1 mL of solution in the vessel.

After samples cooled, 1 mL of 18 MΩ water and 1 mL of 30% $H_2O_2$ were added. Samples were covered with a watch glass and heated to 85°C for 1 hour. Samples were allowed to cool and an additional 1 mL of 30% $H_2O_2$ was added and heated for another 1 hour at 85°C. This process was repeated once. Samples were then heated for an additional ~2 hours at 95°C or until there was ~ 1 mL of solution in the vessel.

After samples cooled, a mixture of 3 mL conc. HF with 1% $H_2SO_4$, 0.5 mL conc. $HNO_3$ and 1 mL conc. $HClO_4$ was added to each sample. Samples were covered with a watch glass and allowed to react overnight at 105°C. The following morning, samples were evaporated at 110°C until dryness (~6 hrs), at which point they were heated to 230°C until white $HClO_4$ fumes were no longer observed (~3 hours). Samples were cooled, gravimetrically diluted with 0.01 M $HNO_3$, and analyzed on the ICP-OES. In

many cases, a white crystalline precipitate of $TiO_2$ was observed at the end of the leaching procedure; these samples were centrifuged before analysis on the ICP-OES. This kind of precipitate has been previously observed in $^{10}Be_{is}$ total digest extractions, and appears to not incorporate Be (Hunt et al., 2008).

### *3.3 $^{9}$Be organic fraction extraction*

In a subset of samples (n = 30), the organic fraction of $^{9}$Be was also measured. After the $HNO_3$ and $H_2O_2$ extraction steps of total digest procedure, samples were evaporated until < 1 mL of solution remained in the Teflon reaction vessel. Samples were gravimetrically diluted with 0.01 M $HNO_3$, centrifuged, and the supernatant was analyzed via ICP-OES. The residual material was rinsed 3 times with MilliQ water, dried overnight, weighed, and digested with HF, $HNO_3$, and $HClO_4$ as described in the total digestion procedure above. $^{9}Be_{min}$ for these samples is reported as the sum of the organic and total digest fractions.

### *3.4 $^{10}Be_{met}/^{9}Be_{reactive}$-derived denudation rate calculations*

We calculated the delivery rate of $^{10}Be_{met}$ for each sample using the approach of Graly et al. (2011). Mean annual precipitation and mean basin latitude were determined via ArcGIS analysis of watershed shapefiles (generated from the ArcGIS hydrology toolset with GIS coordinates of sample locations used as "pour points" for watershed calculations) and 30 arc-second current precipitation data from WorldClim.org.

The mean f.factor for each study area was estimated using three methods. First the f.factor was calculated via eq. 1'. Using this equation, *D* was the *in situ*-derived

denudation rate for each sample, $F_{met}^{^{10}Be}$ was the mean $^{10}Be_{met}$ deposition rate for each catchment, $[^{9}Be]_{parent}$ was assumed to be 2.5 μg/g, and the measured $^{10}Be_{met}/^{9}Be_{reactive}$ ratio was used for each sample. This method of calculating the f.factor is effectively a method of calibrating $^{10}Be_{met}/^{9}Be_{reactive}$-derived denudation rates to $^{10}Be_{is}$ –derived denudation rates. Comparing denudation rates calculated this way is circular. A second method of estimating the f.factor assumes that the $^{9}Be_{diss}$ is a small fraction of the total $^{9}$Be pool in these study regions. Assuming negligible $f_{diss}^{^{9}Be}$ in the catchments, the f.factor is estimated by dividing the $^{9}Be_{reactive}$ concentration by the sum of $^{9}Be_{min}$ and $^{9}Be_{reactive}$ concentrations (eq. 2).

$$f.factor = \frac{^{9}Be_{reactive}}{^{9}Be_{reactive} + ^{9}Be_{\min}} \quad \text{eq. 2}$$

The assumption that $^{9}Be_{diss}$ concentrations are low is supported by the high $K_d$ of Be compounds under most natural conditions (Measures and Edmond, 1983; Hawley et al., 1986; You et al., 1989; You et al., 1994; Aldahan et al., 1998; Takahashi et al., 1999) and by the small (< 0.03) $F_{diss}$ calculated by von Blanckenburg et al. (2012) in 4 of the 5 highly weathered, tropical subcatchments of the Amazon River; only the highly acidic (~pH 4 river water) Rio Negro exhibited $^{9}Be_{diss}$ constituting greater than 3% of the total $^{9}$Be (Brown et al., 1992; von Blanckenburg et al., 2012).

A third method of estimating f.factor assumes that the total $^{9}$Be concentration is equal to 2.5 μg/g. With this assumption, $^{9}Be_{diss}$ is calculated by subtracting $^{9}Be_{min}$ and $^{9}Be_{reactive}$ from 2.5 μg/g. The f.factor is subsequently calculated via eq. 3.

$$f.factor = \frac{^{9}Be_{reactive} + ^{9}Be_{diss}}{2.5} \quad \text{eq. 3}$$

If total $^{9}$Be concentrations are assumed to be 2.5 μg/g for the f.factor (eq. 3) when using eq. 1 to calculate $^{10}Be_{met}/^{9}Be_{reactive}$-derieved denudation rates, then 2.5 μg/g is also used for $[^{9}Be]_{parent}$ . However, if $^{9}Be_{min}+^{9}Be_{reactive}$ is used to calculate f.factor (eq. 2), then the mean basin specific $^{9}Be_{min}+^{9}Be_{reactive}$ is also used for $[^{9}Be]_{parent}$ .

## 4. Results

Using over 200 river sediment samples (7 different study sites) for which meteoric and *in situ* $^{10}$Be concentrations had already been measured, we performed additional chemical extractions and elemental analyses. These data allow us to understand the distribution of $^{9}$Be and the relationship of different beryllium isotopes to major element concentrations in both grain coatings and underlying mineral matrixes. We use this information to compare existing models that interpret meteoric and *in situ* $^{10}$Be measurements as landscape-scale denudation rates.

### *4.1 Grain coatings leached with HCl*

Experimental results indicate that leaching with 6 M HCl effectively removes grain coatings without dissolving underlying mineral matrixes. 6 M and 3 M HCl-extractable Be, Fe, Al, and Mg concentrations plateau over 24 hours of reaction time for the fluvial sediment sample (QLD), the soil sample (CPA), and the glacial lake sediment sample (varve), (Fig. 3). 6 M HCl extracts more material than 3 M HCl for soil and glacial lake sediment samples, but not fluvial sediment samples. Extractable concentrations of Si do not have the same increasing and then plateauing trend in concentration over time as other elements and overall concentrations of leached Si are low. Minimal leaching of Si

(leached Si remains less than 45 ug/g of sample for all substrates) indicates that 6 M HCl extraction method does not leach Be incorporated in silicate mineral matrixes. We duplicated 6 M HCl extractions for 19 samples and found that the percent difference between the extractable Be concentrations in duplicates is normally distributed with 0.2% average difference between replicates and a standard deviation of 5.6% (SI). The Be concentration of a multi-element standard measured after every 11 samples on the ICP-OES has a standard deviation of 1.7% (SI). These replication data indicate that the 6 M HCl-leaching method reproducibly leaches grain coatings from fluvial sediment samples and that low concentrations of Be can be reliably detected using ICP-OES.

### *4.2 Significant correlations between $^{10}Be_{is}$, $^{10}Be_{met}$, $^{10}Be_{met}/^{9}Be_{reactive}$, and $^{10}Be_{is}$-derived denudation rates*

Be isotope data included in this study span a wide range of concentrations, and study areas include watersheds that are eroding relatively slowly ($^{10}Be_{is}$-derived denudation rate of 7.5 ± 0.8 t km$^{-2}$ yr$^{-1}$) and quickly (1000 ± 230 t km$^{-2}$ yr$^{-1}$). $^{10}Be_{met}$ concentrations range from 2.61 x $10^{6}$ to 6.18 x $10^{9}$ atoms/g, $^{10}Be_{is}$ concentrations range from 2.27 x $10^{5}$ to 1.67 x $10^{7}$ atoms/g, $^{9}Be_{reactive}$ concentrations range from 3.88 x $10^{15}$ to 2.79 x $10^{17}$ atoms/g, and $^{10}Be_{met}/^{9}Be_{reactive}$ ratios (unitless) range from 8.03 x $10^{-11}$ to 8.38 x $10^{-8}$.

Some statistically significant ($p < 0.05$) bivariate correlations between Be isotopic measurements exist in individual study areas and other significant correlations between measurements exist when considering all samples (n = 202), but few significant correlations exist when considering all samples and regional scale data. When considering all samples, there is a positive and significant correlation between $^{10}Be_{met}$ and

$^{10}Be_{is}$ ($R^2 = 0.40$), and a stronger positive correlation between $^{10}Be_{met}/^{9}Be_{reactive}$ and $^{10}Be_{is}$ ($R^2 = 0.58$), (Fig. 4). However, when considering individual study areas, correlations between $^{10}Be_{met}$ and $^{10}Be_{is}$ are only significant in CH1xx and CHb study areas, and correlations between $^{10}Be_{met}/^{9}Be_{reactive}$ and $^{10}Be_{is}$ are only significant in CH1xx, CHb and CHa study areas (Table 2).

$^{10}Be_{met}$ and $^{9}Be_{reactive}$ are positively correlated in individual study areas; the correlations are statistically significant in all study areas except CHc (Fig. 5). The strong correlation between $^{10}Be_{met}$ and $^{9}Be_{reactive}$ is not evident when considering data across all study areas; $^{10}Be_{met}$ and $^{9}Be_{reactive}$ are weakly correlated ($R^2 = 0.08$) in all samples.

$^{10}Be_{is}$-derived denudation rates show a statistically significant correlation with $^{10}Be_{met}/^{9}Be_{reactive}$ in CH1xx, CHa, and CHb study areas, but these correlations do not have $R^2 > 0.30$. When considering all samples, the correlation between $^{10}Be_{is}$-derived denudation rates and $^{10}Be_{met}/^{9}Be_{reactive}$ is significant, but the effect size is small ($R^2 = 0.11$), (Table 2). $^{10}Be_{is}$-derived denudation rates do not significantly correlate to $^{9}Be_{reactive}$ or $^{10}Be_{met}$ when considering all samples.

*4.3 Chemical compositions of grain coatings and mineral matrixes*

HCl-extractable materials primarily consist of Fe and Al, which represent an average of 54.5% and 18.7% of total elemental abundances by mass, respectively. Fe, Mn, and Al significantly and positively correlate to $^{10}Be_{met}$ in individual study areas, and $R^2$ ranges from 0.15 (study area CHa) to 0.94 (G) for correlations with Al, 0.00 (CHa) to 0.98 (G) for correlations with Fe, and 0.00 (GLD) to 0.92 (G) for correlations with Mn (Fig. 6). When considering all samples, the correlation between $^{10}Be_{met}$ and concentrations of Al,

Mn, Fe, and total measured acid-extractable elements is weak ($R^2 < 0.18$ for all correlations). $^{9}Be_{reactive}$ has strong positive correlations to total HCl-extractable elemental abundances in several study areas (G: $R^2 = 0.99$, CHb: $R^2 = 0.87$, POT: $R^2 = 0.63$) and no correlation in others (QLD: $R^2 = 0.01$, CHa: $R^2 = 0.00$). Over the entire dataset, the correlation between $^{9}Be_{reactive}$ and total grain coating mass is significant ($R^2 = 0.28$).

Study areas have a wide range of $^{9}Be_{reactive}$ (0.06-4.18 μg/g) and $^{9}Be_{min}$ (0.03-3.76 μg/g) concentrations. The average sum of $^{9}Be_{min}$ and $^{9}Be_{reactive}$ concentrations between study areas varies from 0.72 ± 0.28 to 2.09 ± 1.12 μg/g with an average of 1.23 ± 0.82 μg/g (n=140). $^{9}Be_{min}$ and $^{9}Be_{reactive}$ are not correlated when considering all samples ($R^2 = 0.01$), but are significantly correlated in QLD ($R^2 = 0.46$), POT ($R^2 = 0.18$), and CHb ($R^2 = 0.70$).

The $H_2O_2$ and $HNO_3$-extractiable (organic) fraction of $^{9}Be$ ranges from 0.01 μg/g to 0.25 μg/g, with the average percentage of $^{9}Be$ in the organic phase representing 4.0 % of total $^{9}Be$ (the sum of $^{9}Be_{min}$, $^{9}Be_{reactive}$, and organic $^{9}Be$). The highest measured percentage of $^{9}Be$ in the organic phase is 8.0%. Unlike the HCl-extractable phase, the leached elements from the organic phase of grain coatings are primarily Na (33% of total organic extractable by mass), Al (30%), and K (19%).

*4.4 Variation in correlations between basin characteristics and Be isotopes by study area*

Few basin characteristics significantly correlate with Be isotope concentrations and ratios (Table 3). $^{10}Be_{met}/^{9}Be_{reactive}$ is significantly correlated to MAP in 4 of 7 study areas; 3 of these correlations are negative, and 1 is positive. $^{10}Be_{met}/^{9}Be_{reactive}$ is only significantly correlated to total basin relief in 2 of 7 study areas and both correlations are

negative (Table 3). MAP is significantly correlated to $^{10}Be_{is}$ (positive correlations), $^{10}Be_{met}/^{9}Be_{reactive}$ (negative correlations) and $^{10}Be_{is}$-derived denudation rates (negative correlations) for G and CHa study areas, but is not strongly correlated to $^{10}Be_{is}$, $^{10}Be_{met}/^{9}Be_{reactive}$, or $^{10}Be_{is}$-derived denudation rates for all samples. Total basin relief is positively and significantly correlated to $^{10}Be_{is}$-derived denudation rates for all samples ($R^2 = 0.55$), but not for most individual study areas. Mean basin slope is positively and significantly correlated to $^{10}Be_{is}$-derived denudation rates in the QLD study area ($R^2 = 0.53$), and across all samples ($R^2 = 0.46$), but is either not correlated (POT, G, CHc) or significantly and negatively correlated (CHb) in other study areas. Mean elevation is positively and significantly correlated to all samples ($R^2 = 0.42$), but for the 2 individual study areas with $R^2 > 0.30$, CHa has a negative correlation and G has a positive correlation. Though $^{10}Be_{is}$-derived denudation rates for all samples significantly and positively correlate to mean elevation ($R^2 = 0.43$) and mean basin size ($R^2 = 0.33$), $^{10}Be_{is}$ and $^{10}Be_{met}/^{9}Be_{reactive}$ do not strongly and significantly correlate to any of the measured basin parameters for all samples (Table 3).

$^{10}Be_{met}/^{9}Be_{reactive}$-derived denudation rates are significantly correlated to MAP in 5 of the 7 study areas, though 3 study areas have a positive correlation (CHc, G, POT) and 2 study areas have a negative correlation (CH1xx, QLD), (Table 3). Considering all data, there is not a significant correlation between $^{10}Be_{met}/^{9}Be_{reactive}$-derived denudation rates and MAP. $^{10}Be_{met}/^{9}Be_{reactive}$-derived denudation rates positively correlate to total basin relief in 2 study areas (CHb and CH1xx), and across all study areas ($R^2 = 0.42$). $^{10}Be_{met}/^{9}Be_{reactive}$-derived denudation rates only significantly correlate to mean basin slope

in the CHc study area (negative correlation), but have significant and positive correlation to mean basin slope across all samples ($R^2 = 0.17$).

*4.5 $^{10}Be_{met}/^{9}Be_{reactive}$ and $^{10}Be_{is}$-derived denudation rates significantly correlate across all samples*

An important unknown in the mass balance model used to determine $^{10}Be_{met}/^{9}Be_{reactive}$-derived denudation rates (eq. 1) is the f.factor, which represents the fraction of $^{9}Be$ in the reactive and dissolved phase (von Blanckenburg et al., 2012). The 3 methods of estimating f.factor used in this study result in significantly different mean f.factors for all samples (ANOVA $F(2, 201) = 63.8$, $p < 0.001$). When using eq. 1' to calculate f.factors, POT and CH1xx have several samples with calculated f.factors that are greater than 1 – an outcome that violates the assumptions of the mass balance model and is impossible to replicate using eq. 2 or 3 (Fig. 8). Using eq. 1 to calculate f.factors and again to calculate $^{10}Be_{met}/^{9}Be_{reactive}$ -derived denudation rates results in a calibrated method of determining denudation rates in which the central tendencies must align. For this reason, when comparing $^{10}Be_{is}$-derived denudation rates to $^{10}Be_{met}/^{9}Be_{reactive}$-derived denudation rates, we calculate the mean f.factor for each basin using eq. 2 or eq. 3.

Another unknown in the mass balance model is the parent $^{9}Be$ concentration. We test two methods of estimating the parent $^{9}Be$ concentrations: we either assume the parent $^{9}Be$ concentration is 2.5 μg/g or we assume that the mean sum of $^{9}Be_{min}$ and $^{9}Be$ concentrations of fluvial sediments in the basin reflects the parent $^{9}Be$ concentration in the study area. Though the $R^2$ between $^{10}Be_{is}$-derived denudation rates and $^{10}Be_{met}/^{9}Be_{reactive}$ derived denudation rates calculated with parent $^{9}Be$ of 2.5 μg/g and eq. 3

or the mean $^{9}Be_{min}$+$^{9}Be_{reactive}$ and eq. 2 are the same ($R^2$ = 0.381 and $R^2$ = 0.376, respectively) the value of the mean $^{10}Be_{met}/^{9}Be_{reactive}$-derived denudation rate is significantly influenced by the estimate of parent $^{9}Be$ concentrations (Table 4). For all samples, using eq. 3 and an assumed parent concentration of 2.5 μg/g results in a central tendency for $^{10}Be_{met}/^{9}Be_{reactive}$-derived dentation rates that is only 1% larger than the mean $^{10}Be_{is}$-derieved denudation rate. In 3 of the 7 study areas, using the measured $^{9}Be_{min}$ + $^{9}Be_{reactive}$ concentrations for f.factor and parent $^{9}Be$ concentration results in more similar central tendencies to $^{10}Be_{is}$-derived denudation rates than assuming $^{9}Be$ parent concentrations are 2.5 μg/g and eq. 3 f.factors; $^{10}Be_{met}/^{9}Be_{reactive}$-derived denudation rates in CHb and CHc watersheds underestimate $^{10}Be_{is}$-derieved denudation rates by 17% and 12%, respectively. However, in 4 of the 7 study areas, using $^{9}Be_{min}$ and $^{9}Be_{reactive}$ based estimates of parent $^{9}Be$ concentrations and f.factors results in $^{10}Be_{met}/^{9}Be_{reactive}$ derived denudation rates that significantly overestimate $^{10}Be_{is}$-derived denudation rates, while assuming 2.5 μg/g for parent $^{9}Be$ concentration and f.factors results in similar central tendencies (10-37% difference) between both measures of denudation rates (Table 4). In individual study areas, CHa, CH1xx, CHc, and POT have significant positive correlations between $^{10}Be_{is}$-derived denudation rates and $^{10}Be_{met}/^{9}Be_{reactive}$-derived denudation rates when $^{9}Be_{min}$+$^{9}Be_{reacive}$ based assumptions about parent $^{9}Be$ concentrations and f.factors are used. However, with the exception of CHa ($R^2$ = 0.60), the $R^2$ of correlations in individual study areas are < 0.30, regardless of the assumptions made about total $^{9}Be$ concentrations (Fig. 9). When 2.5 μg/g is assumed for parent $^{9}Be$ concentrations and f.factors, only CH1xx, CHc, and POT have statistically significant correlations between $^{10}Be_{is}$-derived and $^{10}Be_{met}/^{9}Be_{reactive}$-derived denudation rates.

## 5. Discussion

This study examines $^{10}Be_{is}$, $^{10}Be_{met}$, and $^{9}Be$ dynamics in fluvial systems. Our method of extracting $^{9}Be$ from grain coatings using HCl results in $^{9}Be_{reactive}$ concentrations that significantly and positively correlate to total $^{10}Be_{met}$ in nearly all of our study areas, supporting the assumption that $^{9}Be_{reactive}$ mixes with $^{10}Be_{met}$ during the formation of grain coatings found on fluvial sediments. However, variability in $^{9}Be$ concentrations of source materials (including bedrock, dust, and organic material) influences $^{9}Be$ abundances in grains and grain coatings; we observe a wide range of $^{9}Be_{min}$ and $^{9}Be_{reactive}$ concentrations within and across study areas. Heterogeneous inputs for $^{9}Be$ ($^{9}Be$ concentrations of parent materials) and $^{10}Be_{met}$ (latitude and climate-dependent delivery rates), combined with site-specific biogeochemical influences on soil mixing and remobilization processes, result in mostly poor correlations between $^{10}Be_{met}/^{9}Be_{reactive}$ and $^{10}Be_{is}$, $^{10}Be_{is}$-derived denudation rates, and basin characteristics when considering all samples.

### *5.1 $^{9}Be_{reative}$ and total $^{10}Be_{met}$ are primarily associated with the HCl-extractable grain coatings*

Our dataset combines $^{9}Be_{reactive}$ concentrations measured in the HCl-extractable phase of fluvial sediment grains and $^{10}Be_{met}$ concentrations measured via total flux fusions; our $^{10}Be_{met}/^{9}Be_{reactive}$ ratios are analogous to other $^{10}Be_{met}/^{9}Be$ studies in which both isotopes were extracted from the "authigenic" phase of sediments (Bourlès et al., 1989; Barg et al., 1997; Wittmann et al., 2012; von Blanckenburg et al., 2012). In our samples, we found a small percentage of total extractable $^{9}Be_{reactive}$ in the organic phase of grain coatings (4%

of total $^{9}$Be), in agreement with other $^{9}$Be and $^{10}Be_{met}$ sequential extraction studies (Bourlès et al., 1989; Wittmann et al., 2012; Taylor et al., 2012). Wittmann et al. (2012) similarly found that concentrations of $^{9}$Be in the organic fraction of fluvial sediment grain coatings consisted of less than 1% of total $^{9}$Be concentrations in 30-40 μm fluvial sediments and Bourlès et al. (1989) found that the organic fraction of marine sediments never contained more than 8% of the total $^{9}$Be or $^{10}Be_{met}$. Though Be complexes readily with organic acids and has been shown to accumulate in organic matter (Lundberg et al., 1983; Veselý et al., 2002; Kabata-Pendias and Szteke, 2015), organometallic Be complexes could sorb to grain coatings by associating with existing metal oxides and hydroxide coatings, allowing organic Be complexes to be removed when the acid-extractable phase of the grain coating is leached. Accordingly, our decision to consider the organic-related $^{9}$Be with $^{9}Be_{min}$ does not significantly influence the $^{10}Be_{met}/^{9}Be_{reactive}$ ratios we calculate because so little $^{9}$Be is associated with organic material.

The strong, positive correlations between total $^{10}Be_{met}$ and acid-extractable Fe, Al, and Mn concentrations (Fig. 7) suggest that $^{10}Be_{met}$ is associated with metal oxides and hydroxides that can be leached in reducing conditions. Zhang et al. (2011) used TEM to visualize and characterize coatings on quartz grains from oxic soils and found that grain coatings were composed of illite, chlorite, allophane, and nanoscale hematite particles cemented with goethite aggregates, a finding that is supported by sequential extraction studies of soil grains (Barg et al., 1997; Taylor et al., 2012). Our method of HCl leaching attacks crystalline and amorphous oxides/hydroxides (Tessier, 1979; Bourlès et al., 1989), but may also partially dissolve mineral grains of phyllosilicates that are known to sequester $Be^{2+}$ ions, such as biotite, illite, and kaolinite (You et al., 1989; Aldahan et al.,

1998; Takahashi et al., 1999; Grew, 2002). The inclusion of significant amounts of $^{10}Be_{met}$ and $^{9}Be_{reactive}$ in soil grain coatings means that the partial dissolution or physical abrasion of grain coatings can influence the concentrations of $^{10}Be_{met}$ and $^{9}Be_{reactive}$ in fluvial sediments.

*5.2 Heterogeneous distributions of $^{9}Be_{min}$ and $^{9}Be_{reactive}$ within and across study areas*

Concentrations of total $^{9}Be_{min}$+$^{9}Be_{reactive}$ vary by study region, suggesting, in agreement with Brown et al. (1992), that $^{9}$Be concentrations of underlying lithology influence regional $^{9}Be_{reactive}$ and $^{9}Be_{min}$ concentrations. Parent material for $^{9}$Be in grains and grain coatings include the minerals that compose the underlying bedrock, surficial materials including regolith and alluvium, dust, and possibly organic-rich materials that have sequestered Be, such as coal or plant matter (Lundberg et al., 1983; Veselý et al., 2002; Conyers, 2014). Our study areas have statistically different averages of $^{9}Be_{min}$+$^{9}Be_{reactive}$ concentrations (ANOVA p value < 0.01) and a wide range of mean $^{9}Be_{min}$+$^{9}Be_{reactive}$ (from 0.72 ± 0.28 μg/g to 2.09 ± 1.12 μg/g) (Fig. 7), which suggests that study areas have a variety of $^{9}$Be concentrations in parent materials. The study area with the lowest mean $^{9}Be_{min}$+$^{9}Be_{reactive}$ is the Weiyuan River watershed (CHb). The basins included in this study area drain a relatively large region within the Lanping-Simao fold belt (mean basin area of CHb study area = 584 km$^2$) that primarily contains Jurassic non-marine redbeds with unconformably overlain upper Triassic sandstone, shale, and limestone (Akciz et al., 2008; Nielson, 2016). However, the Lanping-Simao unit has complex bedrock lithology; the eastern section of the unit is primarily limestone (~900 m thick) and fine-grained sandstone (~1000 m thick) but along the west side of the Lanping-

Simao Unit, closer to the CHb study area, is a thick section (up to 5 km) of mafic and ultramafic volcanics (Burchfiel and Zhilang, 2012). The relatively low concentrations of $^{9}Be$ in this study area may reflect fluvial sediment contributions from regions of the watershed that drain limestone and mafic bedrock units, which are likely to have low $^{9}Be$ concentrations (Grew, 2002). In contrast, study area CHa has the highest $^{9}Be_{min}+^{9}Be_{reactive}$ of our study areas. CHa (the Yongchun River basin) is also located in the Lanping-Simao unit, but ~800 km to the NW of CHb. In the northern region of the Lanping-Simao unit, bedrock is dominated by sandstone, mudstone, siltstone, and breccia that could be relatively enriched in $^{9}Be$, explaining the high CHa $^{9}Be$ concentrations (Grew, 2002; von Blanckenburg et al., 2012).

Our samples also have a wide range of $^{9}Be_{min}+^{9}Be_{reactive}$ within individual study areas. $^{9}Be_{min}+^{9}Be_{reactive}$ of samples from the Georges River catchment (G) range from 0.39 to 3.95 μg/g. In the Georges River catchment, relatively high concentrations of $^{9}Be_{min}$ could be reflecting elevated Be concentrations in bedrock from nearby Be-enriched granitic intrusions, such as the alkali-feldspar granites of the Mount Paris Pluton and Lottah Pluton or biotite adamelites of the Blue Tier Batholith and Mount Pearson Pluton (McClenaghan, 1985). Although Be concentrations of these intrusions have not been measured, Be is known to accumulate in highly differentiated igneous rocks (Grew, 2002); Portenga et al. (2015) observed native $^{9}Be$ concentrations up to 38 μg/g in quartz grains from fluvial sediments in basins with leucogranitic intrusions in the Bhutanese Himalayas. Contributions of fluvial sediment from the granodiorite intrusions like the Georges River Pluton and Pyengana Pluton are likely to have much lower $^{9}Be$ concentrations than sediments derived from granites and adamellites (Grew, 2002; von

Blanckenburg et al., 2012). These varied source materials result in an over 3 μg/g range in $^{9}Be_{min}$+$^{9}Be_{reactive}$ from fluvial sediment samples in the G study area.

We also observe samples with a large range of $^{9}Be_{min}$+$^{9}Be_{reactive}$ (from 0.10 to 3.19 μg/g) in the Potomac River watershed (POT). The Potomac River drains in part the Upper Freeport Coal Bed, which has Be concentrations that range from 0.21-5.0 μg/g and a mean value of 1.80 ± 0.81 μg/g (Ruppert et al., 2000). Whether or not Be-enriched coal grains were included in sieved samples, the presence of coal in the soil system may result in higher $^{9}Be_{diss}$ concentrations in surrounding pore water, and thus higher $^{9}Be_{reactive}$ concentrations in grain coatings. Be-enriched coal grains influence $^{9}Be_{reactive}$ concentrations in grain coatings where coal crops out in the riverbed or is close enough to the surface to be incorporated into the mixed zone of soil profiles, conditions that occur in the Potomac watershed along the North branch of the river (Ruppert et al., 2000). The regional influence of Be-enriched coal is supported in our data – the highest concentrations of $^{9}Be_{reactive}$ measured in the POT watershed (5.4 μg/g, 3.1 μg/g, and 3.0 μg/g) occur in northern reach of the study area where the Freeport Coal Bed crops out, while samples in southern section of the main stem of the river (sample numbers POT 37 and below) have a mean $^{9}Be_{reactive}$ concentration of only 0.5 ± 0.5 μg/g. These large ranges of $^{9}Be_{min}$+$^{9}Be_{reactive}$ in study areas suggest that significant heterogeneities in $^{9}Be$ concentrations of source material for grain coatings can exist within a single, regional river catchment.

The mean $^{9}Be_{min}$+$^{9}Be_{reactive}$ concentration for our sediment samples (1.23 ± 0.82 μg/g, n = 140) is less than the global mean abundance of $^{9}Be$ in parent rocks (2.5 μg/g), which was calculated by averaging previous compilations of Be concentrations in the GERM

Reservoir hosted on earthref.org (von Blanckenburg et al., 2012; Staudigel et al., 1998). However, our $^{9}$Be data agree with total $^{9}$Be concentrations measured in sequential extraction studies of fluvial sediments by Wittmann et al. (2012), who found that total $^{9}$Be concentrations of fluvial sediments had a mean value of 1.26 ± 0.22 μg/g (n = 5). The finding that the mean sum of $^{9}Be_{min}$ and $^{9}Be_{reactive}$ concentrations in 207 fluvial sediments samples from around the globe (202 from this study, 5 from Wittmann et al. 2010) are well below the average global crustal abundance of $^{9}$Be in parent materials may be reflecting the fact that our method of estimating $^{9}Be_{parent}$ from $^{9}$Be abundances in quartz-rich detrital river sediment consistently underestimates parent $^{9}$Be concentrations. Sieved fluvial sand samples are unlikely to include clay minerals known to be enriched in Be (Grew, 2002), may not include organic matter like leaf litter or coal fragments (Lundberg et al., 1983; Veselý et al., 2002), and do not include $^{9}$Be that may be in the dissolved phase after being leached from soil, sediment, or bedrock during weathering (von Blanckenburg et al., 2012; Brown et al., 1992; Bourlès et al., 1989). It is possible that the collection of studies included in the GERM database (Staudigel et al., 1998; https://earthref.org/GERMRD) is biased towards particular rock types. However, our finding that assuming 2.5 μg/g for parent $^{9}$Be concentrations for our dataset as a whole results in a mean $^{10}Be_{met}/^{9}Be_{reactive}$-derived denudation rate that is nearly identical to the mean $^{10}Be_{is}$-derived denudation rate supports the assumption that at a large spatial scale, 2.5 μg/g is an accurate estimate of mean $^{9}$Be concentrations in parent materials.

### *5.3. Study site-specific influences on $^{9}Be_{reactive}$ and $^{10}Be_{met}$ concentrations in sediment grain coatings*

The HCl leaching method of extracting total grain coatings results in $^{9}Be_{reactive}$ concentrations that positively correlate to total $^{10}Be_{met}$ in nearly all study areas, but not when considering all data together. The lack of correlation between $^{10}Be_{met}$ and $^{9}Be_{reactive}$ in our entire dataset reflects the observed variability of $^{9}Be$ concentrations of parent materials (approximated by $^{9}Be_{min}$+$^{9}Be_{reactive}$) and variability of calculated $^{10}Be_{met}$ deposition rates (from 4.88 x $10^{5}$ to 1.95 x $10^{6}$ atoms $cm^{-2}$ $yr^{-1}$). When considering all of our samples, differing spatially and climactically dependent $^{10}Be_{met}$ delivery rates and variable $^{9}Be$ concentrations in parent materials are significant enough to overwhelm correlations between $^{10}Be_{met}$ and $^{9}Be_{reactive}$.

The positive correlations we observe between $^{10}Be_{met}$ and $^{9}Be_{reactive}$, combined with the lack of correlation between Be isotope data in grain coatings and $^{10}Be_{is}$-derived denudation rates, gives insight into the relative influence of remobilization and denudation on Be isotope concentrations in individual study areas. Because $^{9}Be_{reactive}$ and $^{10}Be_{met}$ concentrations are ultimately influenced by inputs ($^{9}Be$ weathering from parent materials, $^{10}Be_{met}$ deposition) and outputs (denudation, leaching, vertical remobilization), any of these processes could be driving the positive correlation between $^{9}Be_{reactive}$ and $^{10}Be_{met}$ in individual study areas (Fig. 2). There are several reasons that $^{9}Be_{reactive}$ and $^{10}Be_{met}$ concentrations in fluvial sediments do not primarily reflect the inputs of these isotopes when considering individual study areas. Factors that contribute to heterogeneities in the weathering flux of $^{9}Be$ from parent materials (the concentration of $^{9}Be$ in these materials and the rate of chemical weathering) are not always or directly related to the spatial and climactic factors that cause heterogeneities in $^{10}Be_{met}$ deposition rates (latitude, precipitation rate). If both $^{9}Be_{reactive}$ and $^{10}Be_{met}$ primarily reflected their

respective input fluxes, their abundances in sediments would not be correlated. There is also no significant and positive correlation between $^{10}Be_{met}$ and calculated $^{10}Be_{met}$ delivery rates in 6 of 7 study areas, which tells us that $^{10}Be_{met}$ is not controlled by delivery rate; rather, it is controlled by processes that remove $^{10}Be_{met}$ from the soil column or river system, such as denudation and leaching. Further, the significant correlation between $^{9}Be_{reactive}$ and total elemental abundances of leached grain coatings in most individual study areas and across all samples indicates that $^{9}Be_{reactive}$ concentrations are controlled by the same processes that result in accumulation and dissolution of grain coatings during pedogenesis. For these reasons, our data indicate that within individual study areas, heterogeneities in $^{10}Be_{met}$ and $^{9}Be_{reactive}$ inputs are likely averaged out via illuvial or eluvial remobilization processes, bioturbation, and fluvial sediment mixing processes; $^{9}Be_{reactive}$ and $^{10}Be_{met}$ concentrations are thus either primarily influenced by remobilization and leaching and/or denudation rates.

Slowly eroding systems have more time to accumulate $^{9}Be_{reactive}$ and $^{10}Be_{met}$ in grain coatings, resulting in a positive correlation between $^{9}Be_{reactive}$ and $^{10}Be_{met}$ that reflects basin-scale denudation rates. If isotopes are equally mixed, $^{10}Be_{met}/^{9}Be_{reactive}$ would not be influenced by leaching, remobilization, or physical abrasion processes because both isotopes would be affected equally. However, we do not observe any strong and significant ($R^2 > 0.30$, $p < 0.05$) correlations between $^{10}Be_{met}/^{9}Be_{reactive}$ and $^{10}Be_{is}$-derived denudation rates in individual study areas (Table 2). This poor correlation between $^{10}Be_{met}/^{9}Be_{reactive}$ and $^{10}Be_{is}$ –derived denudation rates suggest that there are biogeochemical influences on $^{10}Be_{met}/^{9}Be_{reactive}$ ratios.

Several biogeochemical processes in fluvial systems could explain the decoupling of denudation rates from Be isotopes in grain coatings. Although most rivers are oxic environments, reduction of river sediments can take place seasonally if the river fluctuates between turbulent high flow conditions in the wet season and low flow conditions with zones of stagnant water in the dry season; anoxia in stagnant water could promote dissolution of metal oxides and hydroxides that make up grain coatings (Calmano et al., 1993). Similarly, swampy conditions and agricultural terracing can produce anoxic environments that promote dissolution of trace metals from grain coatings (Warren, 1983; Nielson, 2016), and physical abrasion of grains during transport has been shown to remove Fe-Mn grain coatings (Cerling and Turner, 1982). These processes provide an alternative explanation for the significant correlations between $^{9}Be_{reactive}$ and $^{10}Be_{met}$ concentrations – that environments conducive to Be sorption to sediments (near-neutral pH, high surface area to volume ratio of mineral grains, oxidizing conditions, little physical abrasion) retain the most $^{10}Be_{met}$ and $^{9}Be_{reactive}$ in fluvial sediment grain coatings, regardless of denudation rates in the watershed. The relative importance of denudation rate and sorption potential on $^{10}Be_{met}$ and $^{9}Be_{reactive}$ concentration likely varies by study area based on the relative rates of denudation processes versus remobilization and leaching processes.

The only region where $^{9}Be_{reactive}$ does not significantly and positively correlate to $^{10}Be_{met}$ is the Nankai River watershed (the CHc study area). The lack of correlation between total $^{10}Be_{met}$ and $^{9}Be_{reactive}$ in this region may be because the Nankai River watershed is heavily cultivated, with the majority of streams in the catchment diverted to irrigate sugar and rice paddies that cover the valley (Nielson, 2016). Reducing conditions

in rice and sugar paddies (Zheng and Zhang, 2011) may be preventing natural biotic and abiotic mixing processes that allow $^{10}Be_{met}$ deposited on the surface and $^{9}Be$ weathering from buried regolith and bedrock to equilibrate in hillslopes.

### *5.4. Assumptions required to calculate $^{10}Be_{met}/^{9}Be_{reactive}$-derived denudation rates introduce uncertainties*

In order to determine denudation rates from $^{10}Be_{met}/^{9}Be_{reactive}$, (eq. 1), one needs to quantify $^{10}Be_{met}$ deposition rates, $^{9}Be$ concentrations of parent materials, and the fraction of $^{9}Be$ weathered from of parent materials (f.factor); these variables are difficult to determine accurately and precisely. Using eq. 2 or eq. 3 to estimate f.factor allows us to independently compare $^{10}Be_{met}/^{9}Be_{reactive}$ and $^{10}Be_{is}$-derived measures of denudation, but also includes assumptions that increase the uncertainty of $^{10}Be_{met}/^{9}Be_{reactive}$-derived denudation rates.

Using eq. 2 to estimate the f.factor assumes that the dissolved fraction of $^{9}Be$ is inconsequential and that there is negligible enrichment or depletion of $^{9}Be_{min}$ in sediments relative to parent bedrock. There are several reasons why these assumptions may not be valid. $^{9}Be_{reactive}$ concentrations are highest in fine-grained materials due to their high surface area to volume ratio (Wittmann et al., 2012) and the high cation exchange capacities of many clay minerals (Birkeland, 1999). This suggests that analyzing the sand-size fraction of fluvial sediments (250-850 μm) can lead to an underestimate of $^{9}Be_{reactive}$ concentrations.

In contrast, using eq. 3 to estimate f.factor assumes that the average parent $^{9}Be$ concentration in the watershed is the same as the mean global crustal abundance of Be,

and that the difference between $^{9}Be_{min}$ + $^{9}Be_{reactive}$ and 2.5 μg/g is represents the $^{9}Be_{diss}$ concentration. If the portion of the total $^{9}Be$ not included in $^{9}Be_{min}$ + $^{9}Be_{reactive}$ concentrations represents $^{9}Be_{min}$ from fine-grained materials, eq. 3 will overestimate the $^{9}Be_{diss}$ and f.factors. We observe that in every study area f.factors calculated with eq. 3 are higher than the other 2 methods of estimation (Fig. 8), indicating that eq. 3 is likely overestimating $^{9}Be_{diss}$ concentrations. Overall, discrepancies between f.factors calculated via the mass balance model (eq. 1'), f.factors estimated from measured $^{9}Be$ concentrations (eq. 2), and f.factors estimated from a combination of assumed and measured concentrations (eq. 3) highlight the difficulties finding agreement between modeled and observed Be dynamics in natural systems.

Estimating parent $^{9}Be$ concentrations also contributes uncertainty to the $^{10}Be_{met}/^{9}Be_{reactive}$-derived denudation rate calculation. We estimate parent $^{9}Be$ concentrations two ways; we either assume a $^{9}Be$ parent concentration of 2.5 μg/g (von Blanckenburg et al., 2012), or we assume parent $^{9}Be$ concentrations to be the mean $^{9}Be_{min}$ + $^{9}Be_{reactive}$ for each study area. Using the mean crustal abundance of $^{9}Be$ as the parent $^{9}Be$ concentration assumes that spatial heterogeneities in parent $^{9}Be$ concentrations average out to the global mean crustal abundance of $^{9}Be$. In contrast, using the mean $^{9}Be_{min}$ + $^{9}Be_{reactive}$ for each study area assumes that total measured $^{9}Be$ concentrations in fluvial sediments reflect $^{9}Be$ concentrations of unaltered source materials. Though the assumptions inherent in these estimates of parent $^{9}Be$ are different, calculating $^{10}Be_{met}/^{9}Be_{reactive}$-derived denudation rates both ways (eq. 2 and 3) results in a correlation with $^{10}Be_{is}$-derived denudation rates that has essentially the same ($R^2$ = 0.381 and $R^2$ = 0.378, respectively). Although neither method of estimating parent $^{9}Be$ concentrations

and f.factors introduces more variance into the correlation between denudation rates, the methods of estimating $^{9}Be_{parent}$ concentrations and f.factors can result in large differences between central tendencies in each study area and for all samples (Table 4). Using $^{9}Be_{min}$+$^{9}Be_{reactive}$-based assumptions, the mean $^{10}Be_{met}/^{9}Be_{reactive}$-derived denudation rate for all samples is 278% higher than the mean $^{10}Be_{is}$-derived denudation rate, but using 2.5 μg/g -based assumptions, the mean $^{10}Be_{met}/^{9}Be_{reactive}$-derived denudation rate for all samples is only 1% higher than the mean $^{10}Be_{is}$-derived denudation rate.

Though the best agreement between mean $^{10}Be_{met}/^{9}Be_{reactive}$-derived denudation rates and mean $^{10}Be_{is}$-derived denudation rates is found by assuming parent $^{9}Be$ concentrations of 2.5 μg/g (QLD), in 3 of the 7 individual study areas we find better agreement between denudation rates by using $^{9}Be_{min}$+$^{9}Be_{reactive}$-based assumptions for f.factor and parent concentrations (Table 4). In these 3 study areas (CHa, CHb, and CHc), using $^{9}Be_{min}$+$^{9}Be_{reactive}$ to estimate parent $^{9}Be$ concentrations and f.factors results in $^{10}Be_{met}/^{9}Be_{reactive}$ denudation rates that are on average 35% lower than $^{10}Be_{is}$-derived denudation rates, compared to an average 77% lower when using 2.5 μg/g based assumptions. All three of these study areas are located in tropical climates, and previous studies have found that significant portions of total $^{9}Be$ and $^{10}Be_{met}$ can be in the dissolved phase in these environments (Brown et al., 1992; Graly et al., 2010; Bacon et al., 2012; von Blanckenburg et al., 2012). If there is significant leaching of $^{9}Be$ from soils and sediments, $^{9}Be_{min}$+$^{9}Be_{reactive}$ based assumptions underestimate parent $^{9}Be$ concentrations because they do not include $^{9}Be$ in the dissolved phase, and subsequently result in $^{10}Be_{met}/^{9}Be_{reactive}$ denudation rates that are higher than those calculated with assumed $^{9}Be_{parent}$ of 2.5 ug/g. Further, because eq. 2 assumes that the $^{9}Be_{diss}$ is negligible,

regions with significant leaching have f.factors calculated via eq. 2 that are lower than f.factors calculated using eq. 3, also resulting in higher $^{10}Be_{met}/^{9}Be_{reactive}$-derived denudation rates. Considering the propensity for $^{9}Be_{min}+^{9}Be_{reactive}$-based assumptions to overestimate $^{10}Be_{met}/^{9}Be_{reactive}$ –derived denudation rates in regions with $^{9}Be$ leaching, the reason why $^{9}Be_{min}+^{9}Be_{reactive}$ based assumptions result in a more accurate estimate of $^{10}Be_{is}$-derived denudation rates in CHa, CHb, and CHc may be uncertainty in the calculated $^{10}Be_{met}$ delivery rates.

$^{10}Be_{met}$ delivery rate estimates contribute to uncertainty in $^{10}Be_{met}/^{9}Be_{reactive}$-denudation rate calculations due to poorly quantified contributions from dust flux and unknown pre-historic precipitation rates. Ouimet et al. (2015) found $^{10}Be_{met}$ deposition rates in the Boulder Creek Critical Zone Laboratory were 0.3-7 times lower than that predicted by global or annual precipitation-specific models in older sites (possibly due to leaching), but 1.5-4 times higher than predicted in younger sites (possibly due to added $^{10}Be_{met}$ contributions from snowdrifts or interflow). Reusser et al. (2010) found that the integrated $^{10}Be_{met}$ inventory of a well-dated 4.1 m in soil profile in New Zealand suggested that pre-historic precipitation rates in the region were 30% lower than contemporary estimates. Both of these studies suggest that long-term $^{10}Be_{met}$ delivery rates can be significantly different from contemporary values and that the most accurate estimates of $^{10}Be_{met}$ deposition rates require local calibration over the integration time represented by erosion rates. It is possible that the low estimates of $^{10}Be_{met}/^{9}Be_{reactive}$-derived denudation rates found in CHa, CHb, and CHc, are partially attributable to an underestimation of $^{10}Be_{met}$ delivery rates; this region of China has relatively few weather stations that contribute to the interpolated global precipitation database used for this study

(worldclim.org), potentially resulting in inaccurate MAP data in this part of the world. Further, precipitation data is interpolated from averaged precipitation rates measured from 1960-1990, which may not be representative of long-term precipitation regimes in this region.

Due to these uncertainties in $^{10}Be_{met}$ delivery rates, f.factors, and parent $^{9}Be$ concentration, statistically significant correlations between $^{10}Be_{is}$-derieved denudation rates and $^{10}Be_{met}/^{9}Be_{reactive}$-derived denudation rates do not exist unless we consider the entire dataset, which ranges over three orders of magnitude in $^{10}Be_{is}$-derieved denudation rates. Regardless of our method of estimating f.factor and parent $^{9}Be$ concentrations, we do not find that $^{10}Be_{met}/^{9}Be_{reactive}$-derived denudation rates and $^{10}Be_{is}$-derived denudation rates have strong and significant ($p < 0.05$, $R^2 > 0.30$) correlations in most individual study areas (Fig. 9). Furthermore, many study areas have a large difference between mean $^{10}Be_{is}$-derieved denudation rates and mean $^{10}Be_{met}/^{9}Be_{reactive}$-derived denudation rates (Table 4). It appears that in areas with a moderate range of denudation rates (one to two orders of magnitude), biogeochemical influences on $^{10}Be_{met}/^{9}Be_{reacitve}$ concentrations combined with the uncertainties in parent $^{9}Be$ concentrations, f.factor, and $^{10}Be_{met}$ delivery rates, obscure correlation between the $^{10}Be_{is}$ and $^{10}Be_{met}/^{9}Be_{reactive}$ measures of denudation rate.

*5.5. Basin characteristics do not primarily influence Be isotopes or denudation rates*

Many studies have found a positive correlation between basin scale denudation rates and total basin relief, in part because total relief co-varies with factors that are thought to control denudation rates in fluvial systems: slope and rates of rock uplift (Ahnert, 1970;

von Blanckenburg, 2005; Portenga and Bierman, 2011). Portenga and Bierman (2011) found significant correlations between $^{10}Be_{is}$-derived denudation rates and mean basin slope ($R^2 = 0.33$) and $^{10}Be_{is}$-derived denudation rates and total basin relief ($R^2 = 0.20$) in a diverse dataset of fluvial sediment samples (n = 1149). In our dataset, we also observe statistically significant positive correlations between $^{10}Be_{is}$-derived denudation rates and total basin relief ($R^2 = 0.55$) and mean basin slope ($R^2 = 0.46$), but we do not calculate strong correlations in the majority of individual study areas (Table 3). Much like $^{10}Be_{is}$-derieved denudation rates, $^{10}Be_{met}/^{9}Be_{reactive}$-derived denudation rates (calculated using $^{9}Be_{min}+^{9}Be_{reactive}$ as the $^{9}Be$ parent concentration) significantly correlate to mean basin slope ($R^2 = 0.17$, positive correlation) and to total basin relief ($R^2 = 0.42$, positive correlation) for all samples, but not in the majority of individual study areas (Table 3). $^{10}Be_{met}/^{9}Be_{reactive}$-derived denudation and $^{10}Be_{is}$-derived denudation rates both significantly correlate to MAP in the majority of study areas, but not across all data. These trends are in agreement with multivariate analysis of basin parameters and $^{10}Be_{is}$-denuation rates from Portenga and Bierman (2011), which found that the while the basin slope was nearly always the most significant parameter in a stepwise regression model for individual study areas, the remaining nine basin parameters (latitude, elevation, basin relief, MAP, mean annual temperature, seismicity, slope, percent vegetation, and basin area) were highly variable in terms of their regression power. It is likely that the environmental condition that most influences denudation rates varies by study area and depends on factors not considered in our analysis, such as whether or not a study area is tectonically active (Kober et al., 2007; Matmon et al., 2003), the contemporary climate (Peizhen et al., 2001), or the relative strength of bedrock (Palumbo et al., 2009).

We also compare $^{10}Be_{met}$ and $^{9}Be_{reactive}$ concentrations to basin parameters, which gives insight into the environmental conditions that may influence the generation or remobilization of grain coatings (Table 3). In three of the study areas, $^{10}Be_{met}/^{9}Be_{reactive}$ positively and significantly correlates to MAP. This correlation may be due to precipitation dependent $^{10}Be_{met}$ flux; Graly et al. (2011) found that at mid and low latitude study sites, meteoric $^{10}Be$ flux strongly correlates to precipitation ($R^2$ range from 0.93 to 0.98 in three mid-latitude study sites). However, the lack of strong and significant correlations between $^{10}Be_{met}/^{9}Be_{reactive}$ and other basin characteristics in the majority of study areas suggests that no single geomorphic variable has dominant influence on $^{10}Be_{met}/^{9}Be_{reactive}$. We do not observe strong and significant ($R^2 > 30$, p value $< 0.05$) correlations between $^{9}Be_{reactive}$, $^{10}Be_{met}$, or $^{10}Be_{met}/^{9}Be_{reactive}$ and any of the measured basin characteristics (latitude, elevation, MAP, mean basin slope, basin size, and total basin relief) when considering all data. The lack of significant bivariate correlations between $^{10}Be_{met}$ and $^{9}Be_{reactive}$ and basin parameters across all data supports our previous suggestion that when considering $^{10}Be_{met}$ and $^{9}Be_{reactive}$ data collected from many study areas, heterogeneities in $^{9}Be$ and $^{10}Be_{met}$ inputs and differing rates of denudation or remobilization introduce significant amounts of noise, likely obscuring correlations to basin characteristics if they exist.

*6.0 Conclusions*

Unlike $^{10}Be_{is}$, $^{10}Be_{met}$ and $^{9}Be_{reactive}$ are significantly influenced by geochemical and geomorphic conditions in watersheds; we do not observe the same trends in $^{10}Be_{met}$ concentrations as $^{10}Be_{is}$ concentrations within individual study areas or across all data.

Although normalizing $^{10}Be_{met}$ against $^{9}Be_{reactive}$ concentrations improves the correlation between $^{10}Be_{met}$ and $^{10}Be_{is}$ concentrations in fluvial sediments, the spatial variation in parent $^{9}Be$ concentrations and $^{10}Be_{met}$ delivery rates, combined with the observations that $^{10}Be_{met}$ and $^{9}Be$ are not always well mixed in soil systems and influenced by biogeochemical remobilization processes, makes interpreting changes in $^{10}Be_{met}/^{9}Be_{reactive}$ across study areas uncertain. The mass balance model for deriving $^{10}Be_{met}/^{9}Be_{reactive}$ denudation rates (eq. 1) helps control for some variation in $^{9}Be$ concentrations and $^{10}Be_{met}$ delivery rates across study areas, but uncertainties in quantifying these variables and unknown f.factors for each watershed introduce noise into the correlations between $^{10}Be_{met}/^{9}Be_{reactive}$-derived denudation rates and $^{10}Be_{is}$-derived denudation rates. Though overall $^{10}Be_{met}/^{9}Be_{reactive}$ mirrors $^{10}Be_{is}$-derived denudation rates, the $^{10}Be_{met}/^{9}Be_{reactive}$-derived measure is much less sensitive to changes in denudation than the $^{10}Be_{is}$-derived measure.

**Acknowledgements**

We thank Eric Portenga for helpful consideration of methods for calculating meteoric $^{10}Be/^{9}Be$-derived denudation rates. Funding supporting this work is from the University of Vermont and National Science Foundation and US Geological Survey grants: USGS-08ERSA0582, NSF-EAR-310208, NSF-ARC-1023191.

## Citations


Akciz, S., Burchfiel, B.C., Crowley, J.L., Jiyun, Y. and Liangzhong, C. (2008) Geometry, kinematics, and regional significance of the Chonng Shan shear zone, Eastern Himalayan Syntaxis, Yunnan, China *Geosphere* **4**(1), 292-314.

Aldahan, A., Ye, H.P. and Possnert, G. (1999) Distribution of beryllium between solution and minerals (biotite and albite) under atmospheric conditions and variable pH. *Chem. Geol.* **156**, 209-229.

Ahnert, F. (1970) Functional relationships between denudation, relief, and uplift in large mid-latitude drainage basins. *Am. J. Sci*. **268**, 243 – 263.

Bacon, A.R., Richter D., Bierman, P.R. and Rood, D.H. (2012) Coupling meteoric $^{10}$Be with pedogenic losses of $^{9}$Be to improve soil residence time estimates on an ancient North American interfluve. *Geology* **40**, 847-850.

Balco, G., Stone, J.O., Lifton, N. A. and Dunai. T.J. (2008) A quick and easily accessible means of calculating surface exposure ages or denudation rates from $^{10}$Be and $^{26}$Al measurements. *Quat. Geochronol.* **3**, 174-195.

Barg, E., Lal, D., Pavich, M. J., Caffee, M. W. and Southon, J. R. (1997) Beryllium geochemistry in soils; evaluation of $^{10}$Be/ $^{9}$Be ratios in authigenic minerals as a basis for age models. *Chem. Geol.* **140**, 237-258.

Bierman, P., and Nichols, K. (2004) Rock to sediment - Slope to sea with $^{10}$Be - Rates of landscape change. *Annu. Rev. Earth Planet. Sci.* **32,** 215-255.

Birkeland, P.W. (1999) *Soils and Geomorphology, 3rd edition*. Oxford University Press, Oxford.

Bourlès, D., Raisbeck, G.M. and Yiou, F. (1989) $^{10}$Be and $^{9}$Be in marine sediments and their potential for dating. *Geochim. Cosmochim. Acta* **53**, 443-452.

Brown, E.T., Edmond, J.M., Raisbeck, F.M., Bourlès, D.L., Yiou, F. and Measures, C.I. (1992) Beryllium isotope geochemistry in tropical river basins. *Geochim. Cosmochim. Acta* **56**, 1607-1624.

Burchfiel, B.C. and Zhiliang, C. (2012) *Tectonics of the southeastern Tibetan Plateau and its adjacent foreland*. Geologic Society of America, Inc. Boulder, CO. pp 100-104.

Campforts, B., Vanacker, V., Vanderborght, J., Baken, S., Smolders, E. and Govers, G. (2015) Simulating the mobility of meteoric $^{10}$Be in the landscape through a

coupled soil-hillslope model (Be2D). *Earth Planet. Sci. Lett.* **439**, 143-157. http://dx.doi.org/10.1016/j.epsl.2016.01.017

Cerling, T.E. and Turner, R.R. (1982) Formation of freshwater Fe-Mn coatings on gravel and the behavior of $^{60}$Co, $^{90}$Sr, and $^{137}$Cs in a small watershed. *Geochim. Cosmochim. Ac.* **46**, 1333-1343.

Crowley, J.W., Katz, R., Huybers, P., Langmuir, C.H. and Park, S. (2015) Glacial cycles drive variation in the production of oceanic crust. *Science* **347**, 1237-1240. DOI. 10.1126/science.1261508

Field, C.V., Schmidt, G.A., Koch, D., and Salyk, C. (2006). Modeling production of climate-related impacts on $^{10}$Be concentration in ice cores. *J. Geophys. Res.* **111***,* D15107.

Fishbein, L. (1984) Overview of analysis of carcinogenic and/or mutagenic metals in biological and environmental samples. *Int. J. Environ. Anal. Chem.* **12**, 113-170.

Gosse, J.C. and Phillips, F.M. (2001) Terrestrial *in situ* cosmogenic nuclides: theory and application. *Quat. Sci. Rev.* **20**, 1475-1560.

Graly, J.A., Bierman, P.R., Reusser, L.J. and Pavich, M.J. (2010) Meteoric $^{10}$Be in soil profiles - a global meta-analysis. *Geochim. Cosmochim. Acta* **74**, 6814-6829.

Graly, J.A., Reusser, L.J. and Bierman, P.R. (2011) Short and long-term delivery rates of meteoric $^{10}$Be to terrestrial soils. *Earth Planet. Sci. Lett.* **302**, 329-336.

Granger. D.E. and Schaller, M. (2014) Cosmogenic nuclides and denudation at the watershed scale. *Elements* **10**, 369-393. http://dx.doi.org/10.2113/gselements.10.5.369.

Grew, E.S. (2002) Beryllium in metamorphic environments (emphasis on aluminous compositions). *Rev. Mineral. Geochem.* **50**, 487-549.

Heikkila, U., Beer, J. and Alfimov, V. (2008) Beryllium-10 and beryllium-7 in precipitation in Dubendorf (440 m) and at Jungfraujoch (3580 m), Switzerland 1998-2005. *J. Geophys. Res.* **113**, D11104. doi:10.1029/2007JD009160.

Hunt, A.L., Larsen, J., Bierman, P.R. and Petrucci, G.A. (2008) Investigation of factors that affect the sensitivity of accelerator mass spectrometry for cosmogenic $^{10}$Be and $^{26}$Al isotope analysis. *Anal. Chem.,* **80,** 1656-1663.

Jungers, M.C., Bierman, P.R., Matmon, A., Nichols, K., Larsen, J. and Finkel, R. (2009) Tracing hillslope sediment production and transport with *in situ* and meteoric $^{10}$Be. *J. Geophys. Res.* **114**, F04020.

Kober, F., Ivy-Ochs, S., Schlunegger, F., Baur, H., Kubik, P.W. and Wieler, R. (2007) Denudation rates and a topography-driven rainfall threshold in northern Chile: Multiple cosmogenic nuclide data and sediment yield budgets. Geomorphology **83**, 97–120.

Kohl, C.P. and Nishiizumi, K. (1992) Chemical isolation of quartz for the measurement of *in situ*-produced cosmogenic nuclides. *Geochim. Cosmochim. Acta* **56**, 3583-3587.

Kramida, A., Ralchenko, Y., Reader, J. and NIST ASD Team (2015) NIST Atomic Spectra Database (ver. 5.3). Available: http://physics.nist.gov/asd. National Institute of Standards and Technology, Gaithersburg, MD.

Lal, D. and Peters, B. (1967) Cosmic ray produced radioactivity on the earth. *Handbuch der Physik*. Springer, Berlin. pp. 551-612.

Lal, D. (1988) *In situ*-produced cosmogenic isotopes in terrestrial rocks. *Annu. Rev. Earth Planet. Sci.* **16**, 355-388.

Lal, D. (1991) Cosmic ray labeling of denudation surfaces: *in situ* nuclide production rates and denudation models. *Earth Planet. Sci. Lett.* **104,** 424-439.

Lal, D. (2007) Recycling of cosmogenic nuclides after their removal from the atmosphere; special case of appreciable transport of $^{10}$Be to polar regions by Aeolian dust. *Earth Planet. Sci. Lett.* **2007**, 177-187.

Lundberg, L., Ticich, T., Herzog, G.F., Hughes, T., Ashley, G., Moniot, R.K., Tuniz, C., Kruse, T. and Savin, W. (1983) $^{10}$Be and Be in the Maurice River-Union Lake system of southern New Jersey. *J. Geophys. Res*. **88**, 4498-4504.

Matmon, A.S., Bierman, P., Larsen, J., Southworth, S., Pavich, M., Finkel, R. and Caffee, M. (2003) Erosion of an ancient mountain range, the Great Smoky Mountains, North Carolina and Tennessee. *Am. J. Sci.* **303**, 817–855.

McHarque, L.R. and Damon, P.E. (1991) The global beryllium-10 cycle. *Rev. Geophys.* **29**, 141-158.

McKean, J., Dietrich, W. E., Finkel, R. C., Southon, J. R. and Caffee, M. W. (1993) Quantification of soil production and downslope creep rates from cosmogenic $^{10}$Be accumulations on a hillslope profile. *Geology* **22**, 343-346.

Measures, C.I. and Edmond, J.M. (1983) The geochemical cycle of $^{9}$Be: a reconnaissance. *Earth Planet. Sci. Lett.* **66**, 101-110.

Meehan, W.R. and Smythe, L.E. (1967) Occurrence of beryllium as a trace element in environmental materials. *Environ. Sci. Technol.* **10**, 839-844.

Neilson, T.B. (2016) Using long- and short-lived sediment-associated isotopes to track denudation and sediment movement through rivers in Yunnan, SW China, Geology. M.S. thesis. Univ. of Vermont.

Nichols, K.K., Bierman, P.R. and Rood, D.H. (2014) $^{10}$Be constrains the sediment sources and sediment yields to the Great Barrier Reef from the tropical Barron River catchment, Queensland, Australia. *Geomorphology*. **224**, 102-110.

Ouimet, W., Dethier, D., Bierman, P., Wyshnystzky, C., Shea, N. and Rood, D. (2015) Spatial and temporal variations in meteoric $^{10}$Be inventories and long-term deposition rates, Colorado Front Range. *Quat. Sci. Rev.* **109**, 1-12.

Palumbo, L., Hetzel, R., Tao, M. and Li, X. (2009) Topographic and lithologic control on catchment-wide denudation rates derived from cosmogenic $^{10}$Be in two mountain ranges at the margin of NE Tibet. *Geomorphology*, **117**, 130–142.

Pavich, M.P., Brown, L., Klein, J. and Middleton, R. (1984) $^{10}$Be accumulation in a soil chronosequence. *Earth Planet. Sci. Lett.* **68**, 198-204.

Peizhen, Z., Molnar, P. and Downs, W.R. (2001) Increased sedimentation rates and grain sizes 2–4 Myr ago due to the influence of climate change on erosion rates. *Nature* **410**, 891–897.

Portenga, E.W. and Bierman P.R. (2011) Understanding Earth's eroding surface with $^{10}$Be. *GSA Today* **21**, 4-10.

Raymo, M.E., Ruddiman, W.F. and Froelich, P.N. (1988) Influence of late Cenozoic mountain building on ocean geochemical cycles. *Geology* **16**, 649-653.

Reusser, L., Graly, J., Bierman, P. and Rood, D. (2010) A long-term meteoric $^{10}$Be accumulation rate in soil. *Geophys. Res. Lett.* **37**, L19403. doi:10.1029/2010GL044751

Ridge, J.C., Balco, G., Bayless, R.L., Beck, C.C., Carter, L.B., Dean, J.L., Voytek, E.B. and Wei, J.H. (2012) The new North American Varve Chronology: a precise record of southeastern Laurentide Ice Sheet deglaciation and climate, 18.2-12.5 kyr bp, and correlations with Greenland ice core records. *Am. J, Sci*. **312**, 685-722.

Ruppert, L.F., Tewalt, S.J., Wallack, R.N., Bragg, L.J., Brezinski, D.K., Carlton, R.W., Butler, D.T. and Calef, F.J. (2000) A digital resource model of the middle Pennsylvanian Upper Freeport Coal Bed, Allegheny Group, Northern Appalachian Basin Coal Region. U.S. Geologic Survey Professional Paper 1625-C.

Staudigel, H., Albarede, F., Blichert-Toft, J., Edmond, J., McDonough, B., Jacobsen, S.B., Keeling, R., Langmuir, C.H., Nielsen, R.L., Plank, T., Rudnick, R., Shaw, H.F., Shirey, S., Veizer, J. and White, W. (1998) Geochemical Earth Reference Model (GERM): description of the initiative. *Chem. Geol.* **145**, 153–159.

Stone, J. (1998) A rapid fusion method for separation of beryllium-10 from soils and silicates. *Geochim. Cosmochim. Acta.* **62,** 555-561.

Stoops, G., Marcelino, V. and Mees, F. (2010) Micromorphological features and their relation to processes and classification, interpretation of micromorphological features of soils and regoliths. Elsevier, Amsterdam, pp. 15-35.

Takahashi, M., Ambe, S., Makide, Y. and Ambe, F. (1999) Comparison of adsorption behavior of multiple inorganic ions on kaolinite and silica in the presence of humic acid using the multi-tracer technique. *Geochim. Cosmochim. Acta* **63**, 815-836.

Taylor, A., Blake, W.H., Couoldrick, L. and Keith-Roach, M.J. (2012) Sorption behavior of beryllium-7 and implications for its use as a sediment tracer. *Geoderma*, *187-188,* 16-23.

Tessier, A., Campbell, P.G.C. and Bisson, M. (1979) Sequential extraction procedure for the speciation of trace metals. *Analytical Chem.* **51,** 844-851.

Trodick, C.D. (2011) *In situ* and meteoric $^{10}$Be concentrations of fluvial sediment collected from the Potomac River Basin. Univ. of Vermont.

Vance, D., Teagle, D. and Foster, G. (2009) Variable Quaternary chemical weathering fluxes and imbalances of marine geochemical budgets. *Nature* **458**, 493-496.

Veselý J.S., Norton, A., Skřivan, P., Majer, V., Krám, P., Navrátil, T. and Kaste, J.M. (2002) Environmental Chemistry of Beryllium. *Rev. Mineral. Geochem.* **50**, 291-317.

von Blanckenburg, F. (2005) The control mechanisms of denudation and weathering at basin scale from cosmogenic nuclides in river sediment. *Earth Planet. Sci. Lett.* **237**, 462-479.

von Blanckenburg, F., Bouchez, J. and Wittmann, H. (2012) Earth surface denudation and weathering from the $^{10}$Be (meteoric)/$^{9}$Be ratio. *Earth Planet. Sci. Lett.* **351**, 295-305.

von Blanckenburg, F. and Bouchez, J. (2014) River fluxes to the sea from the ocean's $^{10}$Be/$^{9}$Be ratio. *Earth Planet. Sci. Lett.* **387**, 34-43.

von Blanckenburg, F., Bouchez, J., Ibarra, D. and Maher, K. (2015) Stable runoff and weathering fluxes into the oceans over Quaternary climate cycles. *Nature Geoscience*. **8**, 538-542.

West, N., Kirby, E., Bierman, P., Slingerland, R., Ma., L., Rood, D. and Brantley, S. (2013) Regolith production and transport at Susquehanna Shale Hills Critical Zone Observatory, part 2: insights from meteoric $^{10}$Be. *J. Geophys. Res. F.* **118,** 1877-1896.

Willenbring, J. and von Blanckenburg, F. (2010) Meteoric cosmogenic Beryllium-10 adsorbed to river sediment and soil: applications for Earth-surface dynamics. *Earth-Sci. Rev*. **98**, 105-122.

Wittmann, H., von Blanckenburg, F., Bouchez, J., Dannhaus, N., Naumann, R., Christl, M. and Gaillardet, J. (2012) The dependence of meteoric $^{10}$Be concentrations on particle size in Amazon River bed sediment and the extraction of reactive $^{10}$Be/$^{9}$Be ratios. *Chem. Geol.* **318**, 126-138.

You, C.-F., Lee, T. and Li, Y.H. (1989) The partition of Be between soil and water. *Chem. Geol.* **77**, 105-118.

You, C.-F., Morris, J., Gieskes, J., Rosenbauer, R., Zheng, S., Xu, X., Ku, T. and Bischoff, J. (1994) Mobilization of beryllium in the sedimentary column at convergent margins *Geochim. Cosmochim. Acta* **58**, 4887-4897.

Zheng, S.A. and Zhang, M.K. (2011) Effect of moisture regime on the redistribution of heavy metals in paddy soil. *J Environ. Sci. China* **23**, 434-443.

# Tables

Table 1.

Physical characteristics of the studied watersheds.

| Location | Climate | Tectonic setting | Bedrock description | ID | n | MAP [a] (mm/yr) | Mean basin [b] size ($km^2$) | Median basin [b] size ($km^2$) | Mean elevation [b] (m) | Mean total relief [b] (m) | Mean latitude [b] (degrees) |
|---|---|---|---|---|---|---|---|---|---|---|---|
| Potomac River | temperate, never glaciated | passive margin | gneiss, sandstone, shale and carbonates | **POT** | 62 | 730-1030 | 1050 | 21 | 354 | 330 | 39.1 |
| Barron River (NE Australia | humid, temperate, never glaciated | passive margin | granite and biogenetic carbonate | **QLD** | 8 | 1930-2250 | 330 | 33 | 475 | 730 | 16.9 |
| Georges River (SE Australia) | humid, temperate, never glaciated | passive margin | sandstone, granodiorite | **G** | 14 | 970-1260 | 90 | 41 | 390 | 730 | 41.3 |
| China, Mekong River (SE China) | tropical, never glaciated | tectonically active | lightly metamorphosed granite and sedimentary red beds | **CH1xx** | 64 | 510-1660 | 28200 | 3900 | 2290 | 2880 | 25.4 |
| | | | | **CHa** | 15 | 960-1040 | 40 | 19 | 3040 | 960 | 27.1 |
| | | | | **CHb** | 24 | 1080-1250 | 580 | 220 | 1700 | 1450 | 24.0 |
| | | | | **CHc** | 15 | 1520-1610 | 140 | 38 | 1596 | 790 | 21.8 |

[a] Mean annual precipitation (MAP) data downloaded with 30 arc-second resolution from www.worldclim.org/tiles.php.

[b] Mean basin size, mean elevation, mean total relief, and mean latitude calculated for the upstream watershed area of each sample location using the ArcGIS hydrology toolset on the Shuttle Radar Topography Mission (STRM) 1 arc-second global elevation dataset, www.earthexplorer.usgs.gov.

Table 2.

$R^2$ and p values of correlations between Be isotope data for each study area and for all samples.

| | | $^{9}Be_{reactive}$ vs. $^{10}Be_{met}$ | | $^{10}Be_{is}$ vs. $^{10}Be_{met}/^{9}Be_{reactive}$ | | $^{10}Be_{is}$ vs. $^{10}Be_{met}$ | | $^{10}Be_{is}$ denudation rate vs. $^{10}Be_{met}/^{9}Be_{reactive}$ | |
|---|---|---|---|---|---|---|---|---|---|
| Study | n | $R^2$ | p | $R^2$ | p | $R^2$ | p | $R^2$ | p |
| POT | 62 | **0.50** [a] | **<0.01** | 0.00 | 0.83 | 0.07 | 0.05 | 0.03 | 0.18 |
| QLD | 14 | **0.75** | **<0.01** | 0.19 | 0.12 | 0.03 | 0.58 | <0.01 | 0.84 |
| G | 8 | **0.99** | **<0.01** | 0.36 | 0.12 | 0.45 | 0.07 | 0.33 | 0.14 |
| CH1xx | 64 | **0.39** | **<0.01** | **0.53** | **<0.01** | **0.52** | **<0.01** | 0.13 | <0.01 |
| CHa | 15 | **0.75** | **<0.01** | **0.45** | **<0.01** | 0.18 | 0.12 | 0.28 | 0.04 |
| CHb | 24 | **0.31** | **<0.01** | **0.63** | **<0.01** | 0.19 | 0.03 | 0.27 | 0.01 |
| CHc | 15 | 0.03 | 0.53 | 0.05 | 0.43 | 0.00 | 0.88 | 0.09 | 0.28 |
| All samples | 202 | 0.08 | <0.01 | **0.58** | **<0.01** | **0.40** | **<0.01** | 0.11 | <0.01 |

[a] Bolded font highlights statistically correlations significant ($p<0.05$) and $R^2 > 0.30$.

Table 3.

$R^2$ and p values of correlations between Be isotopes concentrations and MAP, mean basin slope, and total relief for each study area and for all samples.

| | | | $^{10}Be_{in situ}$ | | $^{10}Be_{meteoric}/^{9}Be_{carrier}$ | | $^{10}Be_{in situ}$ denudation rate | | $^{10}Be_{meteoric}/^{9}Be_{carrier}$-derived denduation rate [a] | |
|---|---|---|---|---|---|---|---|---|---|---|
| study ID | n | basin parameter | $R^2$ | p | $R^2$ | p | $R^2$ | p | $R^2$ | p |
| POT | 62 | MAP [b] | 0.03 | 0.21 | 0.01 | 0.56 | 0.12 | <0.01 | 0.08 | 0.03 |
| | | mean basin slope [c] | <0.01 | 0.86 | 0.03 | 0.17 | 0.06 | 0.05 | 0.05 | 0.09 |
| | | total relief [c] | <0.01 | 0.96 | 0.05 | 0.07 | 0.01 | 0.44 | 0.03 | 0.16 |
| | | mean elevation | <0.01 | 0.75 | 0.04 | 0.11 | 0.07 | 0.04 | 0.11 | 0.01 |
| | | mean latitude | 0.12 | 0.01 | 0.01 | 0.39 | 0.04 | 0.12 | 0.04 | 0.14 |
| | | basin size | 0.02 | 0.29 | <0.01 | 0.66 | 0.02 | 0.31 | <0.01 | 0.90 |
| QLD | 14 | MAP | 0.09 | 0.31 | **0.36** [a] | **0.02** | 0.27 | 0.06 | **0.46** | **0.01** |
| | | mean basin slope | 0.06 | 0.41 | 0.20 | 0.11 | **0.53** | **<0.01** | 0.17 | 0.14 |
| | | total relief | 0.03 | 0.55 | 0.01 | 0.72 | <0.01 | 0.95 | <0.01 | 0.83 |
| | | mean elevation | 0.07 | 0.38 | 0.02 | 0.67 | 0.23 | 0.09 | 0.07 | 0.37 |
| | | mean latitude | 0.05 | 0.46 | 0.04 | 0.51 | 0.07 | 0.36 | 0.02 | 0.04 |
| | | basin size | 0.06 | 0.42 | 0.13 | 0.21 | 0.10 | 0.26 | 0.14 | 0.19 |
| G | 8 | MAP | **0.91** | **<0.01** | **0.59** | **0.02** | **0.77** | **<0.01** | **0.56** | **0.03** |
| | | mean basin slope | 0.40 | 0.09 | 0.07 | 0.52 | 0.09 | 0.47 | 0.05 | 0.59 |
| | | total relief | 0.13 | 0.38 | 0.28 | 0.18 | 0.03 | 0.68 | 0.26 | 0.19 |
| | | mean elevation | **0.79** | **<0.01** | 0.51 | 0.05 | **0.88** | **<0.01** | **0.52** | **0.04** |
| | | mean latitude | 0.12 | 0.39 | 0.01 | 0.87 | 0.18 | 0.29 | 0.01 | 0.79 |
| | | basin size | 0.06 | 0.55 | 0.04 | 0.62 | 0.09 | 0.48 | 0.25 | 0.63 |
| CH1xx | 64 | MAP | 0.01 | 0.44 | 0.03 | 0.21 | 0.24 | <0.01 | 0.09 | 0.02 |
| | | mean basin slope | 0.02 | 0.25 | 0.02 | 0.22 | 0.12 | <0.01 | <0.01 | 0.76 |
| | | total relief | 0.01 | 0.36 | 0.10 | 0.01 | 0.26 | <0.01 | 0.08 | 0.02 |
| | | mean elevation | 0.01 | 0.50 | 0.03 | 0.18 | 0.25 | <0.01 | 0.09 | 0.02 |
| | | mean latitude | 0.01 | 0.58 | 0.06 | 0.04 | **0.66** | **<0.01** | 0.15 | <0.01 |
| | | basin size | <0.01 | 0.85 | 0.04 | 0.11 | 0.27 | <0.01 | 0.07 | 0.03 |
| CHa | 15 | MAP | **0.69** | **<0.01** | **0.30** | **0.04** | **0.43** | **<0.01** | 0.24 | 0.06 |
| | | mean basin slope | **0.78** | **<0.01** | 0.17 | 0.12 | **0.39** | **0.01** | 0.14 | 0.18 |
| | | total relief | 0.29 | 0.03 | 0.26 | 0.05 | 0.10 | 0.25 | 0.04 | 0.49 |
| | | mean elevation | **0.58** | **<0.01** | **0.35** | **0.02** | **0.33** | **0.03** | **0.41** | **0.01** |
| | | mean latitude | **0.66** | **<0.01** | 0.18 | 0.12 | **0.30** | **0.04** | **0.36** | **0.02** |
| | | basin size | <0.01 | 0.84 | 0.03 | 0.52 | 0.01 | 0.80 | <0.01 | 0.94 |
| CHb | 24 | MAP | 0.34 | **<0.01** | 0.16 | 0.06 | 0.29 | <0.01 | 0.06 | 0.23 |
| | | mean basin slope | 0.08 | 0.18 | 0.01 | 0.06 | 0.22 | 0.02 | 0.03 | 0.43 |
| | | total relief | 0.04 | <0.01 | **0.37** | **<0.01** | 0.21 | 0.03 | 0.28 | 0.01 |
| | | mean elevation | 0.03 | 0.42 | 0.1 | 0.13 | 0.02 | 0.54 | 0.08 | 0.04 |
| | | mean latitude | **0.31** | **<0.01** | 0.09 | 0.15 | **0.36** | **<0.01** | 0.02 | 0.46 |
| | | basin size | 0.11 | 0.11 | 0.08 | 0.18 | 0.04 | 0.32 | 0.03 | 0.39 |
| CHc | 15 | MAP | 0.05 | 0.41 | **0.33** | **0.02** | 0.10 | 0.26 | **0.38** | **0.02** |
| | | mean basin slope | 0.33 | **0.02** | **0.06** | **<0.01** | 0.22 | 0.08 | **0.37** | **0.02** |
| | | total relief | <0.01 | 0.93 | 0.04 | 0.48 | <0.01 | 0.85 | 0.22 | 0.08 |
| | | mean elevation | 0.04 | 0.47 | 0.01 | 0.77 | 0.01 | 0.76 | 0.01 | 0.75 |
| | | mean latitude | **0.61** | **<0.01** | 0.04 | 0.37 | **0.47** | **<0.01** | 0.07 | 0.32 |
| | | basin size | 0.03 | 0.51 | 0.01 | 0.79 | <0.01 | 0.95 | 0.04 | 0.50 |
| All samples | 202 | MAP | <0.01 | 0.53 | 0.03 | 0.01 | 0.01 | 0.18 | <0.01 | 0.45 |
| | | mean basin slope | <0.01 | 0.46 | 0.03 | 0.01 | **0.46** | **<0.01** | 0.17 | <0.01 |
| | | total relief | 0.02 | 0.03 | 0.11 | <0.01 | **0.55** | **<0.01** | **0.42** | **<0.01** |
| | | mean elevation | 0.08 | 0.07 | <0.01 | 0.62 | **0.43** | **<0.01** | 0.22 | <0.01 |
| | | mean latitude | 0.01 | 0.25 | 0.03 | 0.01 | 0.10 | <0.01 | 0.05 | <0.01 |
| | | basin size | 0.01 | 0.09 | 0.04 | 0.01 | **0.33** | **<0.01** | 0.24 | <0.01 |

[a] Bold text highlights correlations with a p value < 0.05 and $R^2$ > 0.30.

[b] Mean annual precipitation (MAP) data downloaded with 30 arc-second resolution from worldclim.org.

[c] Mean basin size, mean elevation, mean total relief, and mean latitude calculated for the upstream watershed area of each sample location using the ArcGIS hydrology toolset on the Shuttle Radar Topography Mission (SRTM) 1 arc-second global elevation dataset, www.earthexplorer.usgs.gov.

[d] $^{10}Be_{meteoric}/^{9}Be_{carrier}$-derived denduation rates are calculated using the mean basin f.factor using eq. 2 and the mean parent $^{10}Be$ concentration estimated from the sum of $^{10}Be_{in}$ and $^{10}Be_{meteoric}$.

Table 4.

Mean denudation rates calculated from $^{10}Be_{is}$ and $^{10}Be_{met}/^{9}Be_{reactive}$ mass balance model (eq. 1) with $^{9}Be$ parent concentrations either assumed to be 2.5 ppm or the mean $^{9}Be_{min}+^{9}Be_{reactive}$ for each basin.

| Study | mean $^{10}Be_{is}$-derived denudation rate [a] | mean $^{10}Be_{met}/^{9}Be_{reactive}$-derived denudation rate (total parent $^{9}Be$ = 2.5) [b] | percent difference from $^{10}Be_{is}$-derived denudation rate | mean $^{10}Be_{met}/^{9}Be_{reactive}$-derived denudation rate (total parent = $^{9}Be_{min}+^{9}Be_{reactive}$) [b] | percent difference from $^{10}Be_{is}$-derived denudation rate |
|---|---|---|---|---|---|
| | t km$^{-2}$ yr$^{-1}$ | t km$^{-2}$ yr$^{-1}$ | % | t km$^{-2}$ yr$^{-1}$ | % |
| POT | 30 ± 16 | 40 ± 26 | 35 | 141 ± 89 | 370 |
| QLD | 74 ± 45 | 81 ± 28 | 10 | 476 ± 162 | 543 |
| G | 44 ± 22 | 30 ± 4 | 35 | 133 ± 18 | 202 |
| CH1xx | 403 ± 268 | 552 ± 396 | 37 | 2030 ± 1450 | 404 |
| CHa | 160 ± 142 | 14 ± 14 | -91 | 24 ± 14 | -85 |
| CHb | 311 ± 88 | 42 ± 15 | -86 | 259 ± 91 | -17 |
| CHc | 128 ± 39 | 61 ± 33 | -52 | 113 ± 61 | -12 |
| all samples | 202 ± 226 | 205 ± 226 | 1 | 768 ± 1190 | 278 |

[a] calculated with the CRONUS erosion rate calculator (Balco et al., 2008) in previous studies (Trodick, 2011; Portenga and Bierman, 2011; Nichols et al., 2014; Nielson, 2016 )

[b] total parent assumption applied to f.factor calculation and $^{9}Be_{parent}$; mean $^{10}Be_{met}$ deposition rate is used for each study area


Fig. 1. Locations of study areas and associated coding. Numbers represent the number of fluvial sediment samples with previously measured $^{10}Be_{is}$ and $^{10}Be_{met}$.

Greene et al., FIGURE 1

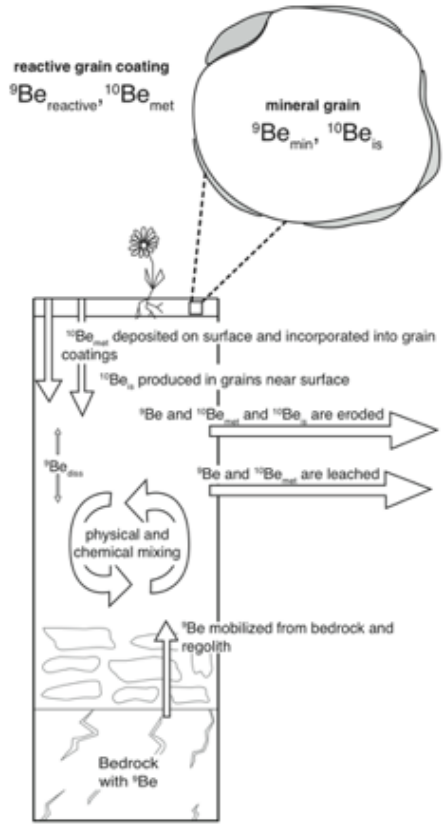


Fig. 2. Schematic diagram of $^{10}Be_{is}$, $^{10}Be_{met}$ and $^{9}Be$ behavior in a typical soil system.

Greene et al., FIGURE 2

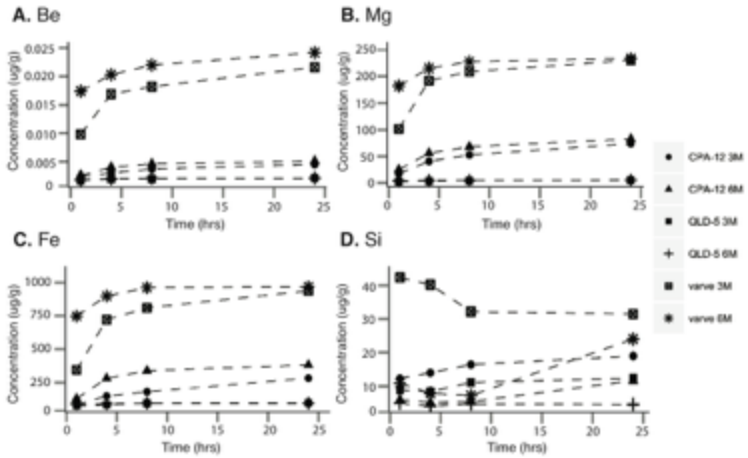


Fig. 3. Evolution of 6M and 3M HCl-extractable elemental concentrations from selected samples over time for (A) Be, (B) Mg, (C) Fe, and (D) Si. CPA-12 is a soil sample from Scotland. QLD-5 is a fluvial sediment sample from Queensland, Australia, and varve is a homogenized lab standard from the New England Varve Chronology (Ridge et al., 2012).

Greene et al., FIGURE 3

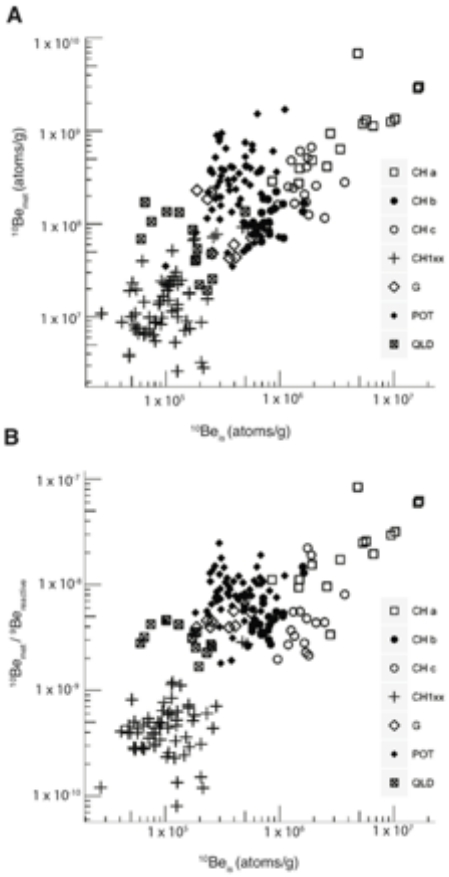


Fig. 4. Correlation between (A) $^{10}Be_{met}$ and $^{10}Be_{is}$, $R^2 = 0.40$, $p < 0.01$ and (B) $^{10}Be_{met}/^{9}Be_{reactive}$ and $^{10}Be_{is}$, $R^2 = 0.58$, $p < 0.01$.

Greene et al., FIGURE 4

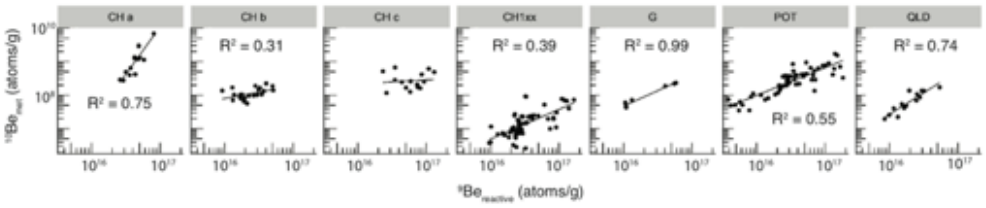


Fig. 5. Comparison of $^{10}Be_{met}$ and $^{9}Be_{reactive}$ concentrations for each study area. All study areas denoted with $R^2$ have $p < 0.05$.

Greene et al., FIGURE 5

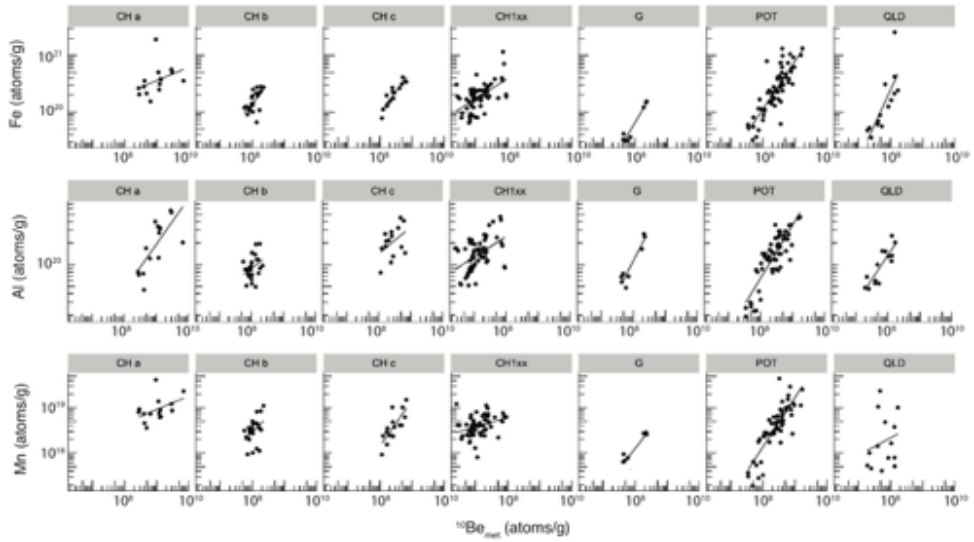


Fig. 6. Correlations between $^{10}Be_{met}$ and HCl-extractable Al, Fe, and Mn for each individual study area.

Greene et al., FIGURE 6

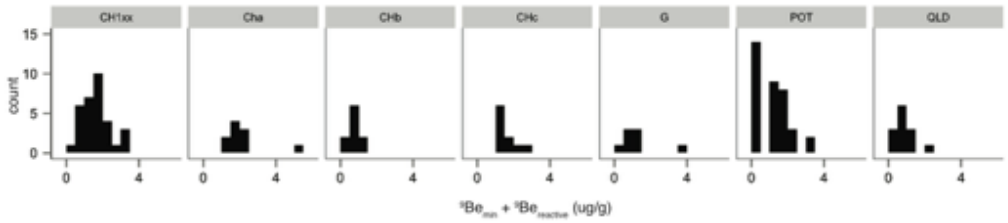


Fig. 7. Histograms of $^{9}Be_{min}$+$^{9}Be_{reactive}$ concentrations in each study area.

Greene et al., FIGURE 7

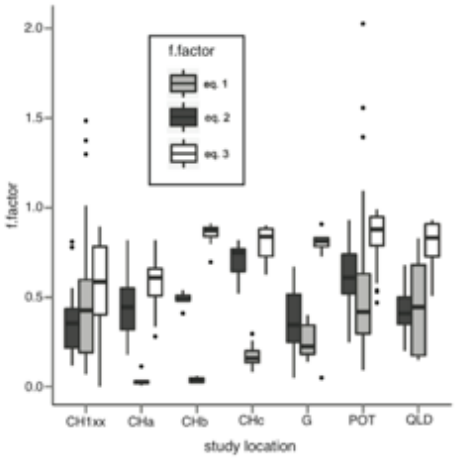


Fig. 8. Boxplot of f.factors calculated with eq. 1, eq. 2 and eq. 3 for each catchment. Dark horizontal lines represent the median, boxes represent the 1st and 3rd quartile, vertical lines represent 95th and 5th percentiles, and points represent data that fall outside of the 95th percentile.

Greene et al., FIGURE 8

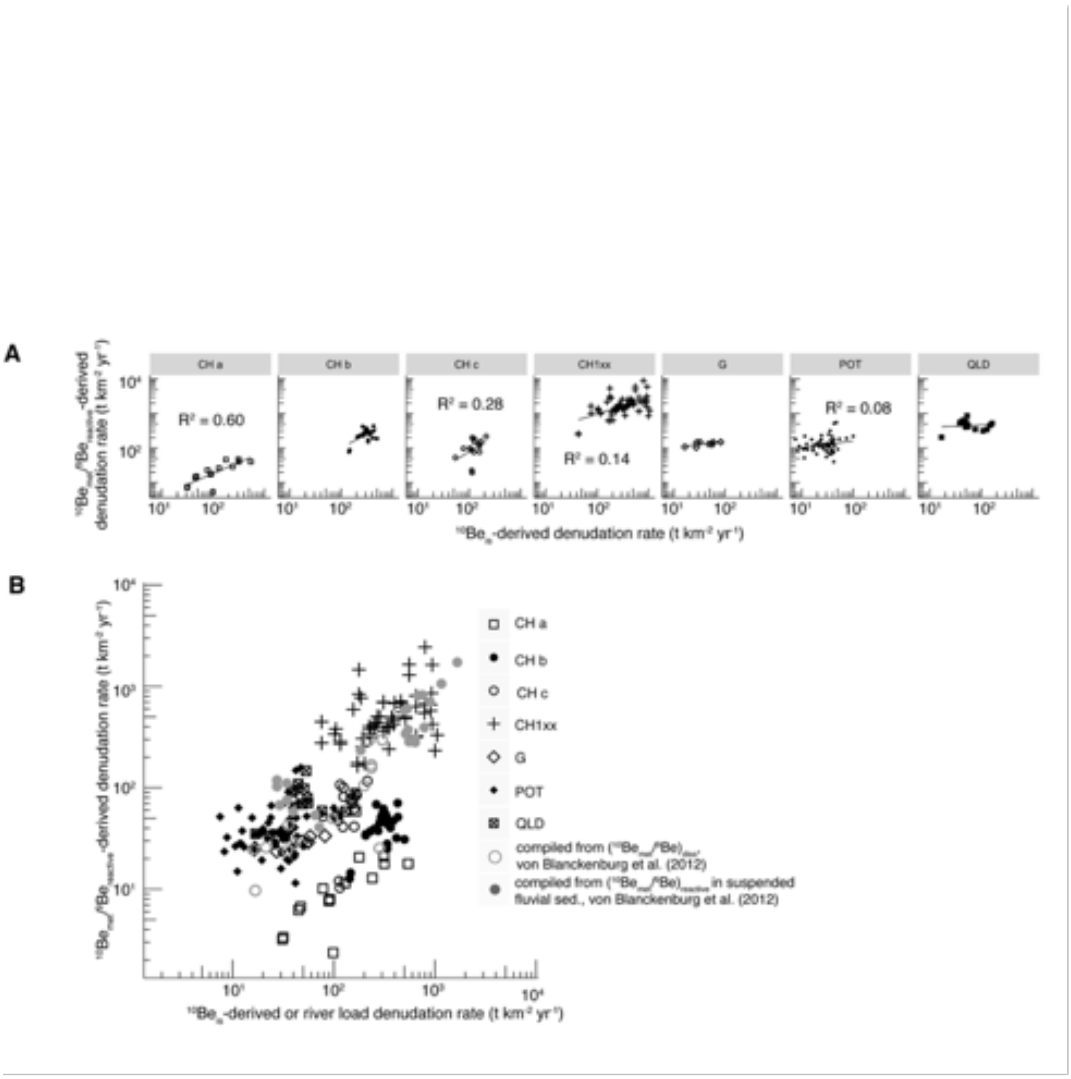


Fig. 9. (A) Comparison of catchment-wide denudation rates calculated from eq. 1 using mean basin-specific f.factors calculated via eq. 2, mean basin-specific parent $^{9}Be$ estimated using $^{9}Be_{min}$+$^{9}Be_{reactive}$, mean basin-specific $^{10}Be_{met}$ deposition rates, and measured $^{10}Be_{met}/^{9}Be_{reactive}$ for each sample. All study areas denoted with $R^2$ have $p < 0.05$; other study areas do not have a statistically significant correlation ($p \geq 0.05$). (B) Black data are an aggregated correlation plot ($p < 0.01$) from all study areas with $^{10}Be_{met}/^{9}Be_{reactive}$-derived denudation rates calculated with mean basin-specific f.factors from eq. 3, an assumed parent $^{9}Be$ concentration of 2.5 µg/g, mean basin-specific $^{10}Be_{met}$ delivery rates, and measured $^{10}Be_{met}/^{9}Be_{reactive}$ for each sample, ($R^2 = 0.38$), and grey data are compiled by von Blanckenburg et al. (2012). Grey open circles are denudation rates calculated from $(^{10}Be_{met}/^{9}Be)_{diss}$, with the x-axis representing suspended sediments and dissolved loads collected in various rivers (von Blanckenburg et al., 2012). Grey closed circles are denudation rates calculated from $^{10}Be_{met}/^{9}Be_{reactive}$ in suspended fluvial sediments, with the x-axis representing $^{10}Be_{is}$-derived denudation rates determined from the same samples (von Blanckenburg et al., 2012).

Greene et al. FIGURE 9

**calibration parameters**

| poly/mono | element | line (nm) | calibration weighting parameter | L background (nm) | R background (nm) | variables in calibration curve fit |
|---|---|---|---|---|---|---|
| poly | Al | 309.271 | 1/c | 0.075 | 0.069 | 2 |
| poly | Be | 234.861 | 1/sqrt C | NA | 0.02 | 2 |
| mono | Be | 234.861 | 1/sqrt(c) | 0.018 | 0.018 | 2 |
| poly | Be | 313.042 | 1/sqrt(std) | NA | 0.036 | 2 |
| mono | Be | 313.042 | 1/sqrt(std) | 0.036 | NA | 2 |
| mono | Be | 313.107 | 1/sqrt C | 0.018 | 0.018 | 2 |
| poly | Ca | 313.997 | 1/c | 0.096 | 0.096 | 2 |
| poly | Fe | 271.441 | 1/c | 0.03 | 0.036 | 2 |
| poly | K | 766.49 | $1/c^2$ | 0.036 | 0.024 | 2 |
| poly | Mg | 279.079 | 1/sqrt C | 0.036 | NA | 2 |
| poly | Mn | 259.373 | 1/sqrt C | 0.05 | 0.05 | 2 |
| poly | Na | 589.592 | 1/sqrt C | 0.05 | 0.05 | 2 |
| poly | Si | 251.611 | none | 0.02 | 0.02 | 2 |
| mono | Si | 251.611 | none | 0.014 | 0.014 | 2 |
| poly | Ti | 334.94 | $1/c^2$ | 0.05 | 0.05 | 2 |

**acquisitions parameters**

| | time (s) | pump speed |
|---|---|---|
| **Rinse** | 10 | normal |
| **Transfer** | 40 | high speed |
| **Integration** | 0.5 | fast |

SI 1. Acquisition parameters for ICP-OES analysis. Some background measurements were not included to the right or left of the peak due to peak interference (elevated baselines). The mono Be 313.107 line is used to determine $^{9}$Be concentrations.

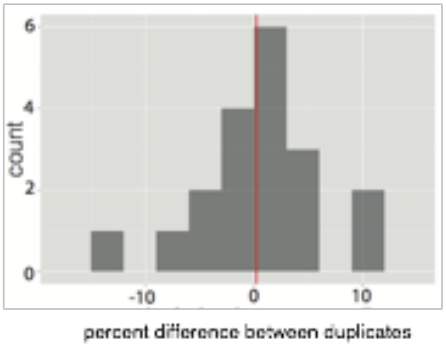


SI 2. percent difference between Be concentration from duplicate samples (n= 19). Red line represents average difference between duplicates.

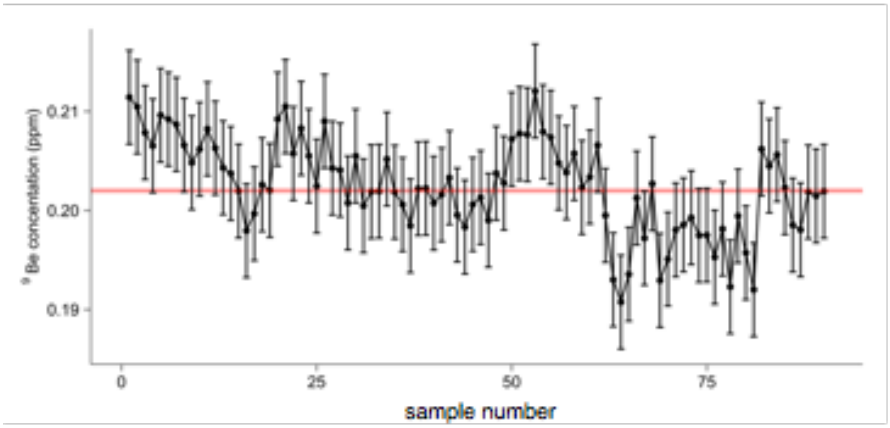


SI 3. Be concentration of a multi-element lab standard over the course of all data collection on the ICP-OES. Standard deviation = 1.7%. Red line represents known Be concentration of standard.

# CHAPTER 4. CONCLUSIONS AND FUTURE WORK

## 4.1. Conclusions

Analysis of 202 fluvial sediments with known meteoric and *in situ* $^{10}$Be concentrations provides new insight into Be dynamics within fluvial systems. For this study, I developed methods of removing grain coatings, totally digesting fluvial sediment samples, and measuring ppb levels of Be leachate via ICP-OES. I also collected basin characteristics (mean basin slope, total basin relief, mean latitude and longitude, mean basin elevation, mean annual precipitation, and basin area) for each sample using ArcGIS and compiled all grain coating, mineral grain, and geospatial data into a comprehensive dataset. In addition to fluvial sediments, soil, suspended sediments, and glacial lake sediment samples with known meteoric or *in situ* $^{10}$Be were chemically characterized, contributing $^{9}Be_{reactive}$ data and major element compositions of grain coatings to future studies.

The fluvial sediment data provided in this study give insight into the $^{10}Be_{met}/^{9}Be_{reactive}$ isotope system. Our method of extracting $^{9}$Be from grain coatings using HCl resulted in $^{9}Be_{reactive}$ concentrations that significantly and positively correlated to total $^{10}Be_{met}$ in nearly all of our study areas, supporting the assumption of previous $^{10}Be_{met}/^{9}Be_{reactive}$ studies that $^{9}Be_{reactive}$ mixes with $^{10}Be_{met}$ in grain coatings of fluvial sediments. However, we found that in a heavily terraced agricultural watershed (CHc), $^{9}Be_{reactive}$ and $^{10}Be_{met}$ were not correlated. This indicates that environments with anoxic conditions or heavily cultivated land use may have limited biological and physical mixing in soils, preventing

$^{9}Be_{reactive}$ from effectively normalizing $^{10}Be_{met}$ against the effects of grain size and remobilization.

This study also found a wide range of $^{9}Be_{min}$ and $^{9}Be_{reactive}$ concentrations within and across study areas, which indicated that variability in $^{9}Be$ concentrations of source materials (such as bedrock, dust, or potentially Be-enriched organic materials) influences $^{9}Be$ abundances in grains and grain coatings. Heterogeneous inputs for $^{9}Be$ ($^{9}Be$ concentrations of parent materials) and $^{10}Be_{met}$ (latitude and climate-dependent delivery rates), combined with study site-specific biogeochemical influences on soil mixing and remobilization processes, resulted in mostly poor correlations between $^{10}Be_{met}/^{9}Be_{reactive}$ and $^{10}Be_{is}$, $^{10}Be_{is}$-derived denudation rates, and basin characteristics when considering all samples. Although a previously published mass balance model for deriving $^{10}Be_{met}/^{9}Be_{reactive}$ denudation rates (eq. 1) helps control for some variation in parent $^{9}Be$ concentrations and $^{10}Be_{met}$ delivery rates across study areas, uncertainties in quantifying these variables and unknown f.factors for each watershed introduce noise into the correlations between $^{10}Be_{met}/^{9}Be_{reactive}$-derived denudation rates and $^{10}Be_{is}$-derived denudation rates.

The assumptions used when estimating f.factors and parent $^{9}Be$ concentrations for $^{10}Be_{met}/^{9}Be_{reactive}$-derived denudation rate calculations have little influence on the correlation between $^{10}Be_{met}/^{9}Be_{reactive}$–derived rates and $^{10}Be_{is}$-derived rates, but do significantly change the central tendency of $^{10}Be_{met}/^{9}Be_{reactive}$-derived denudation rates. Assuming that the total $^{9}Be$ concentration in the study area is 2.5 µg/g (the mean global crustal abundance of Be) when estimating f.factors and parent $^{9}Be$ concentrations resulted in mean $^{10}Be_{met}/^{9}Be_{reactive}$-derived denudation rates for all samples that agreed with $^{10}Be_{is}$-

derived denudation rates (202 ± 226 t $km^{-2}$ $yr^{-1}$ and 205 ± 226 t $km^{-2}$ $yr^{-1}$, respectively). However, assuming that the parent $^{9}Be$ concentrations are better estimated by the mean $^{9}Be_{reactive}$ + $^{9}Be_{min}$ concentrations results in a better agreement between mean denudation rates in many individual study areas. Overall, we find that $^{10}Be_{met}/^{9}Be_{reactive}$ mirrors $^{10}Be_{is}$-derived denudation rates, but that the $^{10}Be_{met}/^{9}Be_{reactive}$ -derived measure is much less sensitive to changes in denudation than the $^{10}Be_{is}$ –derived measure.

### 4.2. Future work

Although this study has provided insight into Be dynamics across a variety of study areas, an analysis of $^{10}Be_{met}/^{9}Be_{reactive}$ in fluvial sediments compared to the $^{10}Be_{met}$ and $^{9}Be_{reactive}$ concentrations in soils, suspended sediments and river water in the same watershed could help understand how site-specific conditions influence in Be isotopes. For example, more $^{10}Be_{met}$ and $^{9}Be$ data could unwrap the complexities of the QLD study area in Queensland, Australia. In this study area, the Barron River transitions from running through flat uplands to coastal lowlands with an abrupt escarpment separating the two regions. I found that $^{10}Be_{met}$ and $^{9}Be_{reactive}$ are well correlated in fluvial sediment samples from QLD, but $^{10}Be_{met}/^{9}Be_{reactive}$-derived denudation rates are not correlated to $^{10}Be_{is}$-derived denudation rates. Further, the central tendency of $^{10}Be_{met}/^{9}Be_{reactive}$-derived denudation rates is 10% - 543% higher than mean $^{10}Be_{is}$-derived denudation rates depending on the method of estimating parent $^{9}Be$ concentrations. A detailed study of $^{10}Be_{met}$ and $^{9}Be$ concentrations in river water and soils in the three distinct regions of this study area (the uplands, the escarpment, and the coastal lowlands) could pinpoint the cause for poor correlation between $^{10}Be_{met}/^{9}Be_{reactive}$-derived and $^{10}Be_{is}$-derived

denudation rates and provide insight into how $^{10}Be_{met}/^{9}Be_{reactive}$ might change as sediment moves from hillslopes to the ocean.

Further analysis of $^{9}Be_{reactive}$ data from suspended sediments could give a better understanding of how grain size and sediment transport mechanisms influence Be compositions of grain coatings. Additionally, analysis of $^{9}Be_{reactive}$ data I collected from the North American Varve Chronology glacial lake sediment samples could help normalize previously measured $^{10}Be_{met}$ data against remobilization and grain size effects. This normalized $^{10}Be_{met}$ data could possibly allow for the glacial lake varves to be correlated to climate events recorded in Greenland ice cores (DeJong et al., 2013).

## Comprehensive Bibliography


Acker, J.G., & Bricker, O.P. (1991). The influence of pH on biotite dissolution and alteration kinetics at low temperature. *Geochimica et Cosmocheimica acta, 56*, 3070-3092.

Akciz, S., Burchfiel, B.C., Crowley, J.L., Jiyun, Y., & Liangzhong, C. (2008) Geometry, kinematics, and regional significance of the Chonng Shan shear zone, Eastern Himalayan Syntaxis, Yunnan, China. *Geosphere, 4*, 292-314.

Aldahan, A., Ye, H.P., & Possnert, G. (1999). Distribution of beryllium between solution and minerals (biotite and albite) under atmospheric conditions and variable pH. *Chemical Geology, 156,* 209-229.

Anhert, F. (1970). Functional relationships between denudation, relief and uplift in large, min-latitude drainage basins. *American Journal of Science, 287*, 243-263.

Bacon, A.R., Richter D., Bierman, P.R., & Rood, D.H. (2012). Coupling meteoric $^{10}$Be with pedogenic losses of $^{9}$Be to improve soil residence time estimates on an ancient North American interfluve. *Geology, 40,* 847-850.

Balco, G., Stone, J.O., Lifton, N. A. & Dunai. T.J.. (2008). A quick and easily accessible means of calculating surface exposure ages or denudation rates from $^{10}$Be and $^{26}$Al measurements. *Quaternary Geochronology, 3,* 174-195.

Barg, E., Lal, D., Pavich, M.J., Caffee, M.W., & Southon, J.R. (1997). Beryllium geochemistry in soils; evaluation of $^{10}$Be/ $^{9}$Be ratios in authigenic minerals as a basis for age models. *Chemical Geology, 140,* 237-258.

Bierman, P.R. (1994). Using *in situ* produced cosmogenic isotopes to estimate rates of landscape evolution; a review from the geomorphic perspective. *Journal of Geophysics Research B: Solid Earth, 99,* 13885-13896.

Bierman, P., & Turner, J. (1995). $^{10}$Be and $^{26}$Al evidence for exceptionally low rates of Australian bedrock erosion and the likely existence of pre-Pleistocene landscapes. *Quaternary Research*, *44*, 378-382.

Bierman, P., & Steig, E.J. (1996). Estimating rates of denudation using cosmogenic isotope abundances in sediment. *Earth Surface Processes and Landforms, 21* 125-139.

Bierman, P., & Caffee, M. (2002). Cosmogenic exposure and erosion history of Australian bedrock landforms. *Geological Society of America Bulletin, 114,* 787-803.

Bierman, P., Caffee M., Davis, P., Marsella, K., Pavich, M., Colgan, P., Mickelson, D., & Larsen, J. (2002). Rates and timing of earth surface processes from *in situ*-produced cosmogenic Be-10. *Reviews in Mineralogy and Geochemistry, 50,* 147-205.

Bierman, P., & Nichols, K. (2004). Rock to sediment - Slope to sea with $^{10}$Be - Rates of landscape change. *Annual Reviews in Earth and Planetary Science, 32,* 215-255.

Birkeland, P.W. (1999). *Soils and Geomorphology, 3rd edition*. Oxford: Oxford University Press.

Bourlès, D., Raisbeck, G.M., & Yiou, F. (1998). $^{10}$Be and $^{9}$Be in marine sediments and their potential for dating. *Geochimica et Cosmochimica Acta, 53,* 443-452.

Brown, L., Pavic, M.J., Hickman, R.E., Klein, J., & Middleton, R. (1988). Erosion of the eastern United States observed with $^{10}$Be. *Earth Surface Processes and Landforms, 13*, 441-457.

Brown, E.T., Edmond, J.M., Raisbeck, F.M., Bourlès, D.L., Yiou, F., & Measures, C.I. (1992). Beryllium isotope geochemistry in tropical river basins. *Geochimica et Cosmochimica Acta, 56,* 1607-1624.

Brown, E.T., Stallard, R.F., Larsen, M.C., Raisbeck, G.M., & Yiou, F. (1994). Denudation rates determined from the accumulation of *in situ* produced $^{10}$Be in the Luquillo Experimental Forest, Puerto Rico, *Earth and Planetary Science Letters, 192,* 193-202.

Bouchez, J., Gaillardet, J., & von Blanckenburg, F. (2014). Weathering intensity in lowland river basins: from the Andes to the Amazon mouth. *Procedia Earth and Planetary Science, 10*, 280-186.

Burchfiel, B.C. and Zhiliang, C. (2012) *Tectonics of the Southeastern Tibetan Plateau and Its Adjacent Foreland*. Geologic Society of America, Inc. Boulder, CO. pp 100-104.

Calmano, W., Hong, J., & Förstner, U. (1993). Binding and mobilization of heavy metals in contaminated sediments affected by pH and redox potential. *Water and Science Technology, 28,* 223-235.

Campforts, B., Vanacker, V., Vanderborght,J., Baken, S., Smolders, E., & Govers, G. (2015). Simulating the mobility of meteoric $^{10}$Be in the landscape through a coupled soil-hillslope model (Be2D). *Earth Planetary Science Letters, 439,* 143-157.

Cerling, T.E., & Turner, R.R. (1982). Formation of freshwater Fe-Mn coatings on gravel and the behavior of $^{60}$Co, $^{90}$Sr, and $^{137}$Cs in a small watershed. *Geochimica et Cosmochimica Acta, 46,* 1333-1343.

Chmeleff, J., von Blanckenburg, F., Kossert, K., & Jakob, D. (2010). Determination of the $^{10}$Be half-life by multicollector ICP-MS and liquid scintillation counting. *Nuclear Instruments and Methods in Physics Research, 268,* 192-199.

Conyers, G. (2014). *Cosmogenic beryllium cycling in a natural forest setting* (MS thesis). Perdue University, Indiana.

Crowley, J.W., Katz, R., Huybers, P., Langmuir, C.H., & Park, S. (2015). Glacial cycles drive variation in the production of oceanic crust. *Science, 347,* 1237-1240.

DeJong, B.D., Balco, G., Ridge, J.C., Rood, D.H., & Bierman, P.R. (2013). Synchronizing the North American Varve Chronology with Greenland ice core records during late MIS 2 using meteoric $^{10}$Be flux. *EGU General Assembly Conference Abstracts, 15,* EGU2013-1140.

Delunel, R., van der Beek, P. A., Carcaillet, J., Bourlès, D.L., & Valla, P.G. (2010). Frost-cracking control on catchment denudation rates: Insights from in situ produced $^{10}$Be concentrations in stream sediments (Ecrins-Pelvoux massif, French Western Alps). *Earth and Planetary Science Letters, 293*, 72–83.

Desilets, D., & Zreda, M. (2003). Spatial and temporal distribution of secondary cosmic-ray nucleon intensities and applications to in situ cosmogenic dating. *Earth Planet. Sci. Lett.* 206, 21-42.

Desilets, D., Zreda, M., & Pradu, T. (2006). Extended scaling factors for *in situ* cosmogenic nuclides: New measurements at low latitude. *Earth and Planetary Science Letters, 246,* 265-276.

Dixon, J., & Riebe, C. (2014). Tracing and pacing soil across slopes. *Elements, 10,* 363-368.

Dunai, T. (2000). Scaling factors for production rates of in situ produced cosmogenic nuclides: a critical reevaluation. *Earth and Planetary Science Letters, 176,* 157-169.

Dunai, T. (2001). Influence of secular variation of the geomagnetic field on production rates of *in situ* produced cosmogenic nuclides. *Earth and Planetary Science Letters, 193,* 197-212.

Dunai, T. (2010). *Cosmogenic Nuclides, Principles, Concepts and Applications in the Earth Surface Sciences*. Cambridge: Cambridge University Press.

Dunne, J., Elmore, D., & Muzikar, P. (1999). Scaling factors for the rates of production of cosmogenic nuclides for geometric shielding and attenuation at depth on sloped surfaces. *Geomorphology, 27,* 3-11.

Dunne, J., & Elmore, D. (2003). Monte Carlo simulations of low-energy cosmogenic neutron fluxes near the bottom of cliff faces. *Earth and Planetary Science Letters, 206,* 43-49

Elmore, D., & Phillips, F., (1987). Accelerator mass spectrometry for measurement of long-lived radioisotopes. *Science*, *236,* 543-550.

Field, C.V., Schmidt, G.A., Koch, D., & Salyk, C. (2006). Modeling production of climate-related impacts on $^{10}$Be concentration in ice cores. *Journal of Geophysics Research, 111,* D15107.

Fishbein, L. (1984). Overview of analysis of carcinogenic and/or mutagenic metals in biological and environmental samples. *International Journal of Environmental Analytical Chemistry, 12*, 113-170.

Fulop, R.H., Bishop, P., Fabel, D., Cook, G.T., Everest, J., Schnabel, C., Codilean, Q. T., & Xu, S. (2015). Quantifying soil loss with *in-situ* cosmogenic $^{10}$Be and $^{14}$C depth-profiles. *Quaternary Geology, 27,* 78-93.

Gabet, E.J., Reichman, O.J., & Seablooom, E. (2003). The effects of bioturbation on soil processes and hillslope evolution. *Annual Reviews in Earth and Planetary Science, 31,* 249 – 273.

Gosse, J.C., & Phillips, F.M. (2001). Terrestrial *in situ* cosmogenic nuclides: theory and application. *Quaternary Science Reviews, 20,* 1475-1560.

Graly, J.A., Bierman, P.R., Reusser, L.J., & Pavich, M.J. (2010). Meteoric $^{10}$Be in soil profiles - a global meta-analysis. *Geochimica et Cosmochimica Acta, 74,* 6814-6829.

Graly, J.A., Reusser, L.J., & Bierman, P.R. (2011). Short and long-term delivery rates of meteoric $^{10}$Be to terrestrial soils. *Earth and Planetary Science Letters, 302,* 329-336.

Granger, D.E., Kirchner, J.W., & Finkel, R. (1996). Spatially averaged long-term denudation rates measured from in situ-produced cosmogenic nuclides in alluvial sediments. *Journal of Geology, 104,* 249-257.

Granger, D., Lifton, N.A., & Willenbring, J.K. (2013). A cosmic trip: 25 years of cosmogenic nuclides in geology *Geologic Society of America Bull*etin, *125,* 1379-1402.

Granger. D.E., & Schaller, M. (2014). Cosmogenic nuclides and denudation at the watershed scale. *Elements, 10,* 369-393.

Grew, E.S. (2002). Beryllium in metamorphic environments (emphasis on aluminous compositions). *Reviews in Mineralogy and Geochemistry, 50,* 487-549.

Hawley, N., Robbins, J.A., & Eadie, B.J. (1986). The partitioning of $^{7}$beryllium in fresh water. *Geochimica et Cosmochimica Acta, 50,* 1127-1131.

Heikkila, U., Beer, J., & Alfimov, V. (2008). Beryllium-10 and beryllium-7 in precipitation in Dubendorf (440 m) and at Jungfraujoch (3580 m), Switzerland 1998-2005. *Journal of Geophysical Research, 113,* D11104.

Heisinger, B., & Nolte, E. (2000). *In situ* production of radionuclides: Exposure ages and erosion rates. *Nuclear Instruments and Methods in Physical Research B, 172,* 790-795.

Heimsath, A.M., Dietrich, W.E., Nishiizumi, K., & Finkel, R.C. (1997). The soil production function and landscape equilibrium. *Nature, 388,* 358-361.

Heimsath, A.M., Dietrich, W.E., Nishiizumi, K., & Finkel, R.C. (1999). Cosmogenic nuclides, topography and the spatial variation of soil depth. *Geomorphology, 27*, 151-172.

Hunt, A.L., Larsen, J., Bierman, P.R., & Petrucci, G.A. (2008). Investigation of factors that affect the sensitivity of accelerator mass spectrometry for cosmogenic $^{10}$Be and $^{26}$Al isotope analysis. *Analytical Chemistry, 80,* 1656-1663.

Jungers, M.C., Bierman, P.R., Matmon, A., Nichols, K., Larsen, J., & Finkel, R. (2009). Tracing hillslope sediment production and transport with *in situ* and meteoric $^{10}$Be. *Journal of Geophysical Research, 114,* F04020.

Kabata-Pendias, A. (2011). *Trace Elements in Soils and Plants*. Berlin, New York: Springer.

Kabata-Pendias, A. and Szteke, V. (2015). *Trace Elements in Abiotic and Biotic Environments. 1st ed.*. Florida: Taylor & Francis Group, LLC.

Kober, F., Ivy-Ochs, S., Schlunegger, F., Baur, H., Kubik, P.W., & R. Wieler. (2007). *Geomorphology, 83.* 97-120.

Kohl, C.P., & Nishiizumi, K. (1992). Chemical isolation of quartz for the measurement of *in situ*-produced cosmogenic nuclides. *Geochim. Cosmochim. Acta, 56,* 3583-3587.

Korschinek G., Bergmaier, A. Faestermann, T., Gerstmann, U.C., Knie, K., Rugel, G. Wallner, A., Dillmann, I., Dollinger, G., von Gostomski, C.L., Kossert, K., Poutivtsev M., & Remmert, A. (2010). A new value for the half-life of $^{10}$Be by heavy-ion elastic recoil detection and liquid scintillation counting. *Nuclear Instruments and Meth*ods *in Physical Research, 268,* 187–191.

Kramidea, A., Ralchenko, Y., Reader, J., & NIST ASD Team (2015). *NIST Atomic Spectra Database (ver. 5.3).* Available: http://physics.nist.gov/asd. Gaithersburg, MD: National Institute of Standards and Technology.

Lal, D., & Peters, B. (1967). Cosmic ray produced radioactivity on the earth. *Handbuch der Physik*. Berlin: Springer.

Lal, D. (1988). *In situ*-produced cosmogenic isotopes in terrestrial rocks. *Annual Review of Earth and Planetary Science, 16,* 355-388.

Lal, D. (1991). Cosmic ray labeling of denudation surfaces: *in situ* nuclide production rates and denudation models. *Earth and Planetary Science Letters, 104,* 424-439.

Lal, D. (2007). Recycling of cosmogenic nuclides after their removal from the atmosphere; special case of appreciable transport of $^{10}$Be to polar regions by Aeolian dust. *Earth and Planetary Science Letters, 2007,* 177-187.

Lebatard, A.E., Bourlès, D.L. Duringer, P., Jolivet, M., Braucher, R., Carcaillet, J., Schuster, M., Arnaud, N., Monié, P., Lihoreau, F., Likius, A., Mackaye, H.T., Vignaud, P., & Brunet, M. (2008). Cosmogenic nuclide dating of Sahelanthropus tchadensis and Australopithecus bahrelghazali: Mio-Pliocene hominids from Chad. *Procedings of the National Academy of Sciences, 105,* 3226–3231.

Lifton, N., Bieber, J., Clem, J., Duldig, M., Everson, P., Humble, J., & Pyle R. (2005). Addressing solar modulation and long-term uncertainties in scaling secondary cosmic rays for in situ cosmogenic nuclide applications. *Earth and Planetary Science Letters, 239,* 140-161.

Lifton, N., Smart, D., & Shea, M. (2008). Scaling time-integrated *in situ* cosmogenic

nuclide production rates using a continuous geomagnetic model. *Earth and Planetary Science Letters, 268,* 190-201.

Lundberg, L., Ticich, T., Herzog, G.F., Hughes, T., Ashley, G., Moniot, R.K., Tuniz, C., Kruse, T., & Savin, W. (1983). $^{10}$Be and Be in the Maurice River-Union Lake system of southern New Jersey. *Journal of Geophysical Res*earch*, 88,* 4498-4504.

Matmon, A., Bierman, P.R., Larsen, J., Southworth, S., Pavich, M., Finkel, R., & Caffee, M. (2003). Erosion of an ancient mountain range, the Great Smoky Mountains, North Carolina and Tennessee. *American Journal of Science*, *303,* 817-855.

Mattock, G. (1954). The hydrolysis and aggregation of the beryllium ion*. Journal of the American Chemical Society, 76,* 4835-4838.

McClenaghan, M.P. (1985). Granitoids of northeastern Tasmania. *Journal of Australian Geology & Geophysics, 9,* 303-312.

McHarque, L.R., & Damon, P.E. (1991). The global beryllium-10 cycle. *Reviews in Geophysics, 29,* 141-158.

McKean, J., Dietrich, W.E., Finkel, R.C., Southon, J.R., & Caffee, M.W. (1993). Quantification of soil production and downslope creep rates from cosmogenic $^{10}$Be accumulations on a hillslope profile. *Geology, 22,* 343-346.

Measures, C.I., & Edmond, J.M. (1983). The geochemical cycle of $^{9}$Be: a reconnaissance. *Earth and Planetary Science Letters*, *66,* 101-110.

Meehan, W.R., & Smythe, L.E. (1967). Occurrence of beryllium as a trace element in environmental materials. *Environmental Science Technology, 10,* 839-844.

Merrill, J.R., Lyden, E., Honda, M., & Arnold, J.R. (1959). The sedimentary geochemistry of the beryllium isotopes. *Geochimica et Cosmochimica Acta, 18,* 108-129.

Monaghan, M.C., Krishnaswami, S., & Thomas, J.H. (1983). $^{10}$Be concentrations and the long-term fate of particle-reactive nuclides in five soil profiles from California, *Earth and Planetary Science Letters, 65,* 51-60.

Monaghan, M.C., Krishnaswami, S., & Turekian, K.K. (1986). The global-average production rate of $^{10}$Be. *Earth and Planetary Science Letters, 76,* 279-287.

Neilson, T.B. (2015). *Using long- and short-lived sediment-associated isotopes to track denudation and sediment movement through rivers in Yunnan, SW China.*

(MS thesis). University of Vermont, Burlington.

Nichols, K.K., Bierman, P.R., & Rood, D.H. (2014). $^{10}$Be constrains the sediment sources and sediment yields to the Great Barrier Reef from the tropical Barron River catchment, Queensland, Australia. *Geomorphology*, *224,* 102-110.

Nishiizumi, K, Lal, D., Klein, J., Middleton, R., & Arnold, J.R. (1986). Production of $^{10}$Be and $^{26}$Al by cosmic rays in terrestrial quartz *in situ* and implications for denudation rates. *Nature, 319,* 1468-1470.

Nishiizumi, K., Imamura, M., Caffee, M.W., Southon, J.R., Finkel, R.C., & McAninch, F. (2007). Absolute calibration of $^{10}$Be AMS standards, *Nuclear Instruments and Methods in Physical Research B, 258,* 403-413.

Nyffeler, U.R., Li, Y.-U., & Santschi, P.H. (1984). A kinetic approach to describe trace-element distribution between particles and solution in natural aquatic systems. *Geochimica et Cosmochimica Acta, 48*, 1513-1522.

Olsen, C.R., Larsen, I.L., Lowry, P.D., Cutshall, N.H., & Nichols, M.M. (1986). Geochemistry and deposition of Be-7 in river-estuarine and costal waters. *Journal of Geophysical Research-Oceans, 91,* 896-908.

Ouimet, W., Dethier, D., Bierman, P., Wyshnystzky, C., Shea, N., & Rood, D. (2015) Spatial and temporal variations in meteoric $^{10}$Be inventories and long-term deposition rates, Colorado Front Range. *Quaternary Science Reviews, 109*, 1-12.

Palumbo, L., Hetzel, R., Tao, M., & Li, X. (2009). Topographic and lithologic control on catchment-side denudation rates derived from cosmogenic $^{10}$Be in two mountain ranges at the margin of NE Tibet. *Geomorphology, 117*, 130-142.

Pavich, M.P., Brown, L., Klein, J., & Middleton, R. (1984). $^{10}$Be accumulation in a soil chronosequence. *Earth and Planetary Science Letters, 68,* 198-204.

Pavich, M.P, Brown, L., Harden, J., Klein, J., & Middleton, R. (1986). $^{10}$Be distribution in soils from Merced River terraces, California. *Geochimica et Cosmochimica Acta, 50,* 1727-1735.

Portenga, E.W., & Bierman P.R. (2011). Understanding Earth's eroding surface with $^{10}$Be. *GSA Today, 21,* 4-10.

Raymo, M.E., Ruddiman, W.F., & Froelich, P.N. (1998). Influence of late Cenozoic mountain building on ocean geochemical cycles. *Geology, 16,* 649-653.

Reusser, L., Graly, J., Bierman, P., & Rood, D. (2010). A long-term meteoric $^{10}$Be accumulation rate in soil. *Geophysical Research Letters, 37,* L19403.

Reusser, L., & Bierman, P.R. (2010). Using meteoric $^{10}$Be to track fluvial sand through the Waipaoa River basin, New Zealand. *Geology, 38,* 47-50.

Riebe, C.S., Kirchner, J.W., & Finkel, R.C. (2003). Long-term rates of chemical weathering and physical erosion from cosmogenic nuclides and geochemical mass balance. *Geochimica et Cosmochimica Acta, 67,* 4411-4427.

Smith, C., Ingerman, L., & Amata, R. (2002). U.S. Department of Health and Human Services. *Toxicological profile for beryllium.* Atlanta Georgia: Government Printing Office.

Stone, J. (1998). A rapid fusion method for separation of beryllium-10 from soils and silicates. *Geochemica et Cosmochimica Acta. 62,* 555-561.

Stoops, G., Marcelino, V., & Mees, F. (2010). *Micromorphological features and their relation to processes and classification, interpretation of micromorphological features of soils and regoliths.* Amsterdam: Elsevier.

Šujan, M., Braucher, R., Kováč, M., Bourlès, D.L., Rybár, S., Guillou, V., & Hudáčková, N. (2015). Application of the authigenic $^{10}$Be/$^{9}$Be dating method to Late Miocene-Pliocene sequences in the northern Danube Basin (Pannonian Basin System): confirmation of heterochronous evolution of sedimentary environments. *Global and Planetary Change, 137,* 35-53.

Takahashi, M., Ambe, S., Makide, Y., & Ambe, F. (1999). Comparison of adsorption behavior of multiple inorganic ions on kaolinite and silica in the presence of humic acid using the multi-tracer technique. *Geochimica et Cosmochimica Acta, 63l,* 815-836.

Taylor, A., Blake, W.H., Couldrick, L., & Keith-Roach, M.J. (2012). Sorption behavior of beryllium-7 and implications for its use as a sediment tracer. *Geoderma*, *187-188,* 16-23.

Tessier, A., Campbell, P.G.C., & Bisson, M. (1979). Sequential extraction procedure for the speciation of trace metals. *Analytical Chemistry*, *51*, 844-851.

Trodick, C. D. (2011). *In situ and meteoric $^{10}$Be concentrations of fluvial sediment collected from the Potomac River Basin.* (MS thesis). University of Vermont, Burlington.

Vance, D., Teagle, D., & Foster, G. (2009). Variable Quaternary chemical weathering fluxes and imbalances of marine geochemical budgets. *Nature, 458,* 493-496.

Veselý J.S., Norton, A., Skřivan, P., Majer, V., Krám, P., Navrátil, T., & Kaste, J.M. (2002). Environmental chemistry of beryllium. *Reviews in Mineralogy and Geochemisty, 50,* 291-317.

von Blanckenburg, F. (2005). The control mechanisms of denudation and weathering at basin scale from cosmogenic nuclides in river sediment. *Earth and Planetary Science Letters, 237,* 462-479.

von Blanckenburg, F., Bouchez, J., & Wittmann, H. (2012). Earth surface denudation and weathering from the $^{10}$Be (meteoric)/$^{9}$Be ratio. *Earth and Planetary Science Letters, 351*, 295-305.

von Blanckenburg, F., & Bouchez, J. (2014). River fluxes to the sea from the ocean's $^{10}$Be/$^{9}$Be ratio. *Earth and Planetary Science Letters, 387,* 34-43.

von Blanckenburg, F., & Schuessler, J.A. (2014). Element cycling in the critical zone as viewed by new isotope tools. *Procedia Earth and Planetary Science, 10,* 173-178.

von Blanckenburg, F., Bouchez, J., Ibarra, D., & Maher, K. (2015). Stable runoff and weathering fluxes into the oceans over Quaternary climate cycles. *Nature Geoscience*, *8,* 538-542.

West, A.J., Baly, A., & Bickle, M. (2005). Tectonic and climatic controls on silicate weathering. *Earth and Planetary Science Letters, 235,* 211-228.

West, N., Kirby, E., Bierman, P., Slingerland, R., Ma., L., Rood, D., & Brantley, S. (2013). Regolith production and transport at Susquehanna Shale Hills Critical Zone Observatory, part 2: insights from meteoric $^{10}$Be. *Journal of Geophysical Research: Earth Surface*, *118,* 1877-1896.

Willenbring, J., & von Blanckenburg, F. (2010). Meteoric cosmogenic beryllium-10 adsorbed to river sediment and soil: applications for earth-surface dynamics. *Earth Science Rev*iews, *98,* 105-122.

Wittmann, H., von Blanckenburg, F., Bouchez, J, Dannhaus, N, Naumann, R., Christl, M., & Gaillardet, J. (2012). The dependence of meteoric $^{10}$Be concentrations on particle size in Amazon River bed sediment and the extraction of reactive $^{10}$Be/$^{9}$Be ratios. *Chemical Geology, 318,* 126-138.

You, C.-F., Lee, T., & Li, Y.H. (1989). The partition of Be between soil and water. *Chemical Geology, 77,* 105-118.

You, C.-F., Morris, J., Gieskes, J., Rosenbauer, R., Zheng, S., Xu, X., Ku, T., & Bischoff, J. (1994). Mobilization of beryllium in the sedimentary column at convergent margins *Geochimica et Cosmochimica Acta, 58,* 4887-4897.

Zheng, S.A., & Zhang, M.K. (2011). Effect of moisture regime on the redistribution of heavy metals in paddy soil. *Journal of Environmental Science China, 23*, 434-443.